| | |
|---|---|
| **Titre:** Title: | Biomechanical Impact of Intraoperative Correction and Bone Maturity on Long-Term Outcomes in Pediatric Lumbar VBT |
| **Auteur:** Author: | Marine Gay |
| **Date:** | 2025 |
| **Type:** | Mémoire ou thèse / Dissertation or Thesis |
| **Référence:** Citation: | Gay, M. (2025). Biomechanical Impact of Intraoperative Correction and Bone Maturity on Long-Term Outcomes in Pediatric Lumbar VBT [Mémoire de maîtrise, Polytechnique Montréal]. PolyPublie. https://publications.polymtl.ca/66249/ |



| | |
|---|---|
| **URL de PolyPublie:** PolyPublie URL: | https://publications.polymtl.ca/66249/ |
| **Directeurs de recherche:** Advisors: | Carl-Éric Aubin |
| **Programme:** Program: | Génie mécanique |

**POLYTECHNIQUE MONTRÉAL**

affiliée à l'Université de Montréal

# Biomechanical Impact of Intraoperative Correction and Bone Maturity on Long-Term Outcomes in Pediatric Lumbar VBT

**MARINE GAY**

Département de génie mécanique

Mémoire présenté en vue de l'obtention du diplôme de *Maîtrise ès sciences appliquées*

Génie mécanique

Juin 2025

**POLYTECHNIQUE MONTRÉAL**

affiliée à l'Université de Montréal

Ce mémoire intitulé :

**Biomechanical Impact of Intraoperative Correction and Bone Maturity on Long-Term Outcomes in Pediatric Lumbar VBT**

présenté par **Marine GAY**

en vue de l'obtention du diplôme de *Maîtrise ès sciences appliquées*

a été dûment accepté par le jury d'examen constitué de :

**Farida CHERIET**, présidente

**Carl-Éric AUBIN**, membre et directeur de recherche

**A. Noelle LARSON**, membre et codirectrice de recherche

**Isabelle VILLEMURE**, membre et codirectrice de recherche

**Michelle WELBORN**, membre

# REMERCIEMENTS

Je souhaite en premier lieu exprimer toute ma gratitude à mon directeur de recherche, Carl-Éric Aubin, professeur titulaire au département de génie mécanique de l'École Polytechnique de Montréal, pour m'avoir offert l'opportunité de travailler sur ce projet. Je le remercie chaleureusement pour son accompagnement attentif à chaque étape, la rigueur scientifique dont il a fait preuve, ainsi que la pertinence de ses orientations et de ses réflexions, qui ont grandement enrichi cette recherche et nourri ma progression tout au long du projet. I would also like to sincerely thank my co-supervisors, A. Noelle Larson and Isabelle Villemure, for their invaluable support and for generously sharing their complementary expertise. Their insightful perspectives—both clinical and biomechanical—greatly contributed to the depth and robustness of this work.

Un immense merci à toi, Nikita Cobetto, pour ton aide précieuse, tes conseils avisés et tes encouragements constants tout au long de ce projet. J'ai eu beaucoup de chance de pouvoir compter sur toi.

Je tiens également à remercier toutes les personnes qui ont contribué à l'accomplissement de ce travail, en particulier Christiane Caouette et Marie-Ève Fecteau. Thanks to Dan Hoernschemeyer, Melanie Boeyer, Ron El-Hawary, and Ahmet Alanay for their constructive collaboration.

Je remercie chaleureusement Nathalie Bourassa et Christian Bellefleur pour leur soutien technique et leur grande disponibilité tout au long de ce projet.

Je suis également reconnaissante envers les organismes qui ont financé cette recherche, notamment la Scoliosis Research Society et l'Institut TransMedTech. Merci de m'avoir offert cette précieuse opportunité.

Un grand merci aux étudiant.es du laboratoire — Daphné, Lola, Mathieu, Mohammad, Catherine et tous les autres — pour leur bonne humeur et leur énergie : vous avez été chacun des rayons de soleil qui ont illuminé ce parcours. Merci aussi à mes ami.es, en France comme au Québec, pour avoir toujours été présent.es pour partir à l'aventure et recharger les batteries avant de retourner au travail : Marie, Laure et Gabriel, Jérémy, Charles, Inès, Camille, Paul, Antoine et les autres.

Une pensée particulière pour mes frère et sœurs, Sibille, Jérômine et Paul-Emmanuel : malgré les kilomètres, vos appels et nos soirées films ont toujours été une source de réconfort et de motivation pour continuer à trouver que la vie est belle.

Enfin, je souhaite remercier du fond du cœur mes parents, Stéphane et Fabienne, sans qui cette aventure n’aurait jamais été possible. Merci pour votre soutien indéfectible, vos encouragements constants et votre confiance, qui m’ont permis d’aller aussi loin.

# RÉSUMÉ

La scoliose est une déformation tridimensionnelle de la colonne vertébrale et de la cage thoracique. Lorsque son étiologie est inconnue et qu'elle survient entre 10 et 18 ans, elle est qualifiée de scoliose idiopathique de l'adolescent (AIS), la forme la plus fréquente de scoliose pédiatrique, avec une prévalence de 1 à 4 %. Pour les courbures sévères (angle de Cobb > 40°), évolutives, ou pour lesquelles le traitement par corset s'avère inefficace, une intervention chirurgicale est nécessaire pour arrêter la progression de la scoliose. La procédure standard repose sur l'arthrodèse, une chirurgie qui entraîne une fusion des vertèbres du segment instrumenté, rigidifiant le rachis. Cette chirurgie est inadaptée pour les patients en début de croissance car elle limiterait alors cette croissance. En alternative, des approches plus récentes de techniques chirurgicales sans fusion, notamment la modulation de croissance par Vertebral Body Tethering (VBT), peuvent être utilisées pour les patients pédiatriques avec une déformation progressive. La chirurgie VBT exploite le principe de Hueter-Volkmann, selon lequel une charge accrue sur une plaque de croissance inhibe localement la croissance osseuse, tandis qu'une diminution de pression la stimule. Le principe de cette chirurgie est d'insérer un câble flexible sur le côté convexe de la courbure pour induire une compression asymétrique par rapport au côté concave: la croissance est ralentie du côté convexe et favorisée du côté concave. Après une correction initiale de la courbure obtenue lors de la chirurgie, la croissance résiduelle du patient contribue à la correction progressive de la déformation.

La chirurgie VBT présente encore plusieurs défis, avec des taux relativement élevés de résultats insatisfaisants liés aux bris du câble, à une sous- ou sur-correction, ainsi qu'à l'apparition de déformations secondaires telles des problèmes jonctionnels aux extrémités de l'instrumentation (adding-on). Le taux de réintervention chirurgicale varie ainsi de 20 à 30 %. Au niveau lombaire, le dispositif de VBT est particulièrement sollicité en raison des forces mécaniques, du potentiel de croissance et de la flexibilité du rachis, accrues au niveau lombaire, limitant la correction satisfaisante des courbures (< 35°) à seulement 57 % des cas. Les recherches récentes ont amélioré la compréhension des trajectoires de modulation de la croissance, mais se concentrent principalement sur le rachis thoracique, négligeant les spécificités lombaires. De plus, la planification chirurgicale demeure difficile en raison des incertitudes sur la modulation de la croissance, la dynamique de maturation squelettique et l'interaction entre le VBT et d'autres forces biomécaniques (musculaires, fonctionnelles, gravitationnelles). En l'absence de modèles prédictifs précis, la planification chirurgicale repose encore sur des estimations empirico-heuristiques.

L'objectif de ce mémoire était d'adapter un outil de modélisation permettant de simuler la chirurgie de VBT lombaire puis la croissance et modulation de croissance sur deux ans et de l'exploiter afin d'analyser l'influence du degré de correction intra-opératoire sur l'évolution de la correction de la scoliose après une chirurgie VBT lombaire. L'approche visait à tenir compte de la maturité squelettique préopératoire, et à identifier une stratégie de correction permettant d'optimiser le résultat final tout en minimisant les risques de sous- ou de sur-correction à la fin de la croissance. Cette démarche avait pour but de tester l'hypothèse que la correction obtenue à maturité osseuse peut être prédite, à l'aide du modèle par éléments finis du rachis, en fonction de la correction intra-opératoire réalisée et de paramètres spécifiques au patient, tels que la maturité squelettique, la flexibilité du rachis et le poids corporel.

Pour ce faire, un modèle biomécanique par éléments finis basé sur la reconstruction 3D de patients instrumentés avec un dispositif VBT a été validé. Ce modèle inclut le positionnent en décubitus latéral du patient ainsi que l'insertion des vis dans les corps vertébraux, l'ajout du câble et sa mise en tension. La croissance et la modulation de croissance sont ensuite simulées afin de prédire la correction sur une période de 24 mois. Ce modèle a été utilisé dans le cadre de deux études. La première visait à tester l'influence de niveaux de correction intra-opératoire sur la correction à deux ans. Trois niveaux de correction nominale intra-opératoire (35%, 50%, 70%) ont été simulés pour quatre maturités squelettiques évaluées par le Score de Sanders (SS) au moment de la chirurgie (SS 3A, 3B, 4, 5). Les corrections postopératoires immédiates et à deux ans ont été simulées et analysées. Une correction intra-opératoire de 35% a entraîné une correction immédiate de 37° (23°-54°) mais une sous-correction à deux ans, avec une courbure finale de 38° (22°-63°). Une progression de la courbe a été observée dans 40 % des cas SS 3A, principalement chez les patients plus lourds (54 kg vs. 38 kg, $p < 0,05$). Une correction intra-opératoire de 50% a conduit à une correction immédiate de 27° (16°-40°), avec une amélioration significative à deux ans uniquement pour les SS 3A ($p < 0,05$). Une modulation de croissance cliniquement significative ($\Delta > 5°$) était corrélée à un poids plus faible (40±6 kg vs. 54±6 kg, $p < 0,05$). Pour une correction intra-opératoire de 70%, la correction immédiate était de 17° (11°-22°), avec une amélioration significative pour tous les SS ($p < 0,05$). Les courbures finales à deux ans étaient de 1° (-27° à 10°) pour SS 3A, 10° (-5° à 10°) pour SS 3B, 12° (0° à 18°) pour SS 4, et 13° (4° à 19°) pour SS 5. Une sur-correction a été observée chez 4 patients SS 3A et 1 patient SS 3B. Ces résultats soulignent l'importance d'une correction intra-opératoire adaptée au patient. Chez les SS 3A-3B, la modulation de croissance peut améliorer la correction à long terme, mais son efficacité dépend du poids et du degré de correction intra-opératoire initial. Le modèle suggère qu'une correction intra-opératoire de 70% est correcte pour la VBT lombaire, sauf pour les SS 3A, où 50% pourrait suffire.

Toutefois, les variations observées entre les résultats des différents cas, ainsi que la simulation de sur-correction, ont mis en évidence la nécessité d'identifier un indicateur plus directement actionnable par les chirurgiens lors de la planification opératoire. L'objectif était ainsi de déterminer un angle de Cobb optimal à atteindre en intra-opératoire, afin de maximiser les chances d'obtenir, à la fin de la croissance, une correction résiduelle de la scoliose considérée comme satisfaisante (10° ± 5°). Dix niveaux de correction intra-opératoire (de 50% à 100%) ont été simulés, pour deux scénarios de croissance différents correspondant à SS 3A et 3B. La croissance et la modulation de la croissance ont été simulées jusqu'à la fin de la croissance (ou <5% de croissance restante). Les résultats des simulations ont montré qu'une correction optimale en fin de croissance de 10° ± 5° était obtenue à des niveaux de correction intra-opératoire significativement différents ($p<0{,}05$) : 74 % (55-87 %) pour SS 3A et 85 % (85-97 %) pour SS 3B. Les angles de Cobb correspondants étaient respectivement de 12° (5°-18°) et de 8° (1°-14°). La flexibilité et le poids du patient n'ont pas eu d'effet significatif sur la correction per-opératoire. Cependant, le poids du patient a influencé de manière significative la variation de la tension du câble nécessaire pour obtenir une correction maximale à la fin de la croissance ($p<0{,}01$), à la fois pour SS 3A et 3B. En revanche, la flexibilité de la colonne vertébrale n'a pas eu d'influence significative sur la modulation de la croissance.

Ce projet a montré que la variabilité des seuils de correction à viser en fonction des paramètres spécifiques aux patients nécessite une planification préopératoire individualisée. Le cadre de simulation développé permet de définir des objectifs de correction intra-opératoire spécifiques en intégrant des paramètres clés tels que la mesure de la déformation initiale, la maturité squelettique du patient évaluée par la mesure du Score de Sanders, le poids corporel et la flexibilité rachidienne. En anticipant les réponses mécaniques et biologiques propres à chaque patient, cette approche réduit la dépendance aux estimations heuristiques. Elle s'inscrit ainsi dans une démarche visant à optimiser la planification chirurgicale par une approche mécanobiologique prédictive, équilibrant correction chirurgicale et potentiel de croissance afin de limiter les risques de sous- ou sur-correction et d'améliorer les résultats à long terme de la chirurgie VBT.

# ABSTRACT

Scoliosis is a three-dimensional deformation of the spine and rib cage. When its etiology is unknown and it occurs between the ages of 10 and 18, it is referred to as adolescent idiopathic scoliosis (AIS), the most common form of pediatric scoliosis, with a prevalence of 1 to 4%. For severe curves (Cobb angle > 40°), progressive curves, or curves for which treatment with a brace is ineffective, surgery is necessary to stop the progression. The standard procedure is based on arthrodesis, a surgery that causes the vertebrae of the instrumented segment to fuse, thus limiting the patient's growth and mobility. Alternatively, recent approaches to fusionless surgical techniques, including growth modulation by Vertebral Body Tethering (VBT), can be used for pediatric patients with progressive scoliosis. VBT surgery uses the Hueter-Volkmann principle, according to which an increased load on a growth plate locally inhibits bone growth, while a decrease in pressure stimulates it. The principle of this surgery is to insert a tether on the convex side of the curvature to induce asymmetric compression in relation to the concave side: growth is thus slowed on the convex side and promoted on the concave side. After an initial correction of the curvature obtained during surgery, the patient's residual growth contributes to the progressive correction of the deformity.

VBT surgery still presents several challenges, with relatively high rates of unsatisfactory results linked to tether breakage, under- or over-correction, and the appearance of secondary deformities such as junctional problems at the ends of the instrumentation (adding-on). The re-intervention rate varies from 20 to 30%. At the lumbar level, the VBT device is particularly stressed due to the mechanical forces, growth potential and flexibility of the spine, which are greater at the lumbar level, limiting satisfactory correction of curvatures (< 35°) to only 57% of cases. Recent research has improved our understanding of growth modulation trajectories, but focuses mainly on the thoracic spine, neglecting the specific features of the lumbar spine. Furthermore, surgical planning remains difficult due to uncertainties about growth modulation, skeletal maturation dynamics and the interaction between the VBT and other biomechanical forces (muscular, functional, gravitational). In the absence of precise predictive models, surgical planning still relies on empiric and heuristic estimates.

The aim of this thesis was to adapt a modelling tool and use it to analyse the influence of the degree of intraoperative correction on the evolution of scoliosis correction after lumbar VBT surgery. The

aim of the approach was to take account of pre-operative skeletal maturity, and to identify a correction strategy that would optimise the result while minimising the risk of under- or over-correction at the end of growth. The aim of this approach was to test the hypothesis that the correction obtained at bone maturity can be predicted, using the finite element model of the spine, as a function of the intra-operative correction performed and patient-specific parameters such as skeletal maturity, spinal flexibility and body weight.

To this end, a biomechanical finite element model based on 3D reconstruction of patients instrumented with a VBT device was validated. This model includes positioning the patient in lateral decubitus as well as inserting the screws into the vertebral bodies, adding the cable and tensioning it. Growth and growth modulation are then simulated to predict correction over a 24-month period. This model was used in two studies. The first aimed to test the influence of three levels of intra-operative correction on correction at two years. Three levels of nominal intraoperative correction (35%, 50%, 70%) were simulated for four skeletal maturities assessed by the Sanders Score (SS) at the time of surgery (SS 3A, 3B, 4, 5). Immediate and two-year post-operative corrections were simulated and analysed. An intra-operative correction of 35% resulted in an immediate correction of 37° (23°-54°) but an under-correction at two years, with a final curvature of 38° (22°-63°). Curve progression was observed in 40% of SS 3A cases, mainly in heavier patients (54 kg vs. 38 kg, $p < 0.05$). Intra-operative correction of 50% led to an immediate correction of 27° (16°-40°), with significant improvement at two years only for SS 3A patients ($p < 0.05$). Clinically significant growth modulation ($\Delta > 5°$) correlated with lower weight (40±6 kg vs. 54±6 kg, $p < 0.05$). For an intraoperative correction of 70%, the immediate correction was 17° (11°-22°), with significant improvement for all SS ($p < 0.05$). Final curvatures at two years were 1° (-27° to 10°) for SS 3A, 10° (-5° to 10°) for SS 3B, 12° (0° to 18°) for SS 4, and 13° (4° to 19°) for SS 5. Over-correction was observed in 4 SS 3A patients and 1 SS 3B patient. These results underline the importance of intraoperative correction adapted to the patient. In SS 3A-3B patients, growth modulation may improve correction in the long term, but its effectiveness depends on weight and the degree of initial intraoperative correction. The model suggests that an intraoperative correction of 70% is correct for lumbar VBT, except for SS 3A, where 50% may be sufficient.

However, the variations observed between the results of the different cases, as well as the simulation of over-correction, highlighted the need to identify an indicator that surgeons could use more directly when planning surgery. The aim was to determine an optimal Cobb angle to be achieved intraoperatively, to maximise the chances of obtaining, at the end of growth, a residual correction of the scoliosis considered satisfactory (<5°). Ten levels of intraoperative correction (from 50% to 100%) were simulated, for two different growth scenarios corresponding to SS 3A and 3B. Growth and growth modulation were simulated until the end of growth (or <5% growth remaining). Simulation results showed that an optimal end-of-growth correction of ±5° was achieved at significantly different levels of intraoperative correction ($p<0.05$): 74% (55-87%) for SS 3A and 85% (85-97%) for SS 3B. The corresponding Cobb angles were 12° (5°-18°) and 8° (1°-14°) respectively. Flexibility and patient weight had no significant effect on intraoperative correction. However, patient weight significantly influenced the variation in cable tension required to achieve maximum correction at the end of growth ($p<0.01$) for both SS 3A and 3B. In contrast, spinal flexibility had no significant influence on growth modulation.

This project has shown that the variability of the correction thresholds to be targeted as a function of patient-specific parameters requires individualised preoperative planning. The simulation framework developed makes it possible to define specific intra-operative correction targets by integrating key parameters such as the measurement of initial deformity, the patient's skeletal maturity as assessed by the Sanders Score, body weight and spinal flexibility. By anticipating the mechanical and biological responses specific to each patient, this approach reduces reliance on heuristic estimates. It is therefore part of an approach aimed at optimising surgical planning using a predictive mechanobiological approach, balancing surgical correction and growth potential to limit the risks of under- or over-correction and improve the long-term results of VBT surgery.

# TABLE OF CONTENTS

# LIST OF TABLES

# LIST OF FIGURES

# LISTE OF SYMBOLS AND ABBREVIATIONS

| | |
|---|---|
| 2-yr | 2 years |
| 2-yr Post-op | Follow up at years post operation |
| 3D | Three dimensional |
| AIS | Adolescent Idiopathic Scoliosis |
| ASME V&V 40 | Verification and Validation of Computational Models in Medical Device Applications (Standard ASME V&V 40) |
| BMI | Body Mass Index |
| C1-C7 | Cervical 1 to Cervical 7 (vertebrae) |
| COU | Context of Use |
| CT-Scan | Computed Tomography Scan |
| Δ | Delta Symbol (difference/variation between two things) |
| EOS | Low-dose Biplanar Radiographic Imaging System (EOS Imaging System) |
| e.g. | Exempli gratia (for example) |
| FEM | Finite Element Model |
| G | Actual Local Growth Rate |
| Gm | Mean Baseline Growth under normal stress |
| Kg | Kilograms |
| L1-L5 | Lumbar Vertebrae |
| LAT | Lateral |
| LIV | Lower Instrumented Vertebra |
| Max | Maximum |
| Min | Minimum |
| MRI | Magnetic Resonance Imaging |

| | |
|---|---|
| MPa | Megapascal |
| MT | Main Thoracic |
| N | Newtons |
| Nb, n | Number of Cases in a Sample |
| PA | Postero-Anterior |
| S1-S5 | Sacral Vertebrae |
| Sigma | Actual Local Stress |
| Sigma m | Mean Physiological Stress |
| SO | Sub-objectives |
| SS | Sanders Score |
| SSX | Sanders Score evaluated at level X |
| TL/L, TLL | Thoraco-lumbar/lumbar |
| TRC | Triradiate Cartilage |
| USA | United States of America |
| UIV | Upper Instrumented Vertebra |
| VBT | Vertebral Body Tethering |
| VVUQ | Verification, Validation, and Uncertainty Quantification |
| β | Sensitivity Factor to mechanical stress |
| ° | Degree |
| % | Percentage |

# LIST OF APPENDICES

# CHAPTER 1 INTRODUCTION

Between 1% and 4% of teenagers suffer from idiopathic scoliosis, a three-dimensional deformity of the spine, most often affecting girls during puberty (Cheng et al., 2015). Depending on the severity of the curvature, measured by the Cobb angle, different treatment options are considered: simple monitoring for curvatures less than 20°, conservative treatment using a brace between 20° and 45°, and surgical treatment above 45° to limit the risk of progression and its functional consequences in adulthood. (Ghanem & Rizkallah, 2020). Posterior arthrodesis, in which the instrumented vertebrae are fused together, is currently still the surgical technique preferred. However, it results in a significant loss of spinal mobility, which has led to the development of so-called "non-fusion" surgical techniques, such as vertebral body tethering surgery (VBT). This approach, based on the Hueter-Volkmann principle, aims to modulate vertebral growth asymmetrically by applying controlled mechanical loads to the vertebral growth plates. By compressing the convex side of the curvature, growth is slowed, while it is stimulated on the concave side, allowing progressive correction of the deformity during residual growth (Cobetto, Aubin, et al., 2018b; Martin et al., 2023; Stokes et al., 2006)

VBT surgery is essentially interesting for patients who are still growing, where bone modulation can be exploited to avoid irreversible fusion (McDonald et al., 2022; Photopoulos et al., 2024). It offers clinical advantages such as reduced operating time, less blood loss and, above all, preservation of spinal mobility (Newton et al., 2020). However, despite encouraging results, several complications have been reported, including the risk of over- or under-correction, tether breakage, and a less predictable correction than with arthrodesis (Pahys et al., 2025; Todderud et al., 2025). VBT surgery remains complex, and its clinical results are variable. The success rate, defined by a final curvature of less than 35°, is reported to be 77%, with re-operation rates between 20% and 30% (Mathew et al., 2022; Newton et al., 2020). The lumbar VBT presents specific challenges linked to the mobility, flexibility and high growth potential of this region, leading to an increased risk of over- or under-correction. The success rate for lumbar curvatures is only 57% (Boeyer, Farid, et al., 2023; C. R. Louer, Jr. et al., 2024; Trobisch et al., 2023). While the modulation of thoracic growth is increasingly well understood, the lumbar region remains little studied and represents a major challenge for future research (Boeyer, Groneck, et al., 2023).

Building on previously validated models (Cobetto, Aubin, et al., 2018b; Cobetto et al., 2020; Martin et al., 2023; Raballand et al., 2023), a patient-specific FEM has been developed to simulate VBT surgery and post-operative growth modulation (Cobetto et al., 2025). This model incorporates the specific three-dimensional geometry of each patient's spine, reconstructed from medical images. It considers the mechanical properties of the vertebrae, intervertebral discs and instrumentation used, as reported in the literature. Growth modulation principles are incorporated as a function of Sanders' stage of bone maturity and the anatomical location of the structures concerned. Finally, the model simulates the biomechanical interactions between the correction obtained during surgery and subsequent vertebral growth. This modelling strategy provides a predictive tool to assess the biomechanical effects of VBT and optimize surgical planning according to patient-specific characteristics.

However, the link between the level of intra-operative correction and the correction obtained at two years has not been extensively studied. Thus, even if the effect of the VBT device is credibly predictable thanks to the model developed, general conclusions enabling us to enrich our knowledge of surgical strategies have yet to be established.

The aim of this study was to model and biomechanically analyse the optimal correction to aim for intraoperatively during lumbar VBT surgery, to maximise two-year outcomes while limiting the risk of overcorrection in patients with paediatric idiopathic scoliosis. The analysis considered key patient-specific factors such as initial deformity, spinal stiffness, body weight and level of bone maturity. Ultimately, the aim was to develop a decision-making tool that would enable surgeons to objectively define an intraoperative correction strategy tailored to the specific features of each case.

This Master thesis is divided into 7 chapters, starting with this introduction in Chapter 1, a literature review in Chapter 2. Chapter 3 presents the objectives and hypotheses of this dissertation, as well as the rationale. Then, in Chapters 4 and 5, two studies in the form of scientific articles present the core of its dissertation. A verification and validation study on the moment calculations used for the project was carried out and is presented in the appendix. Finally, Chapter 6 offers a general discussion of the study. The conclusion and recommendations of this project are given at the end of the dissertation in Chapter 7.

# CHAPTER 2 Literature review

## 2.1 Descriptive and functional anatomy of the spine

### 2.1.1 Anatomical reference planes

The anatomical reference planes used to study the spine are defined as follows and illustrated in Figure 2-1:

- The sagittal or lateral plane (A) divides the body into its right and left portions.
- The coronal or frontal plane (B) divides the body into an anterior (ventral) and posterior dorsal) sections.
- The transverse or axial plane (C) divides the body horizontally into cranial (upper) and caudal (lower) parts.

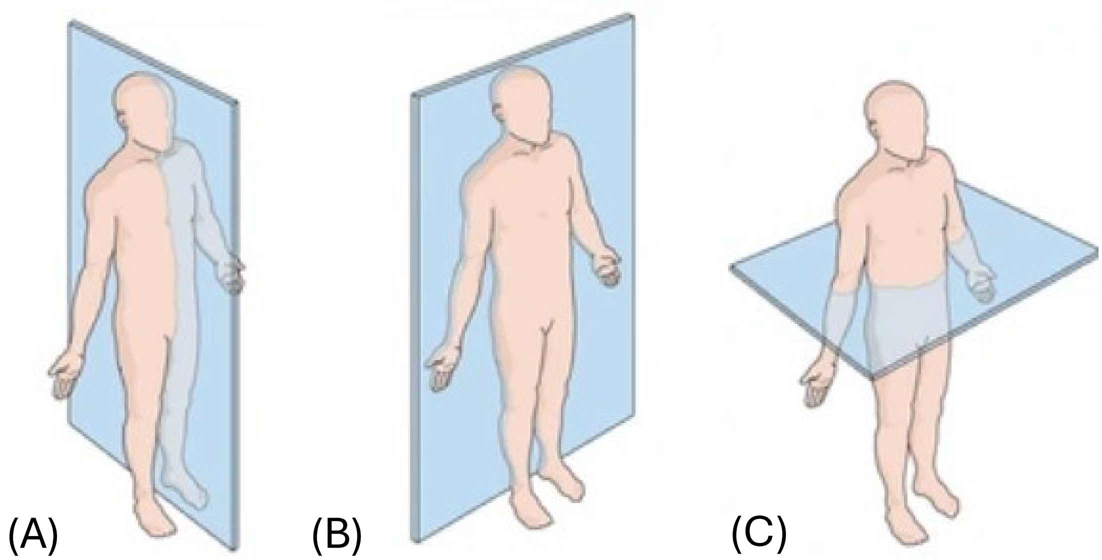


Figure 2-1: Anatomical reference planes (Saurabh, 2019)

The resulting coordinate system is defined by three axes: the anteroposterior axis, the mediolateral axis, and the craniocaudal (or longitudinal) axis (Figure 2-2).

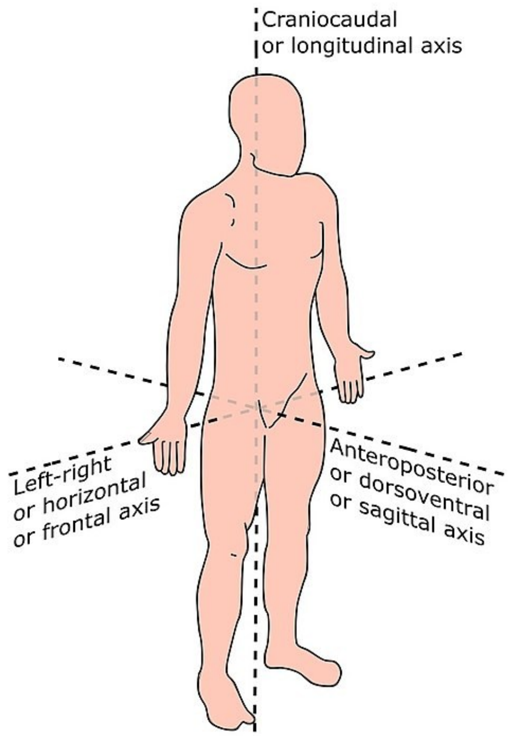


Figure 2-2: Anatomical axes

### 2.1.2 The spine

The spine is subdivided into five functional regions (Figure 2-3): cervical (C1-C7), thoracic (T1-T12), lumbar (L1-L5), sacral (S1-S5, fused), and coccygeal (4 fused vertebrae). It fulfills multiple essential roles, including structural support, load transfer, protection of the spinal cord, and ensuring both stability and mobility of the body.

#### 2.1.2.1 The pelvis

The pelvis, composed of the iliac bones, sacrum, and coccyx, plays a central role in transferring body weight to the lower limbs and ensuring body stability. It also protects abdominal and pelvic organs, contributes to locomotion, and facilitates childbirth in women. The sacrum and coccyx articulate with the iliac bones through the sacroiliac and sacrococcygeal joints, while the acetabulum, formed by the fusion of the ilium, ischium, and pubis, allows articulation with the femur (Figueroa et al., 2025).

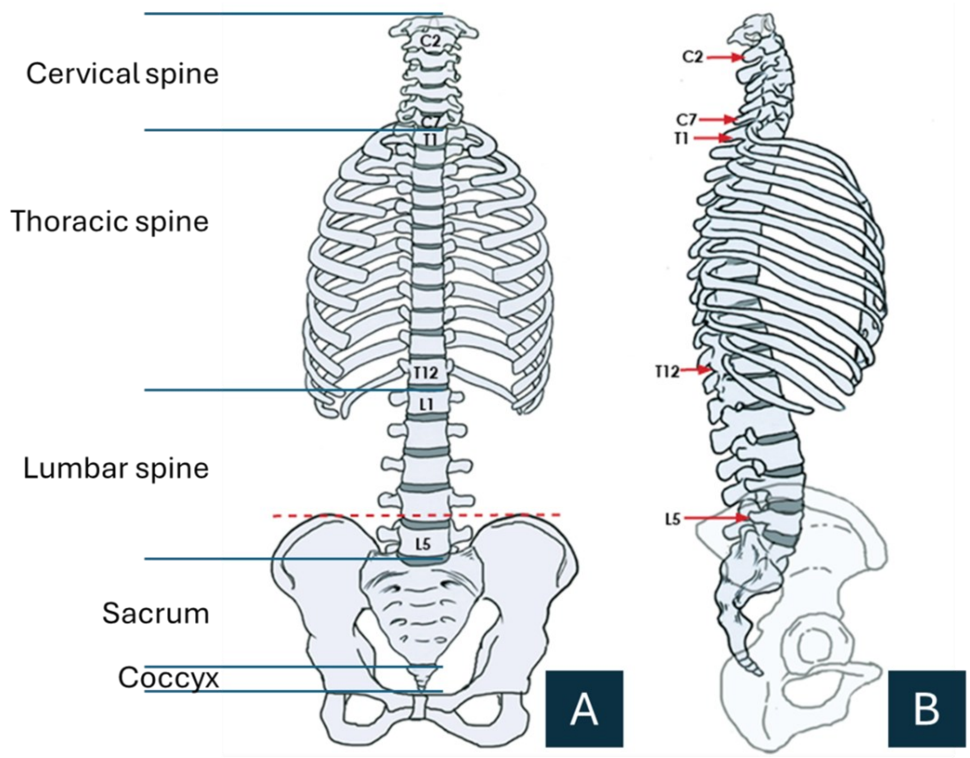


Figure 2-3: Subdivision of the spine (A) Coronal plane, (B) Sagittal plane, adapted from (O'Brien et al., 2005)

### 2.1.2.2 Intervertebral discs

Intervertebral discs are located between vertebrae, allowing spinal mobility while absorbing and distributing compressive loads (Figure 2-4). Each disc is composed of a gelatinous, hydrophilic nucleus pulposus surrounded by a fibrous annulus fibrosus primarily composed of type I collagen (Raj, 2008).

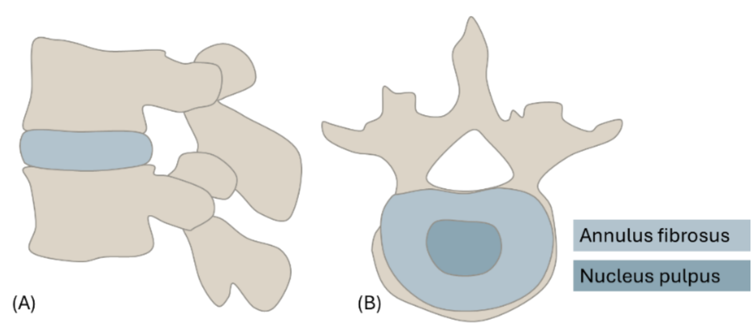


Figure 2-4: Intervertebral disc position and composition. (A) Sagittal plane, (B) Transverse plane.

### 2.1.2.3 Rib cage

The main function of the rib cage is to protect vital organs such as the heart, lungs and main arteries from external compression, which partly explains the limited mobility of the thoracic spine.

The rib cage is anchored posteriorly to the twelve thoracic vertebrae, extends laterally through the ribs, and closes anteriorly with the sternum — a flat, elongated bone located at the centre of the anterior thorax, and ending with the xiphoid process (Figure 2-5).

There are usually twelve ribs on each side. Based on their anterior attachment, ribs are classified into three groups:

- *True ribs* (T1 to T7): directly connected to the sternum via their own costal cartilage.
- *False ribs* (T8 to T10): indirectly connected to the sternum through the costal cartilage of the rib above.
- *Floating ribs* (T11 and T12): not connected to the sternum at all, with their anterior ends free within the abdominal musculature.

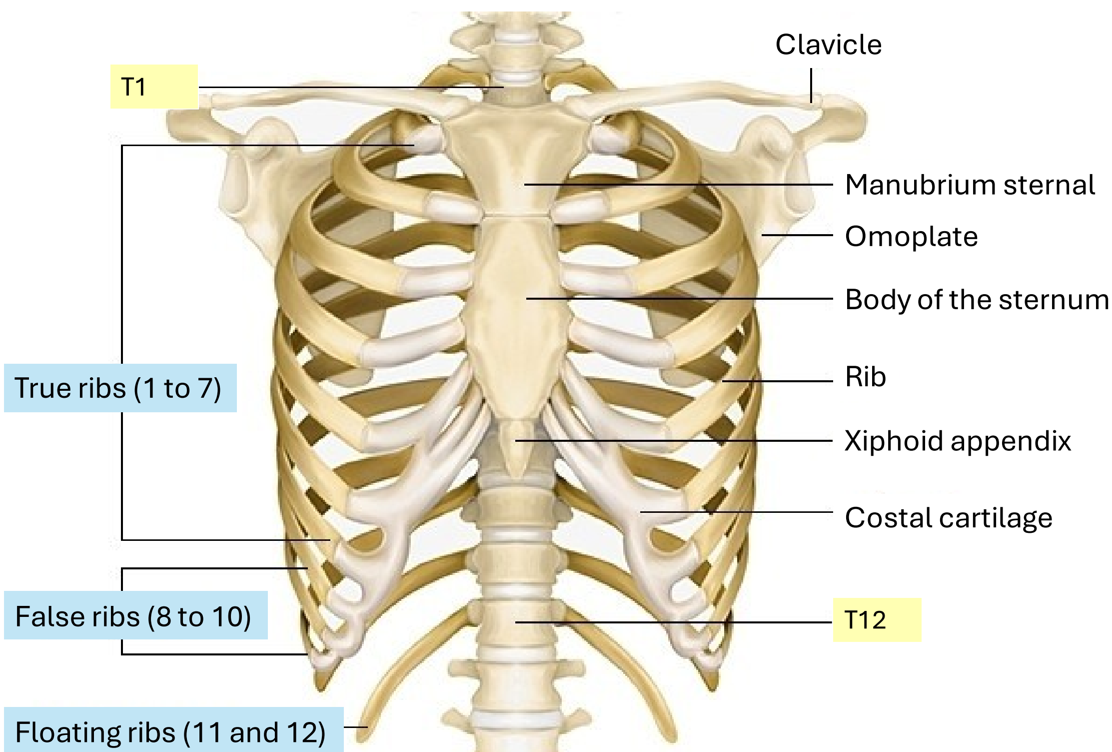


Figure 2-5: Anatomy of the thoracic cage, adapted from Larousse encyclopaedia

### 2.1.2.4 Natural curves of the spine

In a healthy spine, there is no curvature in the coronal plane and no vertebral rotation in the transverse plane. However, four natural curves exist in the sagittal plane, two lordosis (cervical, lumbar) and two kyphosis (thoracic, sacro-coccygeal) (Figure 2-6).

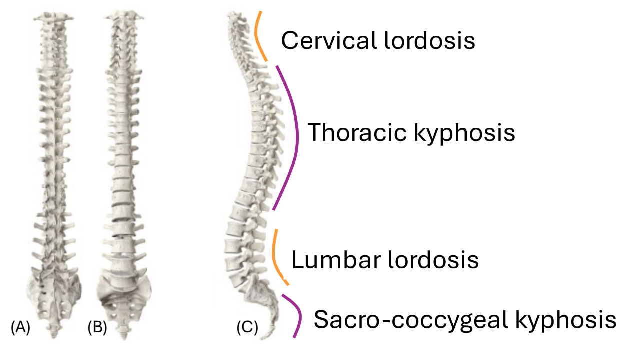


Figure 2-6: Natural curves of the spine, (A) Coronal plane, postero-anterior view, (B) Coronal plane antero-posterior view, (C) Sagittal plane

### 2.1.2.5 Ligaments of the lumbar and thoracic spine

Ligaments are bands of connective tissue rich in collagen fibres. They exist in different shapes and sizes and play a crucial role in stabilizing joints. In the spine, they connect adjacent bones and help maintain their relative position during body movements.

#### 2.1.2.5.1 Ligaments of the lumbar spine

The ligaments of the lumbar spine (Figure 2-7) are the densest and strongest in the spinal column. The spinous processes are connected by the supraspinous and interspinous ligaments, while the transverse processes are connected by the intertransverse ligaments (Oliver & Middleditch, 1991).

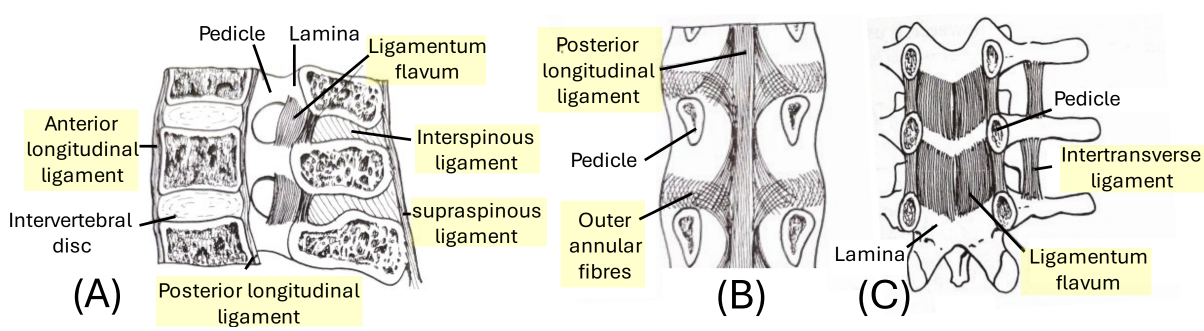


Figure 2-7: Ligaments in the lumbar region, (A) Sagittal plane, (B) Posterior longitudinal ligament, (C) Coronal aspect of ligamenta flava. Adapted from (Oliver & Middleditch, 1991)

#### 2.1.2.5.2 Ligaments of the thoracic spine

The ligamenta flava, thicker at the thoracic level, connect adjacent vertebral laminae and form the posterior boundary of the intervertebral foramen. Composed of elastic fibers, they limit flexion and help restore upright posture. Their elasticity also prevents folding that could compress the dura mater (Oliver & Middleditch, 1991).

The articular capsules of the thoracic zygapophyseal joints attach to the articular processes of adjacent vertebrae.

### 2.1.2.6 Muscles

The back muscles (Henson et al., 2023) are categorized into three groups. The deep intrinsic muscles, known as the transversospinalis group (semispinalis, multifidus and rotatores), contribute to spinal stability, proprioception, and balance. The superficial muscles (splenius capitis and splenius cervicis) are primarily involved in neck and shoulder movements. The intermediate muscles, forming the erector spinae group (longissimus, iliocostalis and spinalis), support flexion, extension, and stabilization of the spine, and assist with thoracic movements.

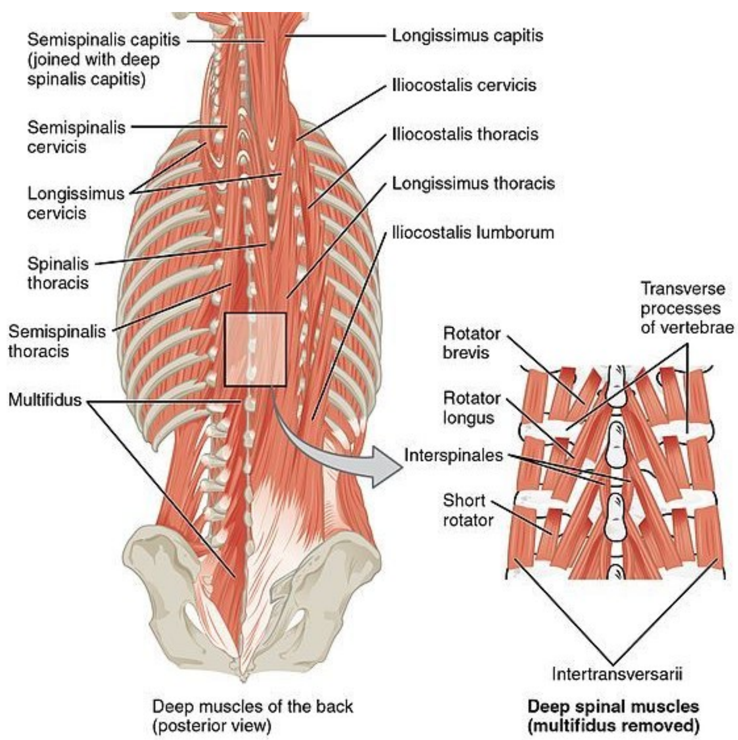


Figure 2-8: Deep muscles of the back (Left), Deep spinal muscles (multifidus removed) (Right), adapted from (Henson et al., 2023)

## 2.2 Biomechanics of the spine

Understanding spinal biomechanics is essential in the context of VBT, as this surgical technique aims to modulate growth through controlled mechanical loading of the spine.

### 2.2.1 Movements of the spine

Each spinal region allows specific types of movement depending on its anatomical features (Figure 2-9):

- Flexion/extension mainly occurs in the cervical and lumbar regions, which are highly mobile. In contrast, the thoracic spine, constrained by the rib cage, allows only limited flexion/extension
- Rotation in the transverse plane occurs primarily in the cervical and thoracic spines. Lumbar rotation is highly restricted due to the sagittal orientation of the facet joints
- Lateral flexion (side bending) in the coronal plane occurs across all spinal regions, with relatively even contribution

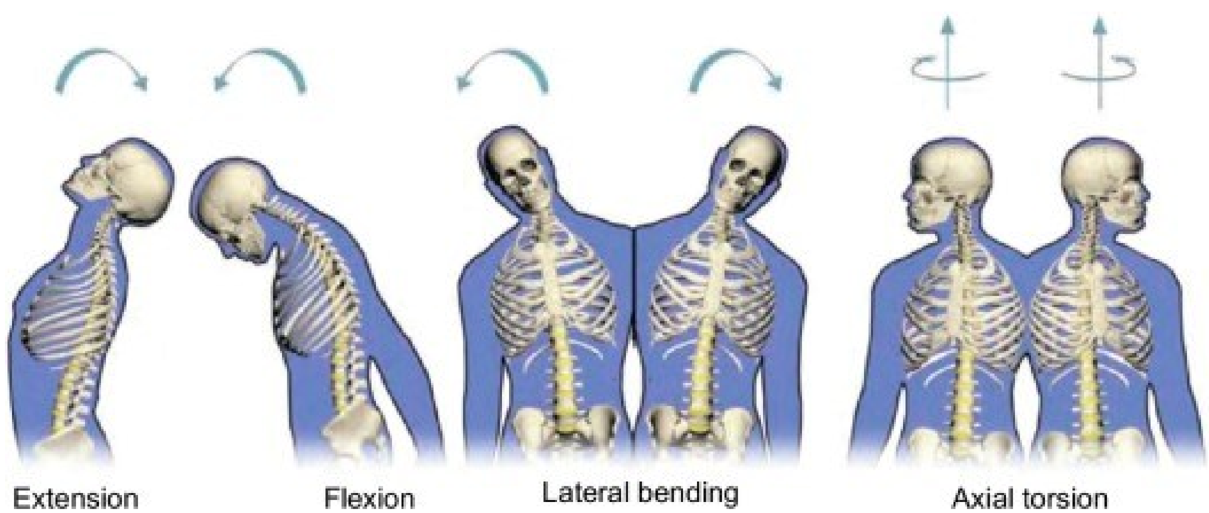


Figure 2-9: Movements of the spine, adapted from (Friis et al., 2017)

### 2.2.2 Loading of the spine

The spine's passive (vertebrae, ligaments, discs, facets) and active (muscles) structures work together to maintain stability and ensure mobility, while constantly supporting compressive forces, even in a neutral standing position.

The magnitude of vertebral loading varies depending on the spinal level and the sagittal alignment (Bruno et al., 2017). For example, increased thoracic kyphosis (TK) leads to higher compressive loads on the vertebrae. However, the loads are always higher in the lumbar spine.

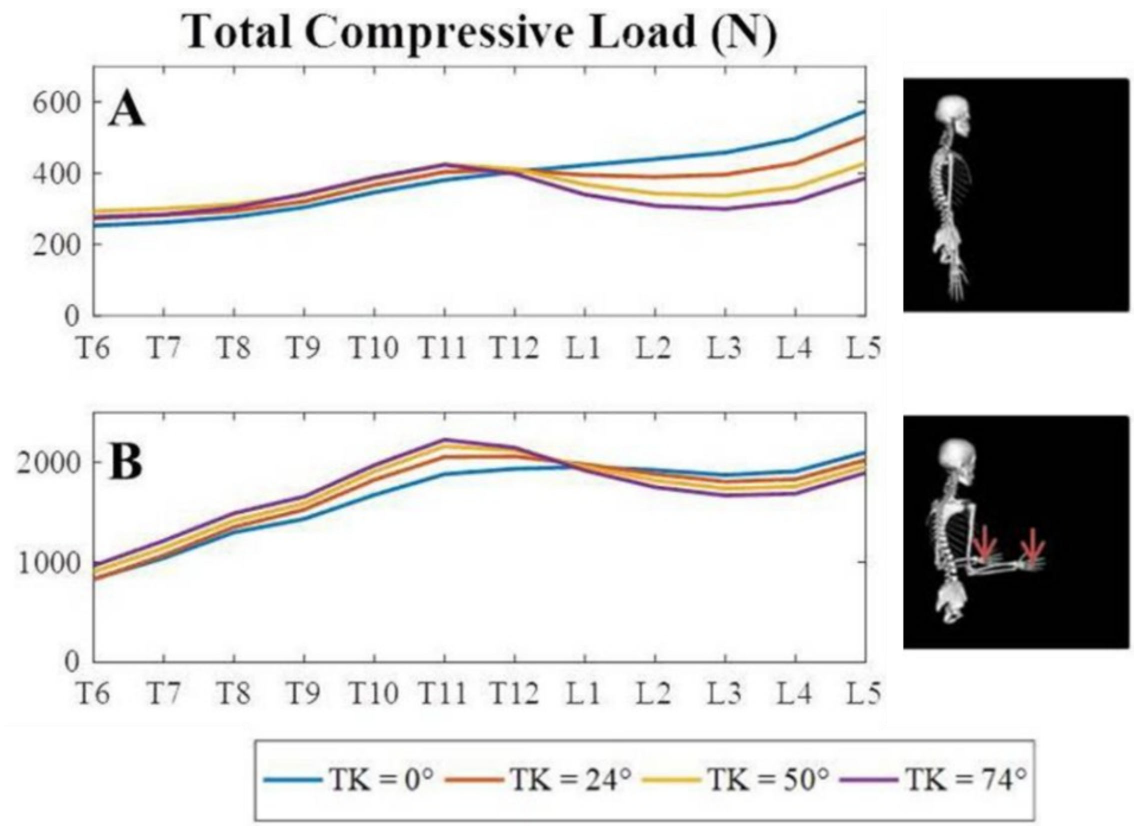


Figure 2-10:Variation in vertebral compressive loading, A: Normal standing position, B: Standing position while carrying an eccentric load (Bruno et al., 2017)

During daily activities, compressive loads typically peak at the thoracolumbar junction (T11-L1), decrease in the mid-lumbar region, then increase again in the lower lumbar spine (Bruno et al., 2017). These loading patterns are particularly relevant in VBT, as they directly influence both the immediate intraoperative correction and the long-term modulation of spinal growth.

## 2.3 Growth of the spine

A detailed understanding of spinal growth mechanisms is critical for the planning and optimization of growth-modulating treatments like VBT. In particular, the distribution and rate of longitudinal growth along the spine determine both the potential for correction and the expected evolution over time after surgery.

### 2.3.1 Mechanisms of vertebral growth

Bone formation in the spine begins early during fetal development, predominantly through a process called endochondral ossification. In this process, new bone forms within a cartilaginous model (Brinker & O'Connor, 2008). This mechanism governs both prenatal vertebral formation and postnatal longitudinal growth, which occurs at multiple growth centers located at the vertebral endplates, the ring apophyses, and the articular process caps.

### 2.3.2 Anatomy and function of the epiphyseal growth plate

The growth plate (physis) is a cartilaginous structure responsible for longitudinal growth. It is composed of distinct layers of chondrocytes surrounded by an extracellular matrix, where cells progress through several maturation stages before being replaced by bone tissue (Ağırdil, 2020). The chondrocytes successively transition from a resting phase, to proliferation, pre-hypertrophy, hypertrophy, and finally a terminal phase leading to cell death and bone replacement (Voller et al., 2020) (Figure 12). In the resting phase, chondrocytes remain relatively inactive, while in the proliferative phase they undergo rapid cell division. As they progress to the pre-hypertrophic and hypertrophic phases, chondrocytes enlarge considerably and modify their extracellular environment, before ultimately ceasing their activity and being replaced by bone tissue. This highly organized maturation process ensures progressive elongation of the vertebrae during growth.

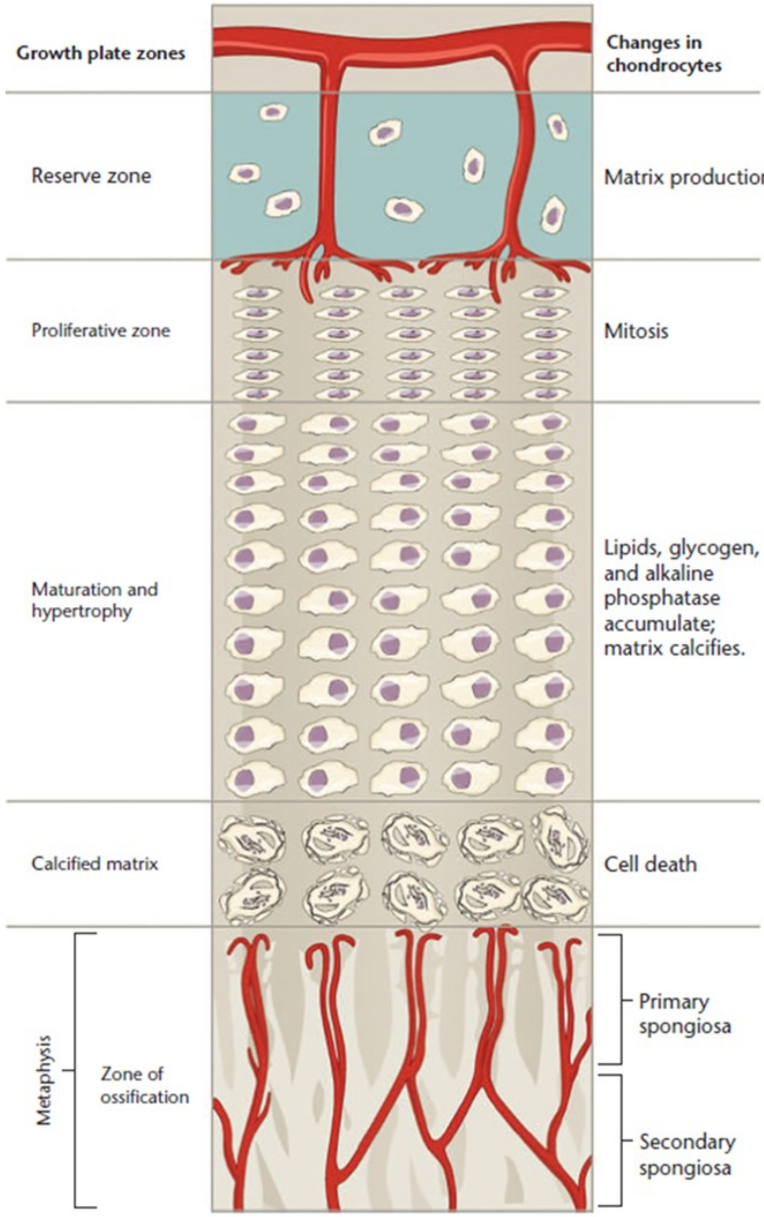


Figure 2-11: Zones of chondrocyte maturation in growth plate (Ağırdil, 2020).

### 2.3.3 Longitudinal growth of the spine

The spine measures around 19 cm at birth and reaches an average length of 47 cm in adulthood (A. DiMeglio et al., 2011). Longitudinal growth occurs symmetrically at the upper and lower vertebral endplates and continues until skeletal maturity, with variations in growth rate throughout childhood and adolescence (Sanders, 2015).

Between birth and one year of age, trunk growth is particularly rapid. The spine lengthens by around 10 cm between birth and age 5, representing a 52% increase in length (Sanders, 2015). This rapid growth may explain the marked progression of certain congenital or infantile spinal deformities during this period. Between the ages of 5 and the onset of puberty, spinal growth continues steadily at a rate of ~5 cm/year, accounting for about 20% of total spinal growth (Sanders, 2015). During puberty, growth accelerates considerably, with the spine gaining up to 10 cm over a 3–4-year period, often two to three times the rate observed during childhood. This pubertal growth spurt occurs earlier in girls but tends to be more pronounced in boys, and primarily affects the trunk and spine rather than the lower limbs (Sanders, 2015). This variability in growth velocity must be carefully considered when selecting the optimal timing for VBT surgery (Sanders, 2015).

### 2.3.4 Growth modulation principles

The principle of growth modulation is at the core of growth-friendly surgical techniques such as VBT. These techniques aim to correct spinal deformities by applying controlled mechanical loads to modulate vertebral growth asymmetrically.

#### 2.3.4.1 Hueter-Volkmann principle

The Hueter-Volkmann principle phenomenologically describes the effect of mechanical loading on the growth rate of the physis. It states that the loading applied to the growth plates influences the rate of bone formation locally. It can be summarized as follows: "In the skeletal immature individuals, bone growth tends to slow down in areas subjected to increased pressure, while it is relatively enhanced in areas experiencing reduced pressure or tensile forces" (Mehlman et al., 1997).

This principle has been mathematically formalized (Stokes, 2002; Stokes et al., 2006):

$$G = G_m * (1 + \beta * (\sigma_m - \sigma))$$

where $G$ is the actual local growth rate, $G_m$ is the mean baseline growth under normal stress, $\sigma$ is the actual local stress applied to the growth plate (compression negative), and $\sigma_m$ is the mean physiological (baseline) stress on growth plate. $\beta$ is the sensitivity factor to mechanical stress (ranging between 1,5 $MPa^{-1}$ and 1,7 $MPa^{-1}$ (Cobetto, Aubin, et al., 2018b; Cobetto et al., 2020; Cobetto et al., 2025; Martin et al., 2023; Stokes et al., 2006).

While this model appropriately captures the role of axial stresses in growth modulation, it does not account for the possible contribution of non-axial or complex stress environments, which may also influence local growth (Lin et al., 2009).

### 2.3.4.2 Loading and growth modulation

#### 2.3.4.2.1 Static loading

According to the Hueter-Volkman principle, local growth at the physis decreases under compressive forces and increases under reduced compressive forces. At the epiphyseal growth plates, this effect is partly explained by morphological changes in the chondrocytes involved in endochondral ossification (Farnum et al., 2000). Compression has been shown to particularly affect the hypertrophic zone of the physis (Stokes et al., 2002), where chondrocytes exhibit a marked reduction in cell volume. For example, under 15% compression, chondrocyte volume decreases across all layers, with the most pronounced effect observed in the hypertrophic zone (Amini et al., 2010). Since hypertrophic chondrocytes play a key role in ossification, reduced cell size slows down bone formation.

Surgical and non-surgical devices designed to correct scoliosis without spinal fusion leverage this principle. By modifying static loading conditions, these techniques promote asymmetric bone growth and progressive correction of vertebral wedging through differential growth (Photopoulos et al., 2024).

#### 2.3.4.2.2 Dynamic loading

Compared to static loading, dynamic loading generates significantly lower lateral and volumetric stresses within chondrocytes (Zimmermann et al., 2017). The intermittent nature of dynamic forces allows cells to better adapt, limiting deformation and reducing the inhibitory effect on growth. As a result, the impact of dynamic loading on local vertebral growth is generally less pronounced than that of sustained static loading.

### 2.3.5 Skeletal maturity and growth rate

The assessment of skeletal maturity is a crucial step in planning growth-modulating VBT treatment, as it provides essential information on the patient’s remaining growth potential and helps determine the optimal timing for surgery.

### 2.3.5.1 Assessment of skeletal maturity

#### 2.3.5.1.1 Risser index

The Risser index evaluates skeletal maturity based on the progression of ossification of the iliac crest apophysis, visible on pelvic radiographs. It is graded from 0 (no ossification) to 5 (complete ossification and fusion of the apophysis to the iliac crest) (Figure 2-12) (Risser, 1958). Although frequently used, the Risser index reflects skeletal changes that occur relatively late, after the peak of pubertal growth.

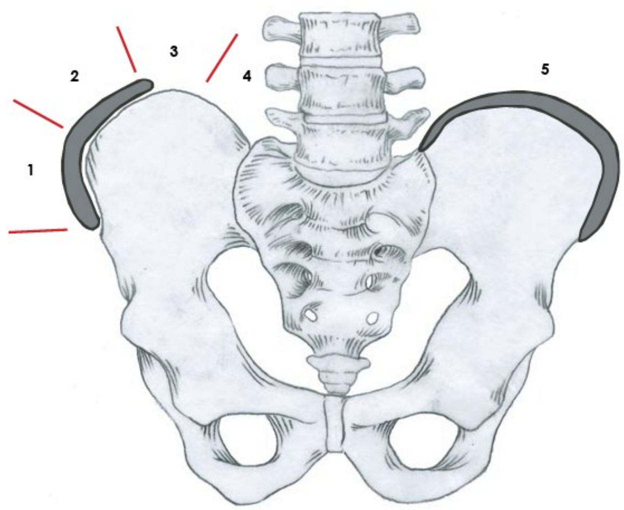


Figure 2-12: US Evaluation of the Risser index (O'Brien et al., 2005)

#### 2.3.5.1.2 Sanders score

The Sanders score (SS) is a more detailed and predictive indicator of skeletal maturity, based on the progressive ossification of the hand and wrist bones. It ranges from 1 (juvenile stage with slow growth) to 8 (skeletal maturity), and captures the different phases of skeletal development before, during, and after the pubertal growth spurt (Table 2-1) (Sanders et al., 2008).

This scoring system provides valuable information for estimating remaining growth potential and is particularly relevant for growth-dependent treatments such as VBT. Unlike the Risser index, which reflects changes occurring after the peak growth phase, the Sanders score captures skeletal changes that occur before and during peak height velocity. It thus allows for a more accurate identification of the onset and peak of the adolescent growth spurt, providing a gradual and precise assessment of skeletal development — a crucial factor for planning growth-modulating treatments (Yucekul et al., 2025).

The main characteristics associated with each stage are summarized in Table 1. Representative images illustrating the extremes of this classification (SS1 and SS8) are shown in Figure 16.

| **Sanders score (SS)** | **Stage** | **Key features** |
|---|---|---|
| 1 (Figure 2-13, A) | Juvenile slow | Digital epiphyses are not covered. |
| 2 | Preadolescent slow | All digital epiphyses are covered. |
| 3 | Adolescent rapid – early | The preponderance of digits is capped. The second through fifth metacarpal epiphyses are wider than their metaphyses. |
| 4 | Adolescent rapid – late | Any of distal phalangeal physes are clearly beginning to close (see detailed description in the text). |
| 5 | Adolescent steady – early | All distal phalangeal physes are closed. Others are open. |
| 6 | Adolescent steady – late | Middle or proximal phalangeal physes are closing. |
| 7 | Early mature | Only distal radial physis is open. Metacarpal physeal scars may be present. |
| 8 (Figure 2-13, B) | Mature | Distal radial physis is completely closed. |

Table 2-1: Sanders score and associated key features

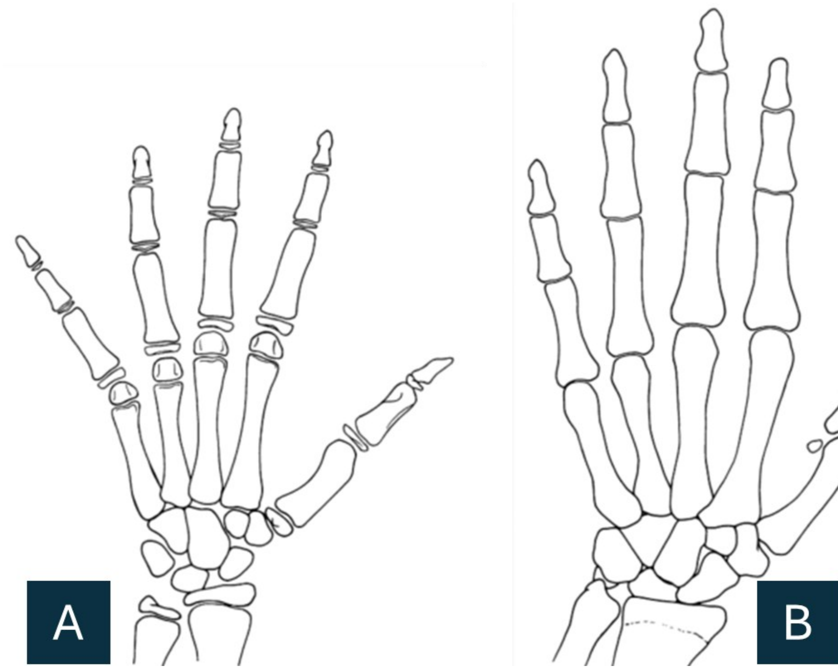


Figure 2-13: Comparison of the level of ossification between a Sanders score of 1 (A) versus a Sanders score of 8 (B) Adapted from (Sanders et al., 2008)

**2.3.5.1.3 Triradiate cartilage**

The triradiate cartilage (TRC), located at the pelvis, is another indicator commonly used to assess skeletal maturity. Its status — whether open, closing, or closed — provides valuable information about the patient's remaining growth potential. An open TRC has been associated with an increased risk of scoliosis progression or failure of brace treatment (Ryan et al., 2007). Figure 2-14 illustrates the progressive closure of the TRC in three different patients.

Although TRC evaluation alone is not sufficient to determine skeletal maturity, it remains a useful complementary tool in borderline or uncertain cases.

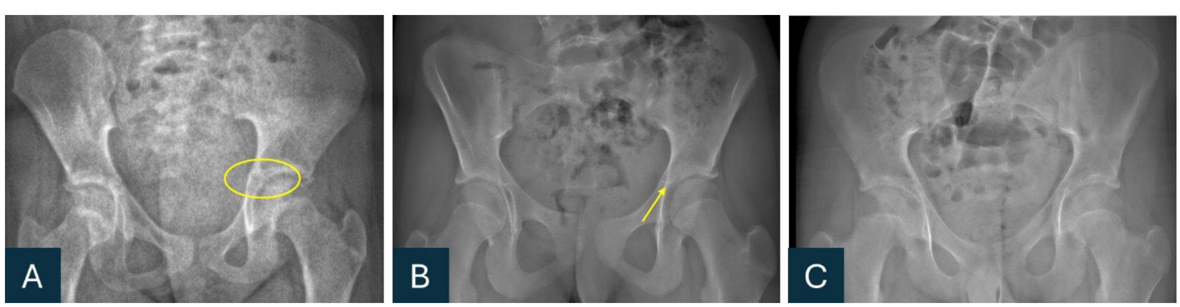


Figure 2-14: Progressive closure of the TRC on three different patients. (A) open, (B) closing, (C) closed.

### 2.3.5.2 Assessment of growth rate in relation to skeletal maturity

#### 2.3.5.2.1 Phase duration and growth rate for each Sanders score

An unpublished study by Boeyer et al., entitled *"Understanding the Tempo of Sanders Staging to Guide Successful AIS Treatments – The Missing Link"* (2024), evaluated the standing height difference between consecutive Sanders Scores (SS).

Anthropometric and radiographic data from two large semi-longitudinal databases were retrospectively reviewed. Inclusion criteria were (1) diagnosis of AIS, and (2) at least two distinct left hand-wrist radiographs with corresponding standing height measurements. The amount of height gained (cm) and the duration of time (months) between two consecutive Sanders stages were calculated

A total of 328 patients met these criteria, a with an average follow-up period of 32.2 months (range: 4.1 to 91.3 months). The greatest mean changes in standing height were observed between SS 1-2 (9.0 cm), SS 2-3 (8.6 cm), and SS 3-4 (4.7 cm), while growth during later stages was much less pronounced (<2 cm) (Figure 2-15).

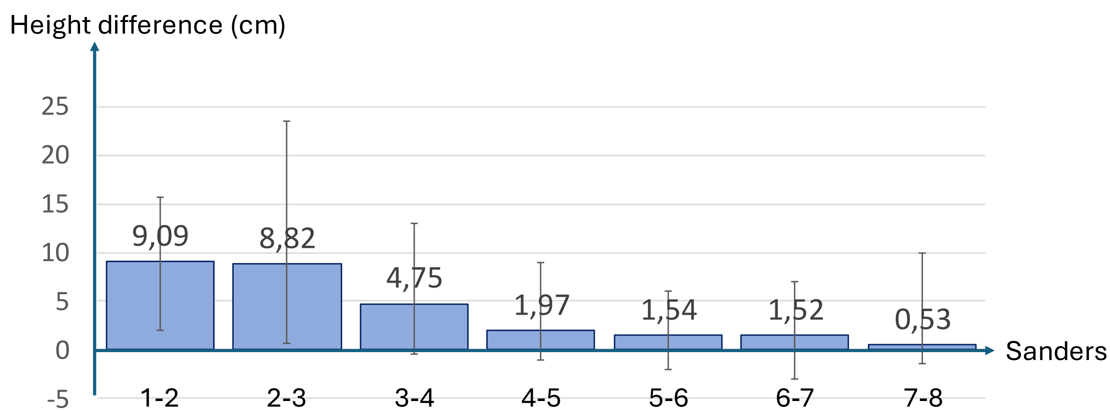


Figure 2-15: Mean height gain between consecutive Sanders stages

The same study also reported the average duration of each Sanders stage (Figure 19), although it did not differentiate between SS 3A and 3B (Figure 2-16).

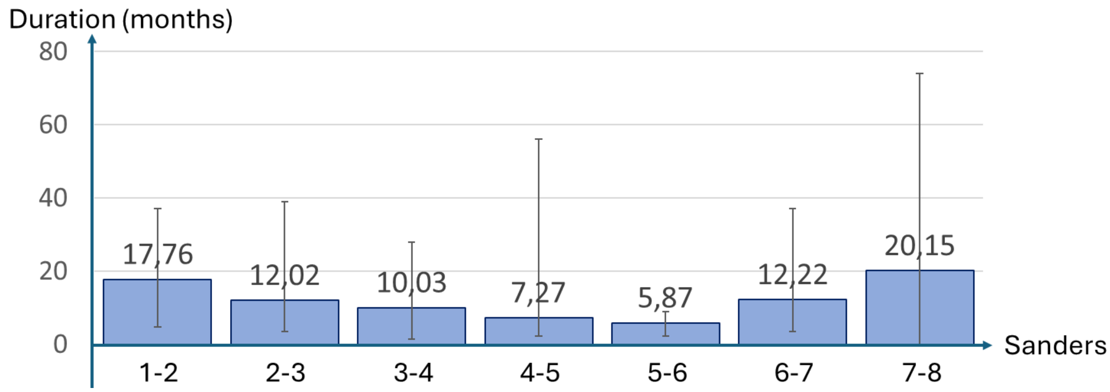


Figure 2-16: Average duration (months) between consecutive Sanders Scores.

(Boeyer, 2023) emphasized the clinical importance of distinguishing between SS 3A and 3B to better predict residual growth. The duration of each Sanders stage — including the separation between SS3A and SS3B — was determined, along with the corresponding growth rates. Their findings are summarized in Figure 2-17.

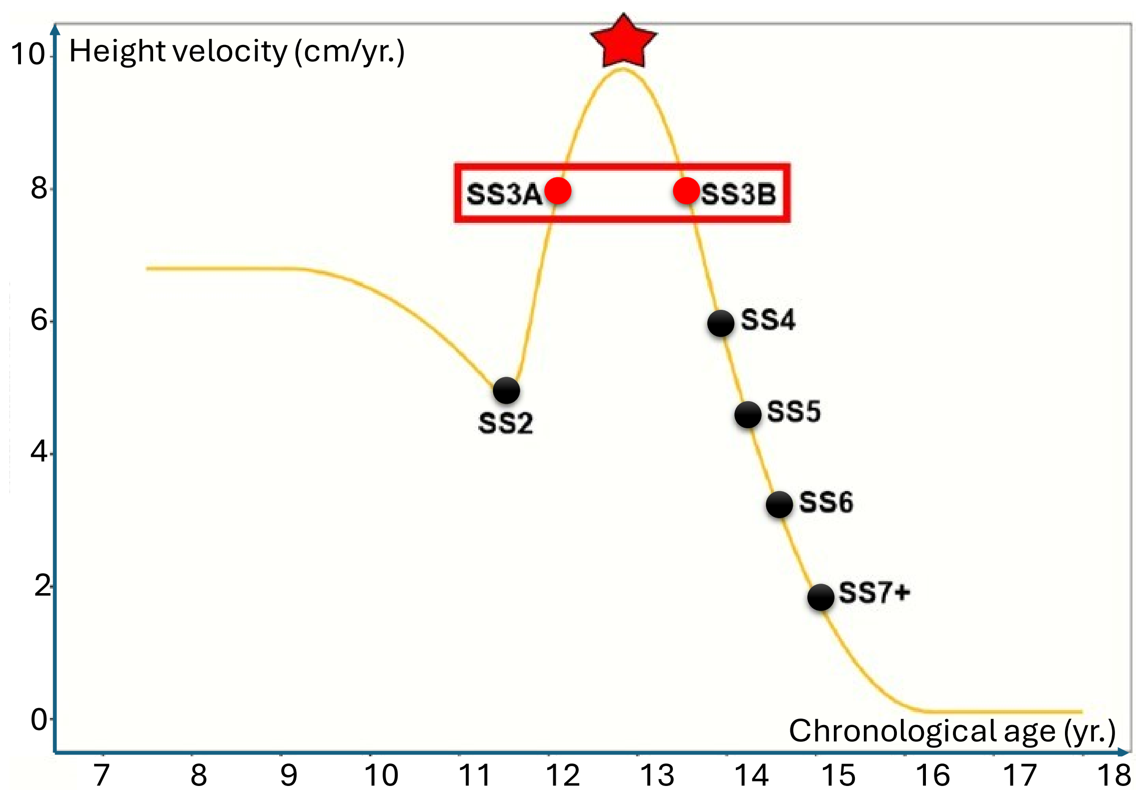


Figure 2-17: Height velocity for different Sanders stages, differentiating between SS 3A and 3B

From this graph was extracted the values gathered in Table 2-2.

Table 2-2: Phase duration and growth rate of each Sanders stage

| Sanders transition | 2 --> 3 | 3A --> 3B | 3B --> 4 | 4 --> 5 | 5 --> 6 | 6 --> 7 | 7 --> 8 |
|---|---|---|---|---|---|---|---|
| Duration (months) | 8 | 15 | 4 | 4 | 4 | 4 | 12 |
| Global growth rate (mm/yr.) | 50 | 92 | 79 | 60 | 46 | 32 | 19 |

From the global growth rate, the spinal growth rate was extracted. Using Figure 2-18 (Dimeglio et al., 2011), 42% of the total growth was associated to the growth of the trunk for SS 2 to 3A, it was calculated at 58% for SS 3B to 4 and 71% for SS 5 to 7+, giving the results summarized Table 2-3.

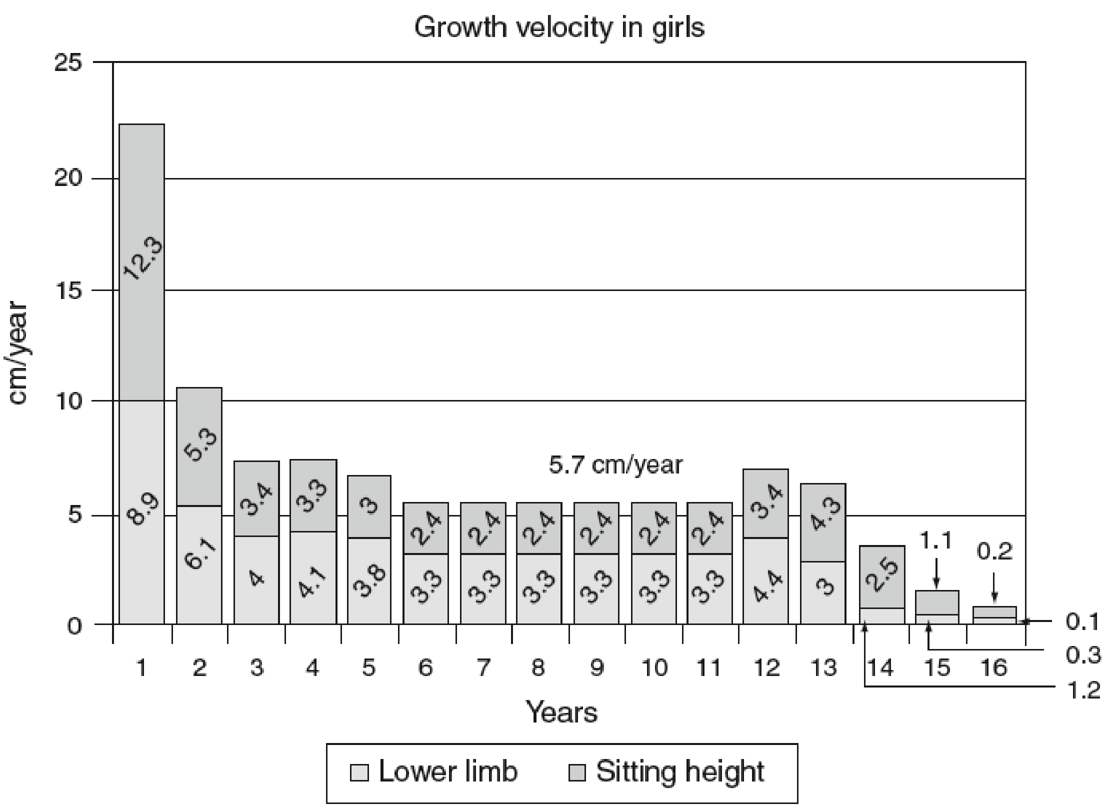


Figure 2-18: Growth velocity of sitting height and lower limb (1–16 years: girls), extracted from (Dimeglio et al., 2011)

Table 2-3: Spinal growth rates for each Sanders transition

| Sanders transition | 2 --> 3 | 3A --> 3B | 3B --> 4 | 4 --> 5 | 5 --> 6 | 6 --> 7 | 7 --> 8 |
|---|---|---|---|---|---|---|---|
| Spinal growth rate (mm/year) | 27,09 | 37,17 | 40,31 | 30,74 | 27,3 | 17,85 | 6,65 |

#### 2.3.5.2.2 Modelling of spinal growth over a 24-month period

Based on the available data, it is possible to estimate the equivalent spinal growth expected over a 24-month period, depending on the SS at the time of surgery. The simulation model considers a sequence of growth phases, with each phase corresponding to a specific SS duration and associated growth rate (Cobetto et al., 2025; Gay et al., 2025; Martin et al., 2023; Raballand et al., 2023). The total spinal growth over 24 months is therefore calculated as the sum of the growth achieved during each SS phase, weighted according to its respective duration within the 24-month timeframe.

To estimate spinal growth over a 24-month period following surgery, the model applies a stepwise calculation based on the Sanders Score (SS) at the time of surgery and the corresponding durations and growth rates of subsequent SS phases.

For example, for a patient evaluated at SS2 at the time of surgery ($P_{SS2}$), the projected spinal growth over 24 months would combine growth (Growth rate : $Tx_{SS2}$) during the remaining duration at SS2 (Duration in months : $D_{SS2}$ ), followed by full phases at SS3A ($D_{SS3A} * Tx_{SS3A}$) and some months (to reach two years in total : $(24 - D_{SS2} - D_{SS3A})$ ) at SS3B, according to:

$$P_{SS2} = D_{SS2} * Tx_{SS2} + D_{SS3A} * Tx_{SS3A} + (24 - D_{SS2} - D_{SS3A}) * Tx_{SS3B}$$

Similarly, for a patient at SS 3A:

$$P_{SS3A} = D_{SS3A} * Tx_{SS3A} + D_{SS3B} * Tx_{SS3B} + (24 - D_{SS3A} - D_{SS3B}) * Tx_{SS4}$$

For later stages:

$$P_{SS3B} = D_{SS3B} * Tx_{SS3B} + D_{SS4} * Tx_{SS4} + D_{SS5} * Tx_{SS5} + D_{SS6} * Tx_{SS6} + (24 - D_{SS3B} - D_{SS4} - D_{SS5} - D_{SS6}) * Tx_{SS7}$$

$$P_{SS4} = D_{SS4} * Tx_{SS4} + D_{SS5} * Tx_{SS5} + D_{SS6} * Tx_{SS6} + D_{SS7} * Tx_{SS7}$$

$$P_{SS5} = D_{SS5} * Tx_{SS5} + D_{SS6} * Tx_{SS6} + D_{SS7} * Tx_{SS7}$$

$$P_{SS6} = D_{SS6} * Tx_{SS6} + D_{SS7} * Tx_{SS7}$$

$$P_{SS7} = D_{SS7} * Tx_{SS7}$$

Estimated spinal growth rates for each Sanders stage evaluated at the time of surgery are presented in Table 2-4.

Table 2-4: Estimated spinal growth rate based on Sanders Score at treatment entry point

| Sanders Score at surgery | Spinal growth rate (mm/yr.) |
|---|---|
| SS 2 | 33,81 |
| SS 3A | 37,43 |
| SS 3B | 21,58 |
| SS 4 | 15,97 |
| SS 5 | 11,43 |
| SS 6 | 7,47 |
| SS 7 | 5,08 |

### 2.3.5.3 Thoracic vs. Lumbar spinal growth

Because the thoracic growth rate is different from the lumbar growth rate, the proportion of the spinal growth rate they each contribute for was assessed using Figure 2-19 (Dimeglio et al., 2011). Between the age of 10- to 15-year-old, 33% of the spinal growth is attributed to the lumbar spine and 67% to the thoracic spine.

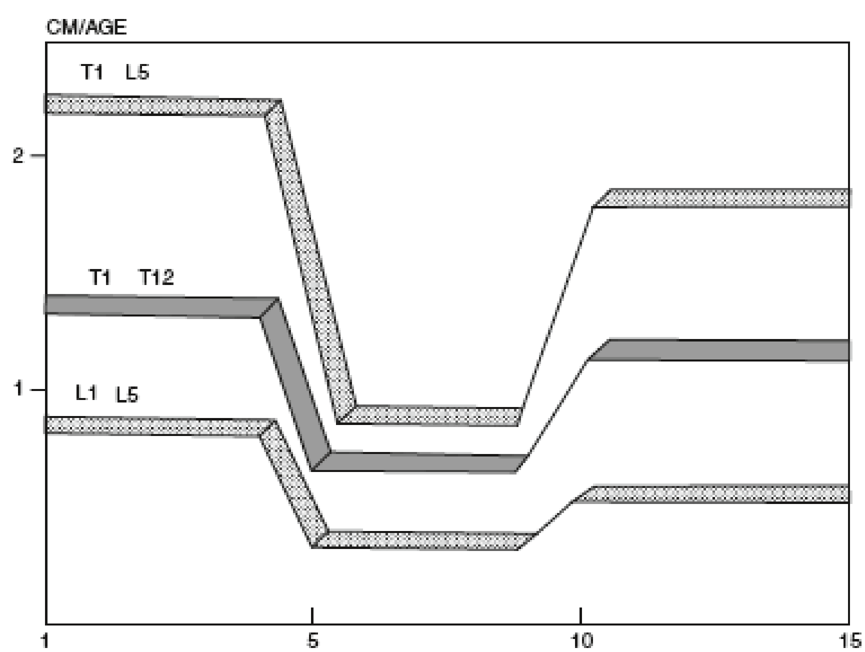


Figure 2-19: Growth velocity of T1–L5, thoracic segment T1–T12, and lumbar segment L1–L5, extracted from (Dimeglio et al., 2011)

The estimated growth rates per vertebra for thoracic and lumbar levels are summarized in Table 2-5.

Table 2-5: Thoracic and lumbar spine growth rates per vertebra for each Sanders Stage at the time of surgery (mm/yr./vertebra)

| Sanders stage at surgery | Thoracic (mm/yr./vertebra) | Lumbar (mm/yr./vertebra) |
|---|---|---|
| SS 2 | 1,80 | 2,13 |
| SS 3A | 2,01 | 2,38 |
| SS 3B | 1,21 | 1,42 |
| SS 4 | 0,89 | 1,05 |
| SS 5 | 0,64 | 0,75 |
| SS 6 | 0,42 | 0,49 |
| SS 7 | 0,28 | 0,33 |

Peak growth rates corresponding to SS 3A/3B were reported at approximately 1.2 mm/year/vertebra for the thoracic spine and 1.6 mm/year/vertebra for the lumbar spine (Alain Dimeglio et al., 2011) and 1.3 mm/year/vertebra for the thoracic spine and 1.6 mm/year/vertebra for the lumbar spine in another study (Aldegheri & Agostini, 1993).

## 2.4 Pediatric idiopathic scoliosis

### 2.4.1 Scoliosis

#### 2.4.1.1 Definition

Pediatric idiopathic scoliosis refers to a spinal deformity of unknown origin occurring during childhood or adolescence. Scoliosis is a three-dimensional spinal deformity involving lateral curvature, vertebral rotation, and alterations in the sagittal profile. When diagnosed before the age of 10, it is termed early-onset scoliosis, irrespective of etiology (Sauri-Barraza, 2023). Between ages 10 and 18, idiopathic cases are classified as Adolescent Idiopathic Scoliosis (AIS) (Menger & Sin, 2025), the most prevalent form, affecting approximately 1% to 4% of adolescents (Cheng et al., 2015).

AIS is characterized by deformities in all three anatomical planes (Figure 2-20):

- **Coronal plane**: Lateral deviation with one or more curves, often accompanied by rib cage asymmetry.
- **Sagittal plane**: Alteration of normal spinal curvatures, such as hypokyphosis.
- **Transverse plane**: Vertebral rotation leading to torsion and potential rib prominence.

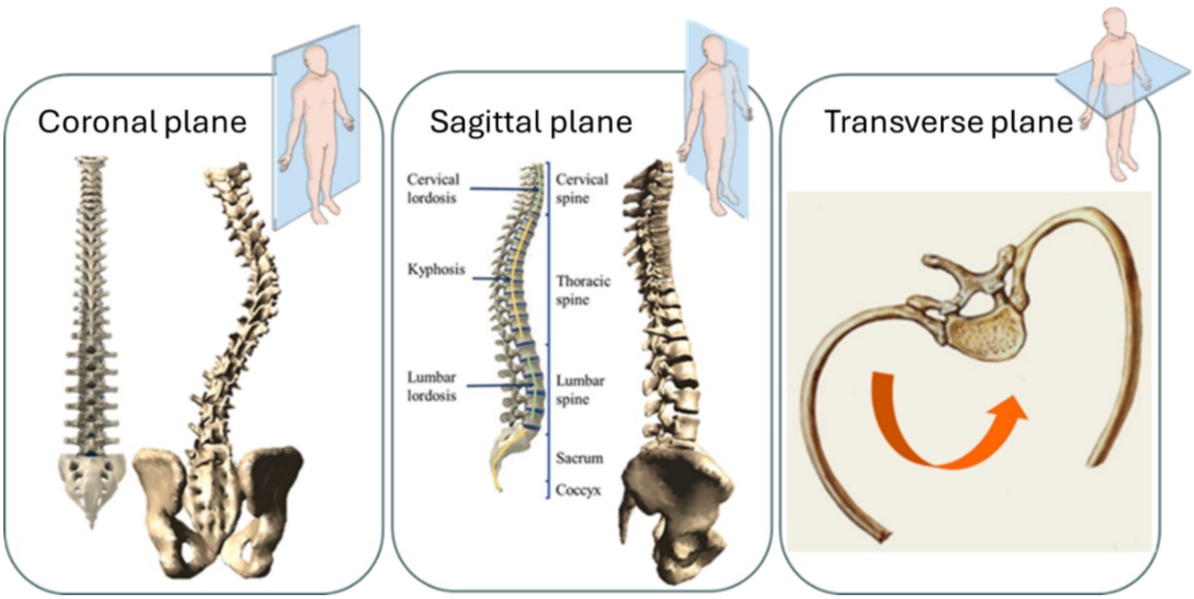


Figure 2-20: Scoliosis results on the spine in the three anatomical planes

This deformation leads to asymmetry in spinal balance and, in the longer term, to pain, neurological disorders and cardiopulmonary problems (Weiss et al., 2016).

The pathological curve is defined by:

- **Apical vertebra**: The most laterally deviated vertebra from the central sacral vertical line.
- **End vertebrae**: The most tilted vertebrae at the upper and lower ends of the curve.

### 2.4.1.2 Measurement of the deformity

The Cobb angle is the standard metric for quantifying scoliosis severity. It is measured on standing posteroanterior radiographs by drawing lines parallel to the superior endplate of the upper end vertebra and the inferior endplate of the lower end vertebra; the angle between these lines represents the curve magnitude ( Figure 2-21). Variations less than 5° are generally considered within the margin of error.

Cobb angles can also be measured in the sagittal plane to assess thoracic kyphosis and lumbar lordosis. Additionally, flexibility radiographs — obtained in side-bending, traction, or prone positioning — are often used to evaluate curve flexibility by measuring the Cobb angle in these different positions, which provides an estimate of the curve's reducibility and helps inform surgical decision-making.

These measurements are crucial for assessing curve progression, evaluating flexibility, and determining treatment strategies, including the suitability for VBT.

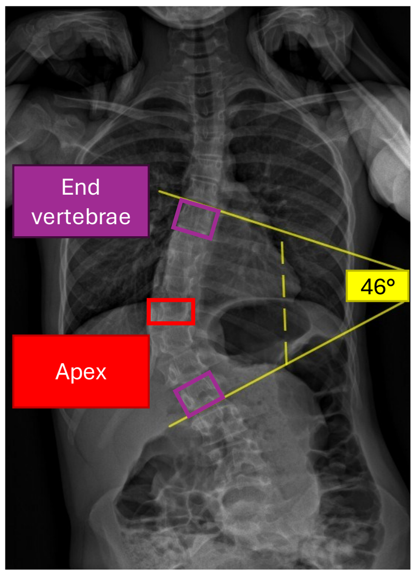


Figure 2-21: TL/L Cobb angle measured in the Coronal plane

#### 2.4.1.3 Lenke's classification

The Lenke classification system is widely utilized for categorizing AIS, particularly in surgical planning. It comprises three components:

1. **Curve Type (1–6)**: Determined by the location and structural nature of the curves.
2. **Lumbar Modifier (A, B, C)**: Based on the relationship between the lumbar curve apex and the central sacral vertical line (CSVL).
3. **Sagittal Thoracic Modifier (-, N, +)**: Reflects the sagittal alignment of the thoracic spine, measured by the T5–T12 kyphosis angle.

### 2.4.2 Mechanism of scoliosis progression

The etiology of scoliosis is multifactorial and complex. However, the mechanisms underlying its progression can be partly explained by the Hueter-Volkmann principle (Arkin & Katz, 1956) and the Stokes' vicious circle model (Stokes et al., 2006; Stokes et al., 2002; Stokes et al., 1996). These principles suggest that vertebral growth modulation depends on mechanical loading: compressive forces inhibit growth, while tensile forces — or relatively lower compressive forces compared to adjacent, more heavily loaded regions — promote it.

In scoliosis, there is an asymmetrical distribution of loads along the spine, with increased compression on the concave side and reduced pressure on the convex side. This loading imbalance leads to progressive vertebral wedging, which in turn accelerates the curvature and further perpetuates the deformity.

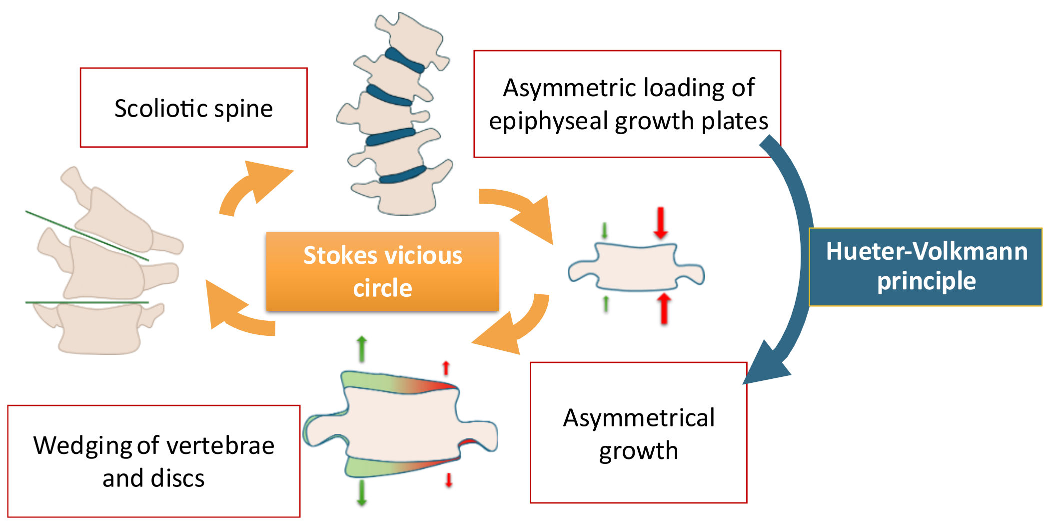


Figure 2-22: Mechanism of scoliosis progression

Clinical studies have shown that a spinal curve measuring 30° at the onset of puberty, or a curve between 20° and 30° progressing by more than 10° per year, is highly predictive of evolution towards the surgical threshold of 45° (Ghanem & Rizkallah, 2020). More recently, further criteria have been identified to predict curve progression, particularly at the peak of pubertal growth. Scoliosis with trunk imbalance, thoracic curves exceeding 40°, or lumbar curves greater than 25° carry a significant risk of progression into adulthood (Angelliaume et al., 2025).

Early identification of these risk factors is critical, as timely non-surgical intervention may prevent curve worsening during growth and ultimately reduce the risk of progression later in life.

### 2.4.3 Non-surgical treatments for scoliosis

Non-surgical management of scoliosis primarily relies on bracing and physiotherapy (Angelliaume et al., 2025). The primary goal of bracing is to stop or slow the progression of the scoliosis deformity. Ideally, bracing may also help reduce curve magnitude and improve spinal balance. While not formally proven, it is generally believed that the Hueter-Volkmann principle may contribute to this effect by modulating vertebral growth through mechanical loading (Guy & Aubin, 2023).

Several studies have shown that bracing can significantly reduce the risk of curve progression toward surgical thresholds in AIS patients identified as high-risk. Its effectiveness is closely related to the duration of daily wear, with greater corrective effects observed with higher compliance (Weinstein et al., 2013).

## 2.5 Vertebral body tethering (VBT)

### 2.5.1 Principle of surgery

VBT is a growth modulation surgical technique that uses a flexible implant, composed of screws and a polyethylene tether, to control scoliosis progression while preserving spinal motion.

During surgery, the patient is positioned in lateral decubitus on the operating table (Figure 2-23), allowing gravity to assist in the initial curve reduction even before instrumentation (Cobetto, Aubin, et al., 2018a).

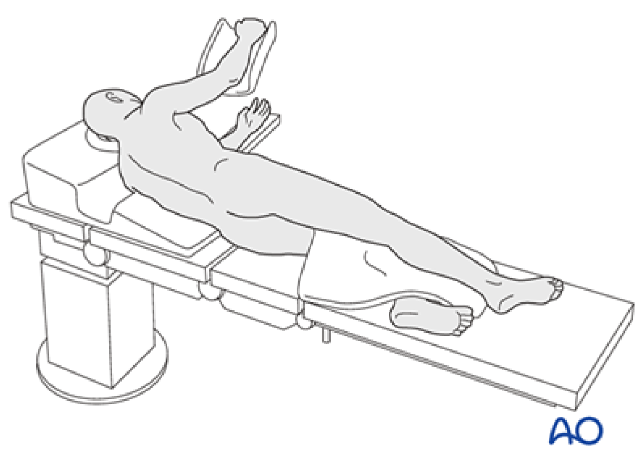

Figure 2-23: Lateral decubitus positioning, from https://surgeryreference.aofoundation.org

The core principle of VBT is to modulate vertebral growth asymmetrically by applying mechanical forces that slow growth on the convex side of the curve while allowing continued growth on the concave side. This strategy aims to gradually correct the deformity over time. This approach can also be seen to reverse the Stokes' vicious cycle of scoliosis progression, where asymmetrical loading perpetuates curve worsening. The flexible cable is placed on the convex side of the deformity, leaving the concave side free (Figure 2-24). Tensioning the tether increases compressive forces on the convex side, where vertebral growth is to be slowed, while reducing pressure on the concave side, thereby promoting growth and progressive correction over time (Baroncini & Courvoisier, 2023; Boeyer, Farid, et al., 2023; Cobetto, Parent, et al., 2018; Courvoisier et al., 2023b; Hammad et al., 2023; Lonner et al., 2022; Raitio et al., 2022; vBizzoca et al., 2022; Zhang et al., 2022).

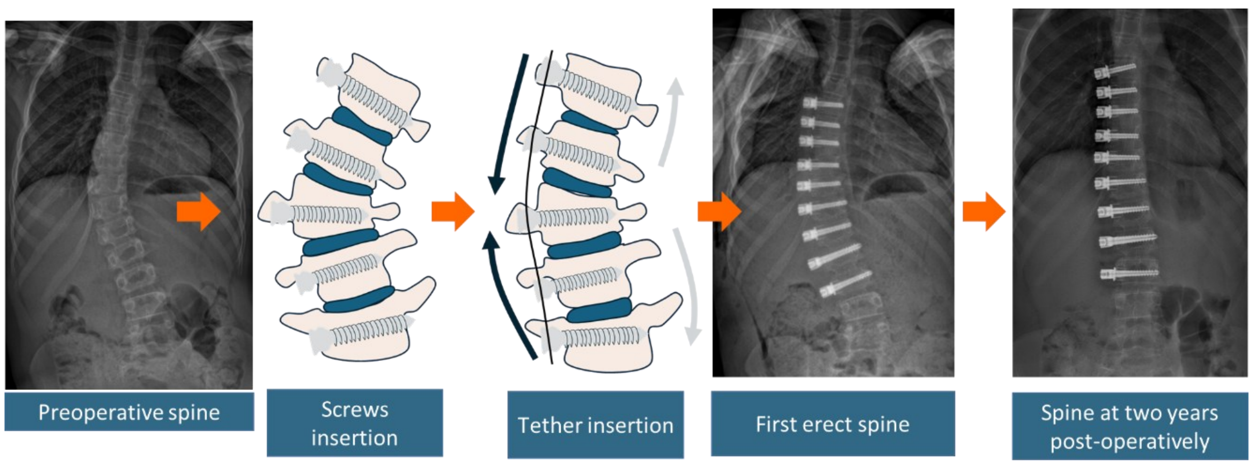


Figure 2-24: Major steps of scoliosis correction after VBT surgery

Initially, the tightening of the tether mainly deforms the intervertebral discs. While concerns have been raised regarding potential long-term disc health, available studies are reassuring. In a series by (Hoernschemeyer et al., 2021), 44% of patients showed recentration of the previously eccentric nucleus pulposus at 2-year follow-up, with none of the patients showing degenerative changes in the disc or the posterior facet. Similar results regarding disc and facet joint preservation were reported by (Yucekul et al., 2021) in a 25-patient study.

### 2.5.2 Effectiveness: success and complications

Despite its promising potential, VBT remains a technically demanding procedure with variable outcomes. Success rates, defined as a final curve below 35°, have been reported in 77% of cases, with reoperation rates between 20% and 30% (Mathew et al., 2022; Newton et al., 2020).

Lumbar VBT presents specific challenges related to the distinct anatomical and biomechanical characteristics of the lumbar spine. Its greater mobility, higher flexibility, and significant growth potential increase the risk of over- or under-correction, making surgical planning and growth prediction more complex. Successful lumbar curve correction has been reported in only 57% of cases (Boeyer, Farid, et al., 2023; C. R. Louer et al., 2024; Trobisch et al., 2023).

Tether breakage is one of the most common complications, often difficult to diagnose because of the radiolucent nature of the polyethylene cable (Wan et al., 2023) (Figure 2-25). Tether breakages occur more frequently in the lumbar region (71%) compared to the thoracic region (29%) (A. Baroncini, F. Migliorini, et al., 2022; A. Baroncini, P. Trobisch, et al., 2022; Yang et al., 2023). The benefit of using double tethers remains debated (Shankar et al., 2022; Trobisch & Baroncini, 2021). Early breakage, particularly within the first year, is associated with significant curve worsening, estimated around 10-15° (A. Baroncini, F. Migliorini, et al., 2022) or 10° ± 6.8° (Trobisch et al., 2022).

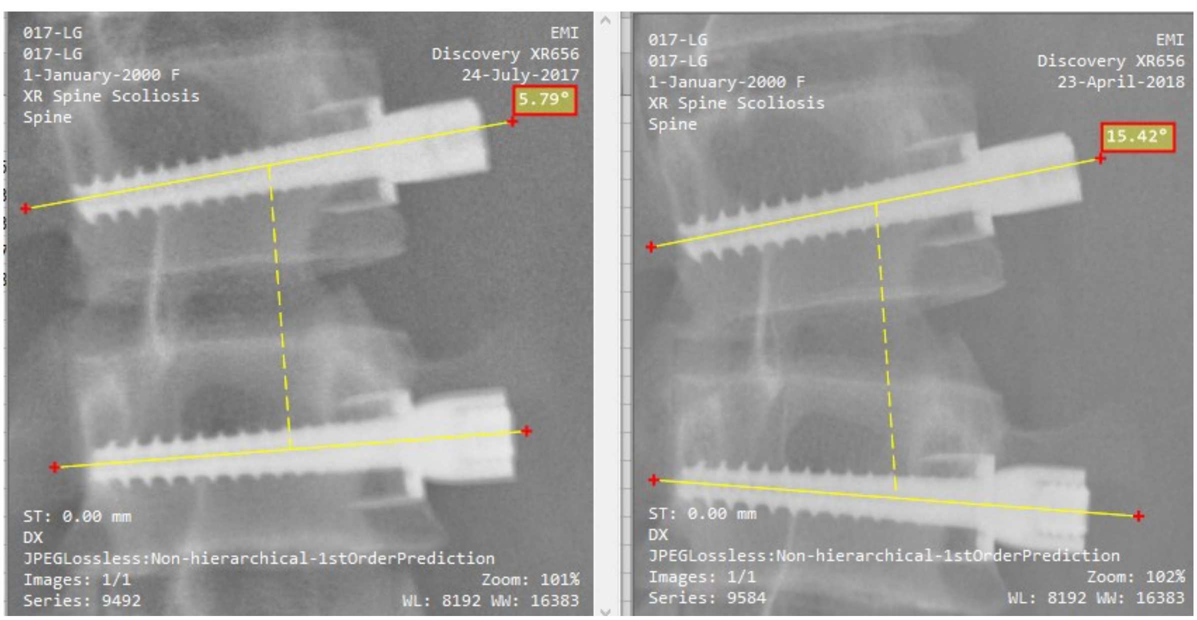


Figure 2-25: Radiographic suspicion of tether breakage

Recent research efforts have improved our understanding of growth modulation mechanisms following VBT (Boeyer, Farid, et al., 2023; C. R. Louer, Jr. et al., 2024), particularly regarding thoracic growth patterns. However, lumbar growth modulation remains less studied and represents a key area for future investigation (Boeyer, Groneck, et al., 2023).

## 2.6 Biomechanical Modelling and Simulation Tools in Spine Instrumentation

### 2.6.1 3D reconstruction

Biplanar radiography (PA and LAT views) remains the standard technique for clinical assessment of spinal deformities. Recent advances in 3D reconstruction techniques now allow for a more accurate assessment of the three-dimensional nature of scoliotic deformities. EOS imaging technology offers low-dose biplanar radiographs with the ability to generate 3D reconstructions of the spine in an upright, weight-bearing position, which is especially valuable for scoliosis assessment. Other technologies also exist to reconstruct 3D models from different types of imaging, as discussed in section 5.1.2. For example, a validated reconstruction method (Cheriet et al., 2007) uses key anatomical landmarks manually refined to compute 3D coordinates via calibration and optimization algorithms (Delorme et al., 2003). The resulting 3D model also captures the patient's spinal alignment in an upright, weight-bearing position (Figure 2-26).

MRI provides excellent tissue contrast without radiation exposure, making it a reference imaging modality in musculoskeletal radiology, particularly for spinal assessment (Fries et al., 2008). However, in the context of VBT, MRI has limitations. The supine position required during acquisition modifies spinal curvature, and the presence of metallic implants postoperatively limits its use.

CT scanning offers high-resolution imaging but exposes patients to significant radiation doses (7 mSv for lumbar imaging vs. 1.9 mSv for X-rays). Like MRI, CT is limited in scoliosis assessment due to the supine acquisition position, which alters curve magnitude. CT is mainly reserved for surgical navigation (Otomo et al., 2022).

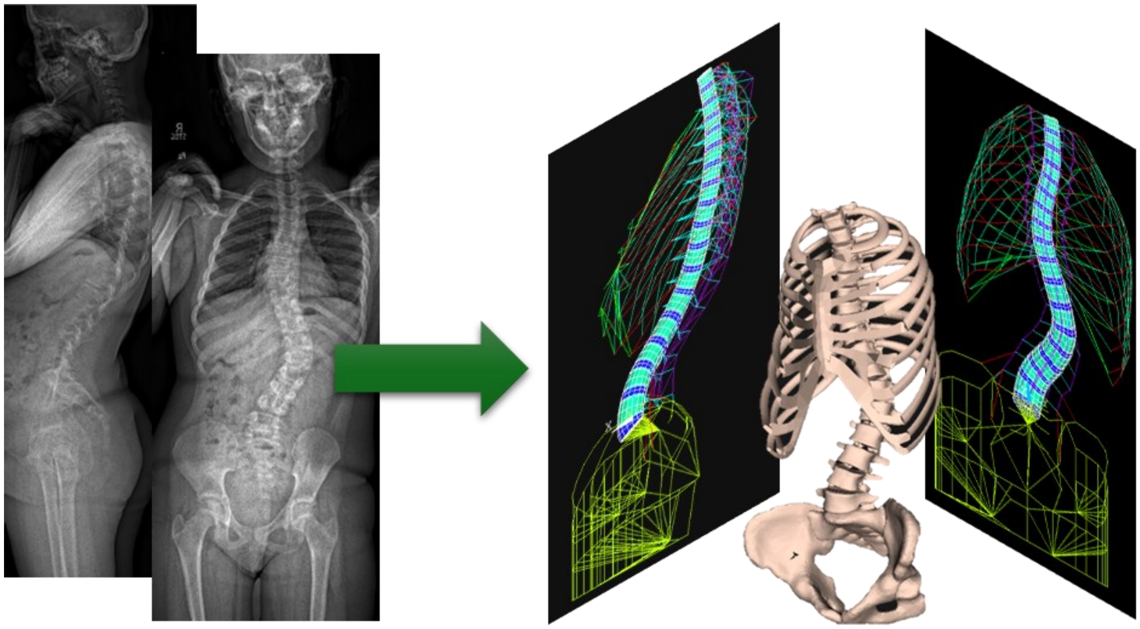

Figure 2-26: 3D reconstruction and finite element modeling from PA and LAT x-rays

### 2.6.2 Finite element modelling of the spine

Finite Element Models (FEM) provide a powerful numerical framework to simulate complex biomechanical behavior of the spine. FEM enables:

- Analysis of the influence of geometry, material properties, and loading conditions.
- Investigation of isolated parameters, otherwise difficult to measure experimentally.
- Testing of multiple surgical scenarios for the same patient.

However, FEM requires several assumptions and simplifications that may affect result accuracy. Sensitivity to input parameters, model convergence challenges, and the need for validation with experimental or clinical data remain key limitations.

### 2.6.3 VBT-Specific Finite Element Modelling and Simulation Approach

Building on previously validated models (Cobetto et al., 2018; Cobetto et al., 2020; Martin et al., 2023; Raballand et al., 2023), a patient-specific FEM has been developed to simulate VBT surgery and post-operative growth modulation (Cobetto et al., 2025). This model integrates:

- Patient-specific 3D spinal geometry.
- Material properties of vertebrae, intervertebral discs, and instrumentation.
- Growth modulation rules informed by Sanders stage and anatomical location.

- Biomechanical interactions between surgical correction and subsequent growth.

This modelling strategy provides a predictive tool to assess the biomechanical effects of VBT and optimize surgical planning according to patient-specific characteristics.

### 2.6.3.1 Representation of the various elements

#### 2.6.3.1.1 Spine model

The thoracic and lumbar vertebrae (T1 to L5), epiphyseal growth plates and intervertebral discs are represented by three-dimensional solid elements. The ribs, sternum, intercostal cartilages and pelvis are modelled using 3D beam elements. The main spinal ligaments (ligamentum flavum, common anterior and posterior, transverse and interspinous ligaments) are simulated by three-dimensional tension-only springs (Cobetto, Aubin, et al., 2018a). The mechanical properties of the various anatomical structures are taken from the literature (Chazal, 1985; Descrimes et al., 1995; Panjabi, 1976; Pezowicz, 2012). Soft tissues are assumed to exhibit linear elastic behaviour, and the intervertebral discs are calibrated to reflect the flexibility of the spine, as assessed from left and right lateral bending radiographs (Cobetto, Aubin, et al., 2018b).

#### 2.6.3.1.2 VBT surgery modeling

The transition from the upright position to the lateral decubitus position is simulated by first identifying an upright posture that matches the radiographic geometry under gravitational loading. The patient is then repositioned in the lateral decubitus orientation, with gravitational forces reoriented and applied to the centre of mass of each vertebra. Boundary conditions are applied on the pelvis and on T1 (fixed) for all patients. Additional constraints are added to simulate contact with the operating table; when the lumbar spine is instrumented, the apical thoracic vertebra is also fixed. For cases involving dual-curve instrumentation, both the proximal thoracic (PT) and lumbar apical vertebrae where fixed.

The components of the VBT construct are modeled using finite elements. Screws are represented by 3D cylindrical elements with titanium material properties, while the tether is modeled with beam elements connecting the screws, with mechanical properties consistent with polyethylene.

Cable tensioning is simulated sequentially. A force is first applied to the most proximal beam element, and then the system is solved. To reproduce the progressive passage, tensioning, and locking of the cable through each screw, the tension is then transferred stepwise to the next segment, with a new solution computed at each step. This sequential method allows the simulation of different configurations based on surgical protocols. Tension is adjusted at each instrumented vertebral level to faithfully reflect the progressive intraoperative tightening process (Cobetto, Aubin, et al., 2018a, 2018b; Cobetto et al., 2020; Cobetto, Parent, et al., 2018; Martin et al., 2023; Raballand et al., 2023). An average force of 165 N is applied, with a maximum at the apical screw and a progressive decrease of 50 N toward the end vertebrae (Cobetto et al., 2020).

Following instrumentation, the spine is repositioned in the upright posture and gravitational loading reapplied. Force magnitudes are scaled based on the patient's weight. To account for the absence of soft tissues (muscles, skin, organs), additional lateral forces perpendicular to the curvature are introduced to preserve the initial geometry. These compensatory forces are patient-specific and can be adjusted to better represent the natural mechanical support of soft tissues (Cobetto, Aubin, et al., 2018a).

#### 2.6.3.1.3 Growth and growth modulation simulations

The model includes predictions of spinal growth over a period expressed in months, with growth rates calibrated for a two-year period.

Growth is modelled as a symmetrical thermal expansion process governed by the growth algorithm developed by Stokes et al, detailed above: $G = G_m * (1 + \beta * (\sigma_m - \sigma))$.

where $G$ is the actual local growth rate, $G_m$ is the mean baseline growth under normal stress, $\sigma$ is the actual local stress applied to the growth plate (compression negative), and $\sigma_m$ is the mean physiological (baseline) stress on growth plate. In this study, the modulation coefficient $\beta$ is set to 1.6MPa$^{-1}$. Since growth cannot be negative, if $\beta * (\sigma_m - \sigma) < -1$ then $G = 0$ and growth is halted.

Growth is computed iteratively on a monthly basis for the entire simulation period. The model has been validated against experimental data for 12- and 24-month growth simulations.

### 2.6.3.2 Validation and verification

To guarantee the reliability of the model used to simulate lumbar VBT, a verification and validation (V&V) process was carried out in accordance with the framework of the ASME V&V40 standard. This work is detailed in a scientific article (APPENDIX 1). The aim of the study was to validate a surgical planning tool based on a personalized FEM, coupled with a mechanobiological growth modulation algorithm considering preoperative bone maturity. The model was tested on a multicentre set of 35 cases of idiopathic scoliosis treated with lumbar VBT. Validation was performed by comparing the model's predictions - both immediately after surgery and two years later - with actual radiographic measurements (Figure 2-27). The results demonstrated clinically relevant accuracy, with deviations of less than 3° on Cobb angles, confirming the credibility of the tool for use in surgical planning.

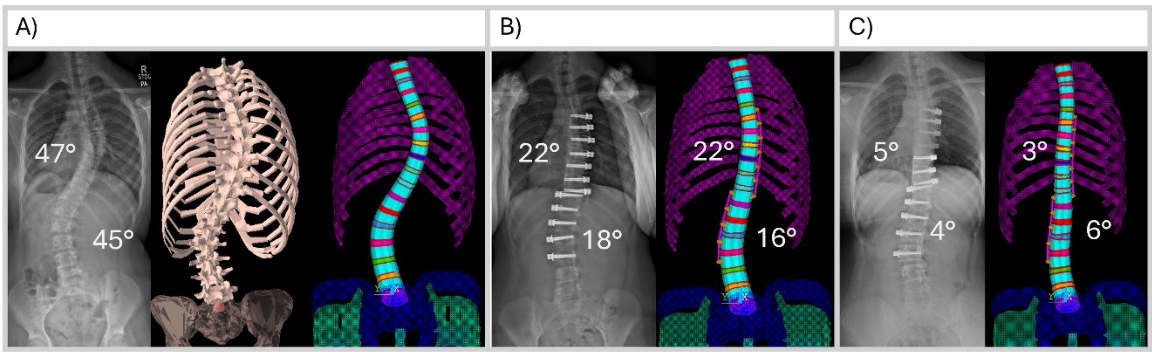


Figure 2-27: A) Presenting deformity, 3D reconstruction obtained from biplanar radiographs and the corresponding FEM calibrated to patient’s flexibility, weight and skeletal maturity (Sanders score); B) Predicted and actual immediate postoperative correction; C) Predicted and actual 2-year growth and growth modulation (ligaments and vertebral posterior elements not shown for clarity), (Cobetto et al., 2025)

# CHAPTER 3 Synthesis of the Clinical Problem, Objectives, and Research Hypotheses

## 3.1 Clinical Context and Unmet Need

In pediatric scoliosis cases with remaining growth potential, VBT surgery is an increasingly popular fusionless alternative. This technique involves placing a lateral tether on the vertebral bodies, on the convex side of the deformity, to guide spinal growth and progressively correct the curvature. Lumbar VBT is particularly attractive due to its ability to preserve spinal mobility.

Despite its growing popularity, VBT poses significant challenges. Postoperative outcomes remain difficult to predict, and complications such as tether breakage, under- or over-correction, and junctional deformities at the ends of the instrumentation are common. Although tether failure is frequent, it does not systematically compromise clinical outcomes. In contrast, the inability to achieve or maintain adequate correction, especially under-correction, can negatively impact cosmetic and functional results. Over-correction, while less frequent, may also result in unfavorable outcomes.

Currently, surgical planning largely relies on clinical experience, as there are no robust, objective tools available to guide intraoperative decision-making in VBT. Understanding how intraoperative correction and patient-specific factors (e.g., curve flexibility, skeletal maturity, body weight) interact to influence long-term outcomes is essential to improve treatment efficacy and consistency.

## 3.2 Objectives

The objective of this study was to biomechanically model and analyze the appropriate intraoperative correction target in lumbar VBT to maximize two-year outcomes while minimizing the risk of overcorrection in pediatric idiopathic scoliosis patients. This analysis considered key patient-specific factors such as the initial deformity, spinal stiffness, body weight, and skeletal maturity. Ultimately, the goal was to develop a decision-support tool that could assist surgeons in objectively defining an optimal intraoperative correction strategy tailored to each patient's characteristics.

This objective was broken down into 3 sub-objectives (SO):

SO1: To adapt, verify and validate a FEM of the spine capable of simulating growth modulation and progressive correction following lumbar VBT.

SO2: To analyze the influence of the intraoperative correction achieved during VBT surgery, as well as patient-specific factors such as flexibility, residual growth potential, and body weight, on the scoliosis correction obtained two years postoperatively.

SO3: To establish recommendations for the intraoperative correction target – in terms of Cobb angle – that should be aimed for during VBT surgery to achieve a residual curve of less than 5° at skeletal maturity.

## 3.3 Hypotheses

The project aims to test the following hypotheses:

H1: The patient-specific FEM of the spine, integrating a growth and growth modulation algorithm, can accurately predict lumbar VBT surgery outcomes, with predicted Cobb angles falling within a ± 3° range of the actual clinical correction, both immediately after surgery and at two-year follow-up.

H2: The intra-operative correction target can be adjusted and optimized to maximize both immediate and long-term (two-year) scoliosis correction, while minimizing the risks of curve progression or over-correction at skeletal maturity.

## 3.4 Rationale

Despite its growing popularity, VBT surgery continues to present significant challenges. Tether breakage is a frequent event following VBT, reflecting the high mechanical demands placed on the construct. However, tether breakage does not systematically lead to complications or poor clinical outcomes. In contrast, one of the most critical challenges for surgeons remains achieving a sufficient and lasting correction of the scoliotic curve. Under-correction is the most common issue, potentially compromising the cosmetic and functional results of surgery, while over-correction — although less frequent — may also lead to unfavorable outcomes. Furthermore, residual deformities outside the instrumented segment, such as junctional problems or progression of unfused curves, represent additional risks that must be anticipated during surgical planning.

In this context, better understanding the relationship between intraoperative correction, patient-specific factors, and long-term outcomes is essential to improve surgical planning and reduce the risk of suboptimal results. However, objective guidelines to help surgeons determine the optimal intraoperative correction target in lumbar VBT are still lacking. This study therefore aims to fill this gap by providing scientifically established recommendations to guide surgical decision-making and personalize VBT correction strategies according to individual patient characteristics.

# CHAPTER 4 ARTICLE 1: PATIENT-SPECIFIC BIOMECHANICAL MODELLING OF INTRAOPERATIVE SCOLIOSIS CORRECTION ON THE 2-YEAR OUTCOMES FOR LUMBAR VERTEBRAL BODY TETHERING

## 4.1 Presentation of the article

The article presented in this section investigates the influence of residual growth and the intra-operative correction achieved during surgery on the correction that can be obtained at two-year post-surgery.

This article entitled “Towards Optimizing Intraoperative Correction in Lumbar Vertebral Body Tethering” was submitted to “Spine Deformity” on March 11$^{th}$, 2025. The lead author contributed approximately 75% to the development of this study, including study design, modeling, analysis, and manuscript preparation.

## 4.2 Article 1: PATIENT-SPECIFIC BIOMECHANICAL MODELLING OF INTRAOPERATIVE SCOLIOSIS CORRECTION ON THE 2-YEAR OUTCOMES FOR LUMBAR VERTEBRAL BODY TETHERING

Marine Gay [1,2], Nikita Cobetto, PhD, Eng.[1,2], Christiane Caouette, PhD, Eng.[1,2], A. Noelle Larson, MD[3], Isabelle Villemure PhD[1,2], Dan Hoernschemeyer, MD[4], Melanie Boeyer, PhD[4], Ron El-Hawary, MD[5], Ahmet Alanay, MD[5], Carl-Eric Aubin, PhD, ScD P.Eng.[1,2]

**Affiliations**

1- Department of Mechanical Engineering, Polytechnique Montréal, Montreal, Quebec, Canada
2- Research Center, Sainte-Justine University Hospital Center, Montreal, Quebec, Canada
3- Department of Orthopedic Surgery, Mayo Clinic, Rochester, Minnesota, USA
4- Department of Orthopaedic Surgery, University of Missouri, Columbia, Missouri, USA
5- Boston Children's Hospital, Boston, Massachusetts, USA
6- Department of Orthopedics and Traumatology, Acibadem Mehmet Ali Aydinlar University School of Medicine, Istanbul, Turkey

### 4.2.1 Abstract

**Purpose:** To biomechanically assess the influence of intraoperative correction and presenting Sanders maturity scores (SS) on growth modulation correction after two years in pediatric idiopathic scoliosis treated with VBT.

**Methods:** Lumbar VBT was simulated using patient-specific finite element models (FEMs) from 20 cases of pediatric idiopathic scoliosis (average lumbar Cobb 47°; min: 34°, max: 63°), calibrated for preoperative SS, weight, and flexibility. The validated FEM included lateral decubitus positioning and VBT instrumentation at the actual upper instrumented vertebra (UIV: T9-T12) and lower instrumented vertebra (LIV: L2-L4). Simulations tested three intraoperative nominal correction levels (35%, 50%, 70%) across SS stages (3A, 3B, 4, 5), with immediate and two-year postoperative corrections computed and analyzed.

**Results:** A 35% intraoperative correction resulted in an immediate post-op correction of 37° (23°-54°) but led to under-correction, with a final deformity of 38° (22°-63°) at two years. Curve progression occurred in 40% of SS3A cases, particularly in heavier patients (54 kg vs. 38 kg, $p < 0.05$). A 50% intraoperative correction yielded an immediate correction of 27° (16°-40°), with significant improvement at two years only in SS3A ($p < 0.05$). Clinically successful growth modulation (>5° improvement) correlated with lower weight (40±6 kg vs. 54±6 kg, $p < 0.05$). A 70% intraoperative correction produced an immediate correction of 17° (11°-22°) and significant improvement across all SS levels ($p < 0.05$), with final two-year corrections of 1° (-27° to 10°) for SS3A, 10° (-5° to 10°) for SS3B, 12° (0° to 18°) for SS4, and 13° (4° to 19°) for SS5. Overcorrection occurred in SS3A (4 cases) and SS3B (1 case).

**Conclusion:** Successful outcomes at 2 years depend on the interaction of key factors such as intraoperative correction, residual growth potential as defined by preoperative SS, patient weight, spinal flexibility, and mechanobiological growth modulation. The advanced and validated planning tool used for the simulations incorporates these elements, integrating both biomechanical and biological growth dynamics to support a more precise and personalized surgical approach.

**Keywords:** Pediatric idiopathic scoliosis – Lumbar Vertebral Body Tethering – Finite element modeling – Growth modulation correction – Biomechanics

### 4.2.2 Introduction

Scoliosis is characterized as a three-dimensional deformity of the spine affecting 2% to 3% of the population, with idiopathic scoliosis constituting 80% of all diagnosed cases. The etiology of scoliosis is multifaceted and complex, and the mechanisms underlying its progression can be partially elucidated by the Hueter-Volkmann principle (Arkin & Katz, 1956) and Stokes' vicious circle (Stokes et al., 2006; Stokes et al., 2002; Stokes et al., 1996), which assert that modulation of vertebral growth depends on loading conditions: compressive forces inhibit growth, while tensile forces facilitate it. In the context of scoliosis, there is an asymmetrical distribution of loading along the spine and on the vertebrae, resulting in increased pressure on the concave side and reduced pressure on the convex side. This differential pressure gradient induces vertebral wedging, which in turn accelerates the progression of spinal curvature.

Vertebral Body Tethering (VBT) is a fusionless surgical intervention designed to address progressive spinal deformities in patients exhibiting residual growth potential (Baroncini & Courvoisier, 2023; Alice Baroncini et al., 2022; Courvoisier et al., 2023b; Hammad et al., 2023). Vertebral body screws and a compressive tether implanted on the convex side of the curve induce immediate correction seen on first erect films (Raitio et al., 2022). The pressure exerted on the scoliotic spine's convex side aims to rebalance asymmetrical stresses on vertebral epiphyseal growth plates, stopping the vicious circle inducing asymmetrical growth and reshaping wedged vertebrae with growth (McDonald et al., 2022; Photopoulos et al., 2024). The objective of VBT surgery is to increase postoperative correction by modulating the growth of the spine (C. R. Louer et al., 2024), primarily addressing the coronal plane deformity (Alice Baroncini et al., 2022).

VBT surgery continues to present significant challenges, with persistently high rates of both over- and under-correction. It has been reported that only 77% of patients achieve a final curve of less than 35°, while reoperation rates range from 20 to 30% (Mathew et al., 2022; Newton et al., 2020). Lumbar VBT is even more challenging due to greater mechanical forces, growth potential, and flexibility of this spinal segment, leading to successful correction of the lumbar curve in just 57% of cases (Boeyer, Farid, et al., 2023; C. R. Louer et al., 2024; Trobisch et al., 2023). Recent research has advanced our understanding of growth profiles (Boeyer, Farid, et al., 2023) and growth modulation trajectories (C. R. Louer, Jr. et al., 2024). Most studies primarily focus on thoracic growth, often overlooking the distinct characteristics of lumbar growth (Boeyer, Groneck, et al., 2023). In addition, surgical planning continues to remain challenging due to the difficulty of accurately assessing growth modulation, residual skeletal maturity dynamics, and the intricate interplay between VBT effects and other biomechanical forces, including muscular, functional, and gravitational forces. Consequently, planning often relies on heuristic estimates, making it particularly complex to determine the optimal degree of initial correction needed to achieve a favorable long-term outcome, given the limited knowledge on how to assess and account for these interacting factors.

This study aims to assess how the degree of intraoperative scoliosis correction influences spinal correction two years after lumbar VBT surgery. Specifically, it investigates this relationship in the context of the patient's preoperative skeletal maturity status, leveraging a validated patient-specific finite element model including a mechanobiological growth modulation algorithm.

### 4.2.3 Methods

**Study Design and Patient Data.** This numerical investigation utilized retrospective clinical data from twenty pediatric patients diagnosed with idiopathic scoliosis who underwent lumbar VBT, with or without concomitant thoracic VBT, at three collaborating institutions. The study was conducted with the approval of institutional ethics review boards. Inclusion criteria required a confirmed diagnosis of idiopathic scoliosis, lumbar VBT instrumentation, and a minimum follow-up of two years. Patients with suspected tether failure, double rows, or non-idiopathic scoliosis (e.g., neuromuscular or congenital scoliosis) were excluded. This cohort had preoperative lumbar Cobb angles ranging from 34° to 63° (mean: 47°) and Sanders maturity scores (SS) between SS3A and SS7 (mean: 4.2). A detailed summary of patient characteristics is provided in Table 1.

**Patient-specific biomechanical modeling (Figure1).** Patient’s specific 3D spinal geometries were reconstructed using postero-anterior (PA) and lateral (LAT) x-rays with a validated in-house software. The 3D reconstruction includes vertebrae from T1 to L5, the pelvis, and the rib cage. A finite element model (FEM) was then generated from the reconstructed 3D geometry. The model incorporated the osseo-ligamentous structures of the spine, with intervertebral discs and ligaments parameterized based on patient-specific flexibility calibration  (Cobetto, Aubin, et al., 2018b; Cobetto et al., 2020; Cobetto, Parent, et al., 2018). This FEM was previously validated for lumbar

VBT (Martin et al., 2023) and allows the simulation of intra-operative positioning and correction. Mechanical flexibility properties of the intervertebral discs were calibrated using flexibility radiographs, adjusting stiffness based on a predefined flexibility index that correlated with curve reduction observed during bending tests (Petit et al., 2004).

**Simulation of VBT Instrumentation.** VBT surgery was simulated by first placing the patient in a lateral decubitus position, replicating the intraoperative setup for instrumentation (Cobetto, Aubin, et al., 2018a; Martin et al., 2023; Raballand et al., 2023). For cases involving both thoracic and lumbar VBT, the thoracic spine was instrumented first. Vertebral screws were modeled as 3D cylindrical beams with titanium material properties and were placed at the selected instrumentation levels. The flexible tether, modeled with polyethylene material properties, was sequentially inserted through the vertebral screws and tensioned, one level at a time. Tensioning was simulated in the cranial to caudal direction following a predefined tensioning protocol where maximal tension was applied at the curve's apex and progressively reduced towards the distal levels. Once the instrumentation was complete, the patient model was returned to an upright standing position by applying gravitational loads and compensatory muscular forces.

**Simulation of growth and growth modulation over 2 years.** Following the simulation of immediate post-operative correction, spinal growth, and growth modulation were modeled over a two-year period using a validated mechanobiological algorithm (Martin et al., 2023). This algorithm is based on in vivo correlations and mechanobiological principles derived from the Hueter-Volkman law (Mehlman et al., 1997; Stokes, 2002; Stokes et al., 2006; Stokes et al., 2002; Stokes et al., 1996), which relates actual stresses (σ) to normal physiological stresses ($\sigma_m$) at vertebral epiphyseal growth plates. The final longitudinal growth rate (G) was calculated as a function of these stresses:

$$G = G_m * (1 - \beta * (\sigma - \sigma_m))$$

where β represents the sensitivity of growth modulation (1.6 $MPa^{-1}$ (Sarwark & Aubin, 2007). When β * (σ - σm) exceeded 1, growth was halted (i.e. G was set to 0). Baseline growth rate (Gm) was adjusted according to the patient's skeletal maturity at surgery, with growth rates modeled for stages SS1 to SS7 (Table 2) distinguishing between SS3A and SS3B. Growth rates were averaged over two years, accounting for the progressive decline in growth with increasing maturity (in house data).

**Simulation configurations.** The initial simulation replicated the actual surgery and was compared with the real two-year postoperative correction, with an average Cobb angle discrepancy of less than 3°.

From this validated base, different configurations were tested by modifying intraoperative correction levels while maintaining the same instrumented vertebrae. Cord tension and a corrective lateral push applied by the surgeon were adjusted to achieve 35%, 50% and 70% of nominal intraoperative correction. Growth was then simulated for 4 levels of possible skeletal maturity level evaluation corresponding to the patient's Sander Score (SS) at surgery (SS 3A, SS 3B, SS 4, SS 5). Considering the independent variables chosen, 12 simulations were performed per patient, leading to a total of 240 simulations.

**Data analysis.** Data analysis aimed to assess the influence of intraoperative correction levels and simulated SS on Cobb angle correction, both immediately postoperatively and two years after surgery (dependent variables). Statistical analysis was conducted using STATISTICA 10.0 software package (Statistica, StatSoft Inc., Tulsa, OK, USA). Normality of the results was verified using Shapiro-Wilk tests. Paired Student t-tests were performed to determine significant differences between simulated configurations. To assess the effect of growth modulation, immediate postoperative correction values were compared with the two-year postoperative results. A statistically significant difference would indicate a substantial effect of growth modulation on the final correction outcomes; growth modulation was considered clinically significant when correction was more than 5° after two years.

### 4.2.4 Results

**Immediate and Two-Year Postoperative Correction.** Three nominal levels of intraoperative correction were achieved: 37% (min 31%, max 43%), 52% (min 47%, max 56%) and 71% (min 68%, max 75%). Correspondingly, the mean immediate correction simulated was 21% (min 10%, max 34%), 43% (min 29%, max 61%) and 63% (min 44%, max 72%), respectively. Results expressed in degrees and percentages are presented in Table 3. The impact of mechanobiological growth modulation on the two-year correction varied according to the intraoperative correction level and skeletal maturity at surgery.

**Impact of growth modulation after a low intraoperative correction (35%).** For 35% intraoperative correction, the mean immediate post-op Cobb angle was 37° (min: 23°, max: 54°). After two years, no significant difference was observed, with the mean simulated correction stabilizing at 38° (min: 22°, max: 63°), indicating insufficient growth modulation across all SS levels:

- SS3A: mean 38° (min: 22°, max: 63°)
- SS3B: mean 38° (min: 24°, max: 58°)
- SS4: mean 38° (min: 23°, max: 57°)
- SS5: mean 37° (min: 23°, max: 56°)

For SS3A, in 10 out of 20 cases, there was no significant change over time. However, in 4 cases curve correction exceeded 5° (up to 10°), while 6 cases exhibited curve progression >5° (up to 11°). SSA3 Patients whose curves worsened were significantly heavier at the time of surgery ($p < 0.05$), as demonstrated by simulation analyses:

- Deformity progression sub-group: mean weight: 54 kg (min: 48 kg, max: 69 kg).
- Correction improvement sub-group: mean weight: 38 kg (min: 35 kg, max: 40 kg).

For SS3B, SS4, and SS5, 19 out of 20 cases showed no significant change over time regardless of weight.

**Impact of growth modulation after moderate intraoperative correction (50%).** A 50% intra-op correction resulted in a mean immediate post-op correction of 27° (min: 16°, max: 40°). After two years, simulated correction varied based on Sanders Score:

- SS3A: 22° (min: 3°, max: 42°, 3/20 cases above 30° at 2-years)
- SS3B: 25° (min: 13°, max: 41°, 3/20 cases above 30° at 2-years)
- SS4: 26° (min: 15°, max: 40°, 4/20 cases above 30° at 2-years)
- SS5: 26° (min: 14°, max: 40°, 7/20 cases above 30° at 2-years)

A significant improvement between immediate post-op and two-year correction was observed only for SS3A ($p < 0.05$), as evidenced by simulations. However, responses within SS3A were heterogeneous:

- Some simulated cases (N=11) exhibited clinically significant growth modulation (>5° correction improvement).
- Others experienced worsening of the curve over time (N=4), with a progression of the curve of 4° (2°-7°).

Dividing the SS3A cohort into simulated cases with effective growth modulation (N = 11) and those without (N = 9) revealed a significant weight difference ($p < 0.05$):

- Growth modulation sub-group: mean weight: 40 kg (min: 31 kg, max: 51 kg).
- Non-modulation sub-group: mean weight: 54 kg (min: 48 kg, max: 69 kg).

The correction at simulated first erect did not differ between the two groups, being in average 27° (16°-36°) for the modulating group and 26° (16°-40°) for the non-modulating group. Flexibility was not significant either.

**Impact of growth modulation after high intraoperative correction (70%).** A simulated 70% intraoperative correction resulted in a significant reduction in deformity ($p<0.05$) between the immediate post-op and two-year follow-up. The residual Cobb angles at two years were:

- SS3A: 1° (min: -27°, max: 10°)
- SS3B: 10° (min: -5°, max: 16°)
- SS4: 12° (min: 0°, max: 18°)
- SS5: 13° (min: 4°, max: 19°)

Clinically significant growth modulation (>5° improvement) was observed in simulations with SS3A, SS3B, and SS4. However, overcorrection occurred in some cases:

- SS3A: 4 cases, with a final Cobb angle of -5° (-8° to -3°), and one at -27°.
- SS3B: 1 case, with a final Cobb angle of -5°.

### 4.2.5 Discussion

This study provides clinically relevant, biomechanical insight into the impact of intra-operative correction, preoperative curve characteristics and skeletal maturity, flexibility, and patient weight on both immediate correction and growth modulation correction following lumbar VBT for idiopathic scoliosis.

**Influence of skeletal maturity on growth modulation.** The simulations performed were consistent with clinical observations (Treuheim et al., 2023), confirming that more skeletally mature patients (SS4 and above) exhibit limited growth modulation. While a statistically significant difference was observed between immediate post-op and two-year correction, this difference remained clinically insignificant (<5°). These findings align with previous reports indicating that more mature patients are at a higher risk of under-correction due to insufficient remaining growth potential. For stiff curves that cannot be adequately corrected intraoperatively, under-correction persists at two years, particularly in patients who are a SS4 or greater. These simulations highlight the importance of achieving full intraoperative correction, as growth modulation alone cannot compensate for inadequate initial correction in patients with limited residual growth.

**Role of patient weight in VBT outcomes.** While similar simulated intraoperative correction can be achieved in both normal-weight and overweight patients, our results confirm that heavier cases are more prone to curve progression during simulated growth modulation (Mishreky et al., 2022). This study further demonstrated that even with identical simulated intraoperative correction, preoperatively lighter patients (40 kg (min: 31 kg, max: 51 kg)) tend to achieve better long-term correction, with lower residual Cobb angles at two years. However, this weight-related discrepancy diminishes when a higher intraoperative correction (≥70%) is achieved. These findings suggest that lumbar VBT remains a viable option for preoperatively heavier patients, provided that sufficient intraoperative correction can be obtained. This has critical implications for patient selection and surgical planning, emphasizing the need for tailored correction strategies based on individual patient characteristics.

**Inter-patient variability and the need for patient-specific modelling.** A key finding of this study is the significant inter-patient variability in simulated VBT outcomes, reflecting the challenge observed clinically by surgeons. Multiple interacting factors—including skeletal maturity, curve flexibility, and body weight—influence correction, making it inappropriate to define a single "ideal" intraoperative correction scenario for lumbar VBT. Instead, our simulation results underscore the importance of patient-specific modelling to refine surgical planning and optimize long-term correction. By simulating individual cases, the validated FEM integrating mechanobiological growth modulation provides valuable insights into:

- The likelihood of successful correction given a patient's preoperative skeletal maturity and flexibility status.
- The expected effect of growth modulation according to the preoperative SS.
- The risk of overcorrection or under-correction based on initial correction, patient weight, and SS.

This predictive approach offers surgeons a robust decision-making tool, enabling a more personalized and biomechanically informed strategy for lumbar VBT. Rather than applying a one-size-fits-all correction approach, patient-specific simulations help refine intraoperative correction levels and mitigate postoperative risks.

**Limitations of the study.** This study has its limitations. Firstly, the simulated growth modulation was based on a fixed rate representing an average over a two-year period, without extending the simulations beyond this timeframe. The current version of the model has not yet been calibrated longer-term predictions. Consequently, the ability to anticipate long-term complications is limited, particularly issues such as cable breakage or growth retardation. The model does not consider potential tether breakage and its impact on correction as a function of bone maturity, which could influence the reliability of long-term outcome predictions.

**Clinical Implications and Future Directions.** These findings suggest that achieving appropriate, patient-specific intraoperative correction is crucial. In patients with significant remaining growth (SS3A-SS3B), growth modulation can enhance long-term correction, but the effect is highly dependent on weight and initial correction level. Our finite element model suggests that a target of 70% intraoperative correction may be appropriate for lumbar VBT surgery, except for SS3A curves, where 50% correction could be sufficient. However, these findings should be interpreted with caution, as they may not be generalizable to all cases.

Future work should focus on i) refining weight-based correction thresholds to further improve surgical planning; ii) Integrating additional patient-specific parameters such as muscle activation, level of activities, and spinal balance into predictive models. iii) Validating these findings in larger, prospective, multicentred studies to enhance generalizability.

Our finite element model suggests that surgeons should aim for 70% intraoperative correction during lumbar VBT surgery when reachable, except for SS3A curves for which 50% intraoperative correction may be sufficient.

Ultimately, this study reinforces the critical role of validated biomechanical modelling in advancing VBT surgical planning, reducing variability in outcomes, and improving patient selection to maximize long-term correction success.

### 4.2.6 Tables and Figures

Table 4-1: Cases specificities

| Case | Instrumented segment(s) | SS | Triradiate cartilage (TRC) | Weight (kg) | Presenting TL/L Cobb | Immediate post-op TL/L Cobb (% correction) | Follow-up (2 years) TL/L Cobb (% correction) |
|---|---|---|---|---|---|---|---|
| 1 | T11-L3 | 4 | Open | 49 | 51° | 34° (40%) | 36° (37%) |
| 2 | T11-L3 | 4 | Closed | 54 | 56° | 24° (59%) | 26° (56%) |
| 3 | T10-L3 | 3 | Open | 51 | 38° | 30° (38%) | 20° (58%) |
| 4 | T10-L3 | 3 | Open | 31 | 55° | 24° (56%) | 1° (98%) |
| 5 | T11-L3 | 4 | Closed | 49 | 52° | 24° (55%) | 24° (55%) |
| 6 | T10-L3 | 6 | Closed | 38 | 51° | 17° (66%) | 10° (80%) |
| 7 | T10-L3 | 6 | Closed | 58 | 38° | 12° (68%) | 11° (71%) |
| 8 | T10-L3 | 3B | Open | 54 | 41° | 23° (48%) | 24° (45%) |
| 9 | T11-L3 | 6 | Closed | 39 | 39° | 9° (76%) | 7° (81%) |
| 10 | T10-L2 | 3A | Closed | 48 | 40° | 9° (77%) | -4° (110%) |
| 11 | T10-L3 | 6 | Closed | 48 | 34° | 9° (75%) | 11° (69%) |
| 12 | T12-L4 | 4 | Closed | 69 | 39° | 20° (55%) | 18° (59%) |
| 13 | T7-L3 | 4 | Closed | 54 | 63° | 28° (59%) | 25° (63%) |
| 14 | T7-L3 | 3A | Open | 35 | 38° | 33° (13%) | 7° (82%) |
| 15 | T7-L3 | 4 | Closed | 31 | 45° | 6° (87%) | -7° (116%) |
| 16 | T11-L3 | 4 | Closed | 48 | 54° | 7° (87%) | 2° (96%) |
| 17 | T7-T12<br>T12-L4 | 7 | Closed | 51 | 40° | 18° (55%) | 14° (65%) |
| 18 | T5-T10<br>T10-L4 | 3B | Closed | 40 | 66° | 23° (65%) | 15° (77%) |
| 19 | T5-T10<br>T10-L3 | 3 | Closed | 38 | 60° | 26° (57%) | 21° (65%) |
| 20 | T5-T10<br>T10-L3 | 4 | Closed | 48 | 47° | 21° (55%) | 11° (77%) |

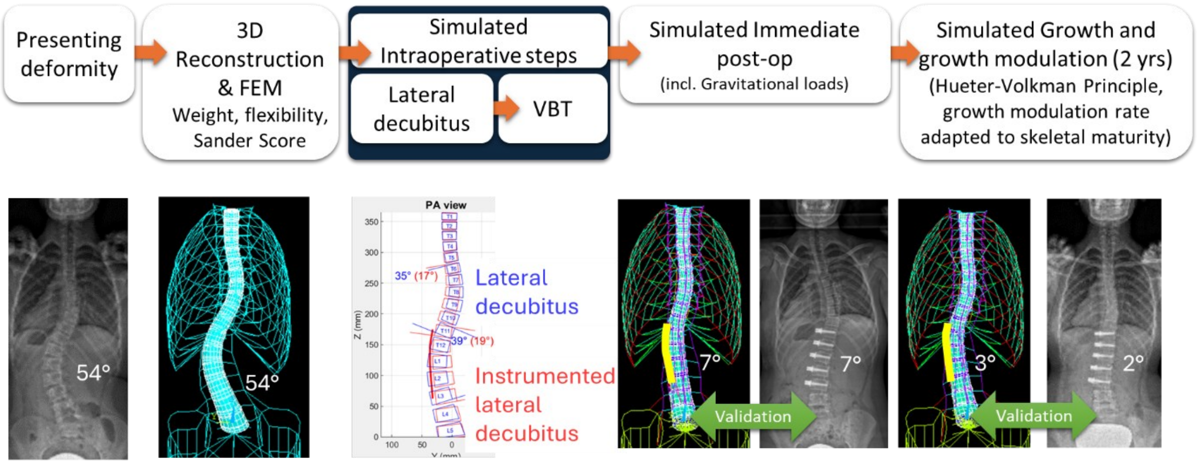


Figure 4-1: Patient specific biomechanical modeling

Table 4-2: Model growth rates as a function of Sanders Score at treatment entry point

| Preoperative Sanders Score | Thoracic growth rate (mm/year/vertebra) | Lumbar growth rate (mm/year/vertebra) |
|---|---|---|
| SS 2 | 1,80 | 2,13 |
| SS 3A | 2,01 | 2,38 |
| SS 3B | 1,21 | 1,42 |
| SS 4 | 0,89 | 1,05 |
| SS 5 | 0,64 | 0,75 |
| SS 6 | 0,42 | 0,49 |
| SS 7 | 0,28 | 0,33 |

Table 4-3: Surgical Outcomes by Intraoperative Correction and Skeletal Maturity

| | | | 35% | | 50% | | 70% | |
|---|---|---|---|---|---|---|---|---|
| | | | Lumbar Cobb (°) | Correction (%) | Lumbar Cobb (°) | Correction (%) | Lumbar Cobb (°) | Correction (%) |
| Preoperative | | Avg | 47° | | 47° | | 47° | |
| | | Min | 34° | | 34° | | 34° | |
| | | Max | 63° | | 63° | | 63° | |
| Intraoperative | | Avg | 30° | 36% | 22° | 52% | 14° | 71% |
| | | Min | 21° | 31% | 15° | 47% | 10° | 71% |
| | | Max | 42° | 42% | 31° | 56% | 18° | 71% |
| Simulated Immediate postoperative | | Avg | 37° | 21% | 27° | 43% | 17° | 64% |
| | | Min | 23° | 8% | 16° | 29% | 11° | 68% |
| | | Max | 54° | 34% | 40° | 61% | 22° | 65% |
| SS3A Simulated | 2-yr post-op | Avg | 38° | 18% | 22° | 53% | 1° | 97% |
| | | Min | 22° | -10% | 3° | 29% | -27° | 179% |
| | | Max | 63° | 49% | 42° | 93% | 10° | 84% |
| SS3B Simulated | 2-yr post-op | Avg | 38° | 19% | 25° | 47% | 10° | 80% |
| | | Min | 24° | 0% | 13° | 29% | -5° | 115% |
| | | Max | 58° | 38% | 41° | 64% | 16° | 75% |
| SS4 Simulated | 2-yr post-op | Avg | 38° | 19% | 26° | 45% | 12° | 76% |
| | | Min | 25° | 3% | 14° | 29% | 0° | 100% |
| | | Max | 57° | 36% | 40° | 60% | 18° | 71% |
| SS5 Simulated | 2-yr post-op | Avg | 38° | 19% | 26° | 44% | 13° | 72% |
| | | Min | 25° | 5% | 15° | 29% | 4° | 88% |
| | | Max | 56° | 35% | 40° | 57% | 19° | 70% |

**CONSORT Flowchart of patient recruited from the participating centers**

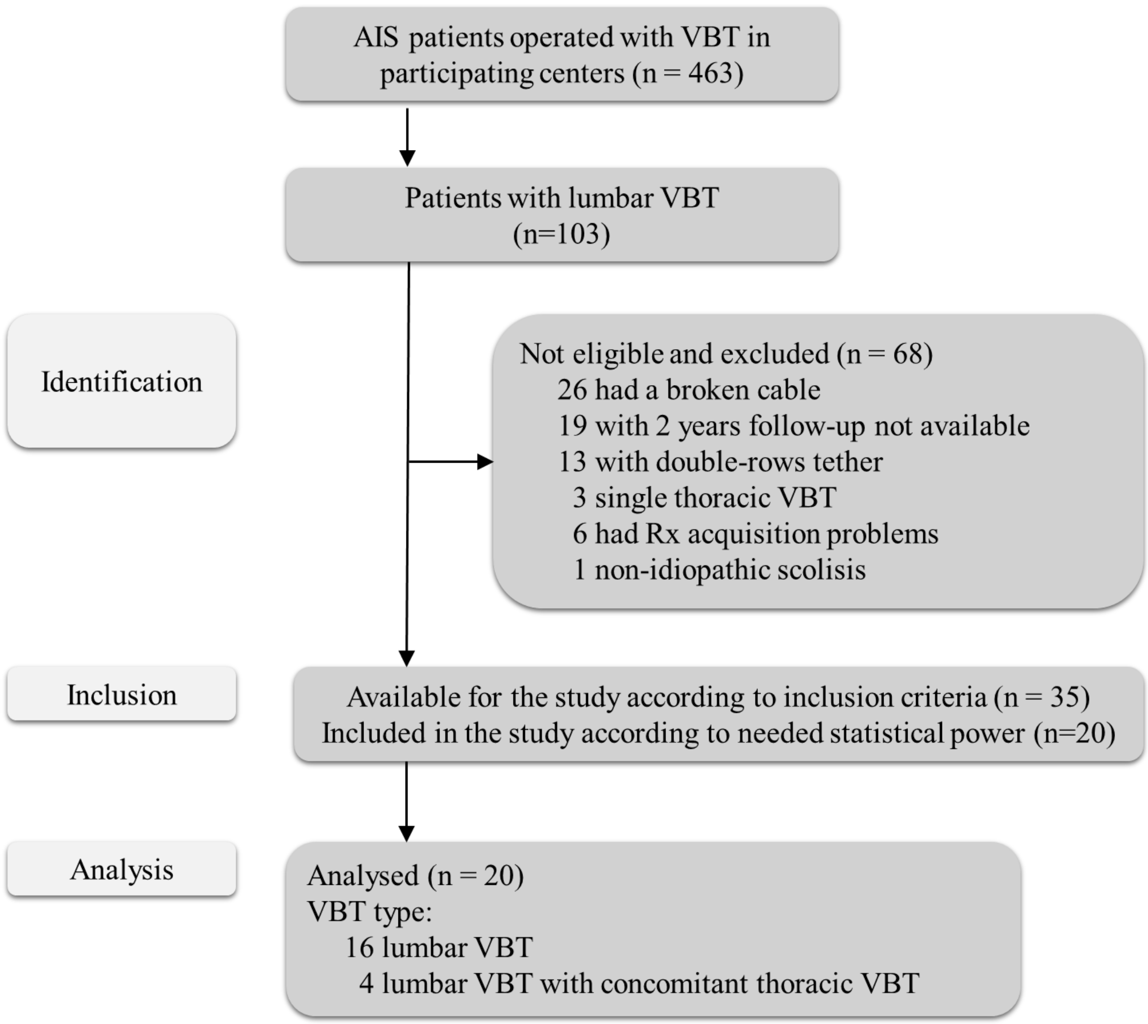

# CHAPTER 5 ARTICLE 2: TOWARDS OPTIMIZING INTRAOPERATIVE CORRECTION IN LUMBAR VERTEBRAL BODY TETHERING

## 5.1 Presentation of the article

Building on the findings of the first study, which demonstrated that intraoperative correction has a direct and predictable impact on long-term scoliosis correction, this article investigates more closely the phenomenon of over-correction. Specifically, it explores how to define an optimal intraoperative correction target to achieve a residual Cobb angle of 10° at two years in SS3A and SS3B patients.

This article, entitled "Towards Optimizing Intraoperative Correction in Lumbar Vertebral Body Tethering" was submitted to "Spine Deformity" on April 25$^{th}$, 2025 The main author contributed approximately 75% to the study, including the conceptualization, model development, simulations, and manuscript writing.

## 5.2 Article 2: TOWARDS OPTIMIZING INTRAOPERATIVE CORRECTION IN LUMBAR VERTEBRAL BODY TETHERING

Marine Gay [1,2], Nikita Cobetto, PhD, Eng.[1,2], Christiane Caouette, PhD, Eng.[1,2], A. Noelle Larson, MD[3], Isabelle Villemure PhD[1,2], Dan Hoernschemeyer, MD[4], Melanie Boeyer, PhD[4], Ron El-Hawary, MD[5], Ahmet Alanay, MD[5], Carl-Eric Aubin, PhD, ScD P.Eng.[1,2]

**Affiliations**

7- Department of Mechanical Engineering, Polytechnique Montréal, Montreal, Quebec, Canada
8- Research Center, Sainte-Justine University Hospital Center, Montreal, Quebec, Canada
9- Department of Orthopedic Surgery, Mayo Clinic, Rochester, Minnesota, USA
10- Department of Orthopaedic Surgery, University of Missouri, Columbia, Missouri, USA
11- Boston Children's Hospital, Boston, Massachusetts, USA
12- Department of Orthopedics and Traumatology, Acibadem Mehmet Ali Aydinlar University School of Medicine, Istanbul, Turkey

### 5.2.1 Abstract

**Purpose:** To identify the appropriate intraoperative correction target in lumbar vertebral body tethering (VBT) to optimize outcomes and to avoid overcorrection at skeletal maturity, by accounting for the presenting deformity, spinal stiffness, body weight and skeletal maturity.

**Methods:** Twenty cases of pediatric idiopathic scoliosis (average lumbar Cobb angle: 47°) were used to build validated 3D patient-specific finite element models, which were calibrated using Sanders score (SS), spine flexibility and body weight. Simulations of VBT were performed in the intraoperative lateral decubitus position, with actual upper (UIV: T7-T12) and lower (LIV: L2-L4) instrumented vertebrae. Ten levels of intra-operative correction (from 50% to 100%) were tested under two different growth scenarios corresponding to SS3A and SS3B. Post-operative growth and growth modulation were simulated over a 2-year period.

**Results:** Simulation showed that achieving an optimal two-year correction, with a security margin of 10°±5° required significantly different intraoperative corrections for SS 3A and 3B ($p<0.01$): 62% (40%-72%) for SS 3A and 70% (50%-79%) for SS 3B, corresponding to Cobb angles of 18° (10°-27°) and 14° (10°-20°), respectively. Patient flexibility and weight did not significantly affect the intraoperative correction target. However, patient weight and flexibility significantly influenced the variation in cord tension required to achieve maximum correction at growth completion ($p<0.05$), for both SS 3A and 3B.

**Conclusion:** The optimal intraoperative correction target in lumbar VBT appears to depend primarily on skeletal maturity. These objectives require verification that the VBT can effectively correct scoliosis and maintain this correction over time. A planning tool can define these targets more precisely, enabling the surgeon to individualize correction strategies.

**Keywords:** Pediatric idiopathic scoliosis – Lumbar Vertebral Body Tethering – Finite element modeling – Growth modulation correction – Biomechanics

### 5.2.2 Introduction

Idiopathic scoliosis is a complex, three-dimensional spinal deformity affecting 2% to 3% of the paediatric population. While its etiology remains elusive, its progression can be mechanobiologically described through the Hueter-Volkmann principle (Arkin & Katz, 1956) and Stokes' vicious circle (Stokes et al., 2006; Stokes et al., 2002; Stokes et al., 1996). These models suggest that asymmetric loading of the growth plates inhibits or promotes vertebral growth depending on the direction and magnitude of mechanical forces, thereby contributing to curve progression.

For progressive curves with a curve magnitude greater than 40°, surgical intervention is typically recommended (Addai et al., 2020). Among surgical options, vertebral body tethering (VBT) has emerged as a promising growth-modulating alternative to spinal fusion. VBT preserves spinal motion and flexibility which are particularly important at the lumbar level and has been associated with higher patient satisfaction and improved quality of life compared to fusion surgery (Courvoisier et al., 2023a; Pehlivanoglu et al., 2021). Lumbar VBT is more challenging due to greater mechanical forces, growth potential, and flexibility of this spinal segment, leading to successful correction of the lumbar curve in just 57% of cases (Boeyer, Farid, et al., 2023; C. R. Louer et al., 2024; Trobisch et al., 2023). Predicting long-term outcomes is also challenging, as the success of lumbar VBT depends heavily on the patient's remaining growth potential (C. R. Louer, Jr. et al., 2024; Pahys et al., 2025).

An accurate assessment of skeletal maturity is therefore critical. The Sanders score (SS), based on maturation of the bones in the hand and wrist (Sanders et al., 2008), provides a more precise estimation of skeletal maturity and growth potential (Sanders et al., 2017) than the traditional Risser sign, particularly during the critical pre-peak and peak growth phases (Yucekul et al., 2025). This makes a detailed assessment of skeletal maturation a potentially valuable metric for planning growth-dependent interventions such as VBT. Importantly, underestimating growth potential may lead to overcorrection, a complication that has been observed in more immature patients SS2. A prior numerical study also reported a residual but reduced risk of overcorrection in SS 3 patients (Gay et al., 2025).

Despite its promise, VBT is still associated with notable revision rates—ranging from 14% to 32%— most commonly due to under- or overcorrection (Abdullah et al., 2021; Baker et al., 2021;

Hoernschemeyer et al., 2020). One key challenge is defining the optimal intraoperative correction: surgeons must carefully balance immediate correction with the anticipated effects of growth. Yet intraoperative decision-making remains largely empirical and guided by clinical intuition, with limited support from predictive, mechanobiologically informed planning tools.

This study aims to determine the optimal intraoperative correction threshold that maximizes 2-year curve correction while minimizing the risk of overcorrection. It investigates how this threshold varies with preoperative skeletal maturity, as assessed by the Sanders score.

### 5.2.3 Methods

**Study Design and Patient Data.** Retrospective data from twenty pediatric patients with idiopathic scoliosis were included. All patients underwent lumbar VBT, with or without concomitant thoracic VBT, at three collaborating institutions. The study received prior approval from the respective institutional ethics committees.

Inclusion criteria comprised a diagnosis of idiopathic scoliosis, lumbar VBT instrumentation and a minimum follow-up of two years. Patients with a suspected broken tether, double-row instrumentation, or non-idiopathic scoliosis (e.g., neuromuscular or congenital) were excluded. The mean preoperative Cobb angle was 47° (range: 34°-63°) and the mean skeletal maturity, assessed using Sanders scores (SS), was 4.2, ranging from SS3A to SS7 (Sanders et al., 2008). Distinction was made between SS3A and SS3B (Sanders et al., 2011). Individual patient characteristics are detailed Table 1.

**Patient-specific biomechanical modeling (Figure 1).** Patient's specific 3D spinal geometries were reconstructed from postero-anterior (PA) and lateral (LAT) radiographs using a validated in-house software. The 3D reconstruction included vertebrae from T1 to L5, as well as the pelvis and rib cage. A finite element model (FEM) was generated from this 3D reconstruction incorporating osseo-ligamentous spinal structures. Intervertebral disc properties were calibrated using patient flexibility tests, with stiffness adjusted based on a predefined flexibility index correlated with curve reduction during bending tests (Petit et al., 2004). This validated FEM provides confidence in simulating intraoperative positioning, VBT instrumentation, and 2-year growth modulation correction, with an average prediction accuracy of 3° (90% statistical power) (Cobetto et al., 2025; Gay et al., 2025).

**Simulation of VBT Instrumentation.** To simulate VBT surgery, patients were first positioned in lateral decubitus, replicating the intraoperative conditions for lumbar and thoracic VBT instrumentation (Cobetto, Aubin, et al., 2018b; Martin et al., 2023). In cases involving both lumbar and thoracic VBT, the thoracic spine was tethered first.

Vertebral screws were modeled as titanium cylindrical beams placed at instrumented levels. A flexible polyethylene tether was then sequentially threaded through the vertebral screws and tensioned sequentially from the cranial to caudal levels. Maximum tension was applied at the apex, with decreasing tension toward distal vertebrae. To replicate the intraoperative technique, a temporary corrective lateral force averaging 25% of the applied tether tension was imposed during the tightening process to simulate the surgeon's manual push. Following tethering, the model was repositioned into upright standing posture, and gravitational and muscle forces were applied.

**Simulation of growth and growth modulation over 2 years.** After simulating the first erect correction, estimated longitudinal spinal growth and growth modulation were modeled over a two-year period using a validated mechanobiological algorithm (Cobetto, Aubin, et al., 2018a; Cobetto et al., 2020; Stokes, 2002; Stokes et al., 2006; Stokes et al., 2002). This algorithm relates actual vertebral stress ($\sigma$) to physiological stress ($\sigma_m$), as perceived at the vertebral epiphyseal growth plates, via the Hueter-Volkmann principle (Mehlman et al., 1997). The longitudinal growth rate (G) was computed as:

$$G = G_m * \left(1 + \beta * (\sigma - \sigma_m)\right)$$

where $\beta$ represents the sensitivity of growth modulation (1.6 $MPa^{-1}$ (Sarwark & Aubin, 2007). Growth ceased when $\beta * (\sigma - \sigma_m)$ exceeded 1 (i.e. G was set to 0). Baseline growth rate ($G_m$) was adapted based on Sanders score at surgery (SS 1–7), distinguishing between SS 3A and 3B (Table 2). Growth rates were averaged over two years, accounting variability in growth rate as skeletal maturity progressed postoperatively.

**Simulation configurations.** An initial simulation replicating each actual VBT surgery was performed to validate the model, with a mean Cobb angle deviation under 3° at two-year follow-up. For this validation study, growth and growth modulation were simulated using the actual Sanders score of the patient.

For comparison purposes, the actual surgeries were also simulated assuming alternate skeletal maturity levels, specifically at SS3A and SS3B.Building on these simulations, additional simulations systematically explored a range of intraoperative corrections (40% to 90%), by progressively adjusting tether tension and lateral forces. The goal was to identify the maximum intraoperative correction achievable to ensure an optimal correction with a safety margin (10° ± 5°) in case of additional residual growth, while maintaining the original instrumentation levels. The simulation period was set at two years to encompass the critical phase of the growth spurt, during which most of the growth occurs.

Physiological growth, and its modulation by mechanical loading, was simulated using two distinct growth profiles representative of SS3A and SS3B. For each case, the maximal intraoperative correction capable of achieving the optimal corrected curve (Cobb angle = 10° ±5°) at two years post-surgery was determined.

Using an iterative process, several simulations were realised to reach optimal correction for each case, for SS3A and SS3B. Approximately 10 simulations per patient were required to converge toward the optimal correction threshold under both SS3A and SS3B conditions, resulting in a total of 200 simulations (Figure 2).

**Data analysis.** Simulated intra-operative, immediate postoperative, and two-year Cobb angles were computed and analyzed for all simulation configurations. Normality was assessed via Shapiro-Wilk tests, and paired Student t-tests were used to identify significant differences between configurations. Statistical analyses were conducted using STATISTICA 10.0 (StatSoft Inc., Tulsa, OK, USA).

### 5.2.4 Results

**Replication of the actual surgery with the actual SS for each case.** The simulation of the actual surgeries, using each patient’s corresponding SS (Table 1), showed reduction of the preoperative lumbar Cobb angle (mean 47°, range: 34°–63°) to an average intraoperative correction of 67% (range: 35%–102%), with corresponding Cobb angles being 16° (range: 1° to 27°). This resulted in a mean immediate postoperative Cobb angle of 18° (range: 5°–37°) and a mean Cobb angle of 13° (range: -3° to 38°) at two years post-surgery.

**Replication of the actual surgery with evaluation of the skeletal maturity at SS3A and SS3B at treatment entry.** For simulations replicating the actual surgeries, intraoperative correction averaged 67% (range: 35%–102%). These cases involved patients with Sanders scores ranging from 3 to 7, with an average maturity score of SS4. When these same cases were simulated using a growth potential corresponding to SS3A (Table 3), the resulting lumbar Cobb angles showed an average overcorrection of 30%. With growth parameters set to SS3B, the average overcorrection decreased to 15%. For SS3A the residual deformation, in over-correction cases, at two years was of -10° (range -26° to -1°), and 6° (range -10° to -2°) for SS3B.

**Scenario of optimal correction for each case for SS3A, SS3B skeletal maturity at treatment entry.** Optimal targeted correction—defined as a final lumbar Cobb angle of 10° ±5°—was achieved in all simulated cases for both SS3A and SS3B. The average intraoperative Cobb angle was 18° (range: 10° to 27°) for SS3A and 14° (range: 10°-20°) for SS3B, with the SS3A group requiring a significantly higher intraoperative angle ($p<0.05$). The corresponding intraoperative corrections were 62% (range: 40%-72%) for SS3A and 70% (range: 50%-79%) for SS3B. Immediate postoperative lumbar Cobb angles averaged 22° (range: 13°-30°) for SS3A and 17° (range 11°-25°) for SS3B.

Neither patient weight nor spinal flexibility had a significant impact on the targeted intraoperative correction threshold ($p>0,05$).

**Variation of tether tension and lateral forces to optimize correction.** Compared to the forces required to replicate the actual surgery, achieving the optimal targeted correction required, on average, 10% lower tension and lateral forces in SS3A simulations, and 12% higher forces in SS3B simulations. The mean apex tension during surgical replication was 238 N (range: 100–400 N), while for the optimal targeted correction it averaged 215 N (range: 120–420 N) in SS3A simulations and 266 N (range: 150–500 N) in SS3B simulations.

Table 4 presents the increase or decrease in tension needed to achieve optimal targeted correction. Interestingly, in 12 out of 20 cases for SS3A and 5 out of 20 cases for SS3B, achieving optimal correction at skeletal maturity required applying less cord tension than in their simulated actual surgery (Table 3). This table shows the percentage variation in tension required to achieve the objective of 10° ± 5° at two years compared to the tension used to achieve the actual surgery. A variation of 0% indicates that the surgery currently being performed is optimal. A positive percentage variation indicates that more tension should have been applied, and a negative percentage variation indicates that less tension should have been applied.

Among SS 3A cases, two subgroups were identified based on the variation in tether tension required to achieve optimal correction. For patients who require less tension to achieve the optimal correction (negative percentage variation), the mean reduction in tension/lateral forces was of 28% (range: -50% to -10%) and the average patient weight for this group was of 42 kg (range: 31-58 kg). In contrast, for patients who require more tension (positive percentage variation) the mean increase of forces was of 26% (range: 0% to +110%) while the average weight for this group of patients was of 52 kg (range: 35-69 kg). The difference in weight between these two groups was statistically significant ($p<0.05$). A similar stratification was applied to SS3B cases, but the difference in weight between subgroups was not significant ($p = 0,3$).

Including all cases, two subgroups were identified according to the patient's flexibility index. The group of patients considered flexible included those whose lumbar Cobb angle had been reduced by 50% or more on the preoperative flexion film, and the group of patients considered less flexible included those whose lumbar Cobb angle had been reduced by less than 50% on the bending film. For the group of flexible cases, these also corresponded to those requiring a reduction in tension to achieve the optimal correction, with a mean value of -23% for SS3A and -5% for SS3B. Conversely, for the group of less flexible patients, these cases corresponded to those requiring an increase in tension to achieve the optimal correction, with mean values of +11% and +36% respectively for SS3A and SS3B.

### 5.2.5 Discussion

This study presents an original simulation framework designed to support the preoperative planning of lumbar VBT, by integrating growth modulation principles and patient-specific biomechanical characteristics within a validated predictive model. By incorporating key factors such as skeletal maturity, body weight, spinal flexibility, and intraoperative forces, this approach provides a rigorous, quantitative foundation to enhance current surgical decision-making. The originality of this approach lies in leveraging a validated FEM to identify the optimal intraoperative correction threshold, specifically accounting for the influence of skeletal maturity, to maximize 2-year curve correction while minimizing the risk of overcorrection. The simulation tool allows simulation of both immediate and 2 years postoperative outcomes of lumbar VBT with clinically relevant accuracy, replicating actual postoperative curve magnitudes within 3° (Cobetto, Aubin, et al., 2018b; Gay et al., 2025). This level of precision is promising and supports the potential of this framework as a robust platform for testing and comparing alternative correction strategies. Ultimately, we hope this surgical planning tool will help minimize the risk of under- or over-correction—two leading causes of revision surgery reported in the literature (Cobetto et al., 2020; Hammad et al., 2023; Martin et al., 2023).

Simulations showed that cases with more immature phenotypes (SS3A) achieved optimal correction with lower intraoperative correction targets and reduced tether tension compared to more mature preoperative phenotypes (SS3B), consistent with prior findings from validated lumbar VBT simulations (Cobetto et al., 2020; Gay et al., 2025). However, SS 3A cases also exhibited a higher risk of overcorrection when intraoperative strategies were not appropriately tailored to their remaining growth potential. This underscores the importance of considering skeletal maturity into the definition of safe and effective intraoperative correction targets.

Spinal flexibility, while not influencing the correction target itself, significantly affected the intraoperative effort required to reach it (Rushton et al., 2021). Simulations showed that stiffer curves demanded greater tether tension to achieve comparable alignment, reflecting the increased biomechanical resistance associated with reduced flexibility (Cobetto et al., 2020). Nevertheless, once target alignment was reached, growth modulation proceeded effectively regardless of initial stiffness, suggesting that flexibility mainly influences the mechanical conditions during surgery, not the long-term correction potential.

Although the model had previously been verified and validated according to the ASME V&V 40 framework (Cobetto, Aubin, et al., 2018b; Martin et al., 2023), supporting its credibility in simulating VBT outcomes with less than 3° deviation from clinical results, — certain limitations must be acknowledged, many of which are typical of numerical simulation studies. One simplifying assumption was that patient body weight remained constant over the entire growth simulation period, whereas adolescents typically experience progressive weight gain. This gain can modify the biomechanical environment, potentially amplifying flexion moments and compressive forces on the concavity of the curve, thereby reducing the effectiveness of growth modulation. Second, estimations of residual growth and its temporal distribution were approximated, which may affect the precision of long-term predictions.

Additionally, the study population primarily included patients with flexible curve types, limiting the generalizability of findings related to stiffness. Further, patients with suspected broken tethers—a frequent complication in lumbar curves—were excluded, potentially biasing results toward more favorable outcomes. The relatively small sample size further limits the statistical power and generalizability of the findings. Finally, direct measurement of intraoperative tether tension remains technically challenging. Despite these limitations, the approach of defining a targeted correction angle in the lateral decubitus position offers a practical and clinically relevant guideline for surgeons.

Despite these clearly defined limitations—many of which are inherent to numerical studies—the model has already successfully replicated growth-modulated correction within a 3° margin two years post-surgery. This promising level of accuracy suggests that a first-order estimation of growth behavior based on preoperative skeletal maturity is sufficient to reproduce clinically relevant spinal responses following VBT, including both longitudinal growth and its modulation. These encouraging results highlight the potential of this simulation framework as a valuable tool to support personalized surgical planning and improve long-term outcomes.

### 5.2.6 Conclusion

The study demonstrated that patients with more immature skeletal phenotypes (SS 3A) achieve optimal correction more easily but are at a higher risk of overcorrection. In contrast, achieving optimal intraoperative correction was more challenging in more skeletally mature patients (SS 3B), though they were less susceptible to overcorrection. These findings highlight the necessity of tailoring the surgical strategy to each patient's skeletal maturity status at the time of instrumentation to optimize outcomes and mitigate complication risks.

The observed variability in correction thresholds and mechanical requirements across simulated patients further highlights the need for individualized preoperative planning. The simulation framework presented in this study offers the potential to define patient-specific intraoperative correction targets based on key parameters such as presenting deformity, skeletal maturity, body weight, and spinal flexibility. By anticipating the mechanical demands and growth response unique to each case, this approach may help reduce the reliance on heuristic-empirical judgment during surgery.

Ultimately, this patient-specific modeling strategy contributes to a paradigm shift towards predictive, mechanobiologically informed surgical planning. It supports the surgeon in planning appropriate intraoperative correction to minimize the risks of under- or over-correction following VBT.

### 5.2.7 Tables and Figures

Table 5-1: Case-specific characteristics

| Case | Instrumented segment(s) | Sanders score (SS) | Triradiate cartilage (TRC) | Weight (kg) | Presenting TL/L Cobb angle | Preoperative bending TL/L Cobb angle | Immediate post-op TL/L Cobb | Follow-up (2 years) TL/L Cobb |
|---|---|---|---|---|---|---|---|---|
| 1 | T11-L3 | 4 | Open | 49 | 51° | 8° | 34° (40%) | 36° (37%) |
| 2 | T11-L3 | 4 | Closed | 54 | 56° | n/a | 24° (59%) | 26° (56%) |
| 3 | T10-L3 | 3 | Open | 51 | 38° | 15° | 30° (38%) | 20° (58%) |
| 4 | T10-L3 | 3 | Open | 31 | 55° | 20° | 24° (56%) | 1° (98%) |
| 5 | T11-L3 | 4 | Closed | 49 | 52° | 6° | 24° (55%) | 24° (55%) |
| 6 | T10-L3 | 6 | Closed | 38 | 51° | 15° | 17° (66%) | 10° (80%) |
| 7 | T10-L3 | 6 | Closed | 58 | 38° | 16° | 12° (68%) | 11° (71%) |
| 8 | T10-L3 | 3B | Open | 54 | 41° | n/a | 23° (48%) | 24° (45%) |
| 9 | T11-L3 | 6 | Closed | 39 | 39° | 25° | 9° (76%) | 7° (81%) |
| 10 | T10-L2 | 3A | Closed | 48 | 40° | 18° | 9° (77%) | -4° (110%) |
| 11 | T10-L3 | 6 | Closed | 48 | 34° | 17° | 9° (75%) | 11° (69%) |
| 12 | T12-L4 | 4 | Closed | 69 | 39° | 14° | 20° (55%) | 18° (59%) |
| 13 | T7-L3 | 4 | Closed | 54 | 63° | 11° | 28° (59%) | 25° (63%) |
| 14 | T7-L3 | 3A | Open | 35 | 38° | 9° | 33° (13%) | 7° (82%) |
| 15 | T7-L3 | 4 | Closed | 31 | 45° | 2° | 6° (87%) | -7° (116%) |
| 16 | T11-L3 | 4 | Closed | 48 | 54° | 15° | 7° (87%) | 2° (96%) |
| 17 | T7-T12 // T12-L4 | 7 | Closed | 51 | 40° | 8° | 18° (55%) | 14° (65%) |
| 18 | T5-T10 // T10-L4 | 3B | Closed | 40 | 66° | 30° | 23° (65%) | 15° (77%) |
| 19 | T5-T10 // T10-L3 | 3 | Closed | 38 | 60° | 21° | 26° (57%) | 21° (65%) |
| 20 | T5-T10 // T10-L3 | 4 | Closed | 48 | 47° | 9° | 21° (55%) | 11° (77%) |

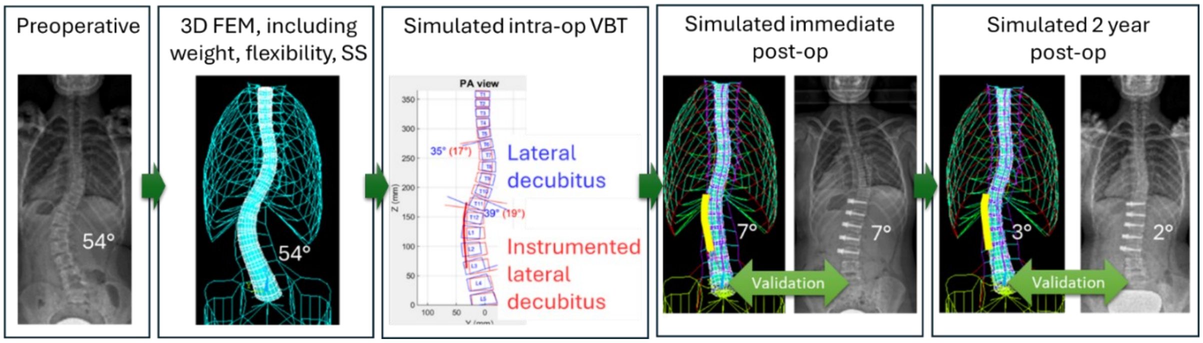


Figure 5-1: Patient specific biomechanical modelling

Table 5-2: Model growth rates as a function of Sanders Score at treatment entry point

| **Sanders score at surgery** | **Thoracic growth rate (mm/year/vertebra)** | **Lumbar growth rate (mm/year/vertebra)** |
|---|---|---|
| SS 2 | 1,80 | 2,13 |
| SS 3A | 2,01 | 2,38 |
| SS 3B | 1,21 | 1,42 |
| SS 4 | 0,89 | 1,05 |
| SS 5 | 0,64 | 0,75 |
| SS 6 | 0,42 | 0,49 |
| SS 7 | 0,28 | 0,33 |

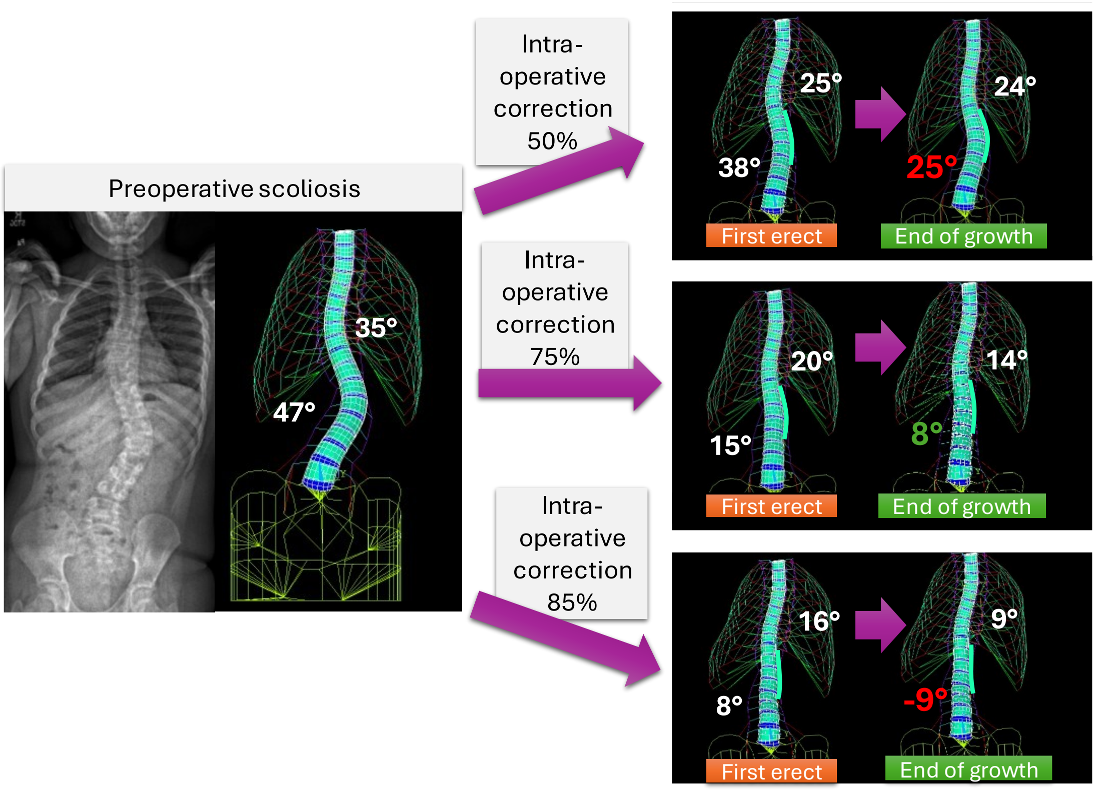


Figure 5-2: Example of three simulations run for a specific case with three different levels of intra-operative correction.

Table 5-3: Residual deformation at two years for the surgical parameters of the actual surgery, for SS3A and SS3B residual growth

| **Case** | **1** | **2** | **3** | **4** | **5** | **6** | **7** | **8** | **9** | **10** | **11** | **12** | **13** | **14** | **15** | **16** | **17** | **18** | **19** | **20** |
|---|---|---|---|---|---|---|---|---|---|---|---|---|---|---|---|---|---|---|---|---|
| **SS3A** | 38° | 12° | 23° | 0° | 11° | -2° | 1° | 17° | 3° | -5° | -4° | 12° | 21° | 10° | -20° | -26° | 5° | -1° | 9° | 1° |
| **SS3B** | 38° | 17° | 24° | 10° | 17° | 5° | 6° | 20° | 6° | 0° | -2° | 15° | 24° | 18° | -10° | -10° | 9° | 8° | 16° | 9° |

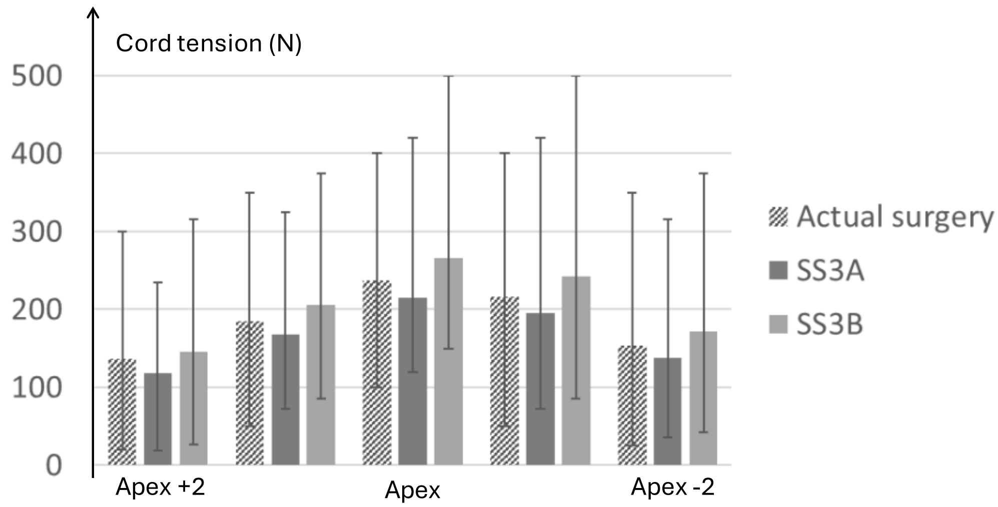


Figure 5-3: Comparison of simulated cord tension (around the apex) needed in the actual surgery vs. optimal targeted correction scenarios for SS 3A and 3B

Table 5-4 : Percentage increase or decrease in tether tension (around the apex) required to achieve optimal targeted correction compared to the simulated actual surgery for the two simulated presenting SS (3A and 3B). Positive values indicate an increase; negative values indicate a reduction.

| Case | Variation in tension (%) for SS 3A | Variation in tension (%) for SS 3B |
|---|---|---|
| 1 | 110% | 150% |
| 2 | 0% | 30% |
| 3 | 30% | 50% |
| 4 | -30% | 10% |
| 5 | 0% | 20% |
| 6 | -20% | 0% |
| 7 | -20% | 0% |
| 8 | 45% | 70% |
| 9 | -10% | -5% |
| 10 | -30% | -20% |
| 11 | -30% | -25% |
| 12 | 0% | 5% |
| 13 | 20% | 20% |
| 14 | 0% | 20% |
| 15 | -50% | -40% |
| 16 | -50% | -30% |
| 17 | -10% | 30% |
| 18 | -30% | 5% |
| 19 | -10% | 20% |
| 20 | -40% | 0% |

# CHAPTER 6 General discussion

This master thesis contributes to advancing the understanding and optimization of lumbar VBT by leveraging a validated patient-specific FEM framework capable of simulating both the intraoperative correction and the long-term growth modulation response of the spine. This modelling approach directly addresses several of the current limitations of lumbar VBT surgery, where decision-making often relies on heuristic and empirical knowledge rather than mechanobiological-scientific-based tools. This study provides new insight into how key patient-specific parameters — including skeletal maturity, body weight, spinal flexibility, and intraoperative correction — interact to influence growth modulation outcomes. This is of particular importance for lumbar VBT, which presents unique biomechanical challenges compared to thoracic VBT due to greater flexibility, higher mobility, and growth potential of the lumbar spine.

By systematically exploring multiple surgical scenarios across a diverse and representative number of simulated lumbar VBT cases, the results of this work contribute to refining surgical strategies for lumbar VBT. The findings confirm the central role of preoperative skeletal maturity (Sanders Score) in determining both the achievable intraoperative correction and the expected contribution of growth modulation in long-term outcomes. In parallel, they reveal that patient weight — while not directly impacting growth modulation capacity — plays a critical role in shaping the biomechanical environment, both intraoperatively and post-operatively. Heavier patients require greater corrective forces to achieve the desired alignment during surgery and are also exposed to higher spinal loading during growth, which can influence the long-term maintenance of correction. Altogether, this work supports the emerging concept that VBT planning should move towards personalized, simulation-informed strategies rather than fixed correction thresholds, in line with recent clinical observations (Pahys et al., 2025; Photopoulos et al., 2024; Todderud et al., 2025) but extending them through a mechanobiological and quantitative modelling perspective.

## 6.1 Influence of skeletal maturity on growth modulation

The study confirmed that skeletal maturity at the time of surgery is a major determinant of growth modulation potential. Less mature patients (SS 3A) benefit from significant additional correction through growth modulation, whereas in more mature patients (≥ SS 4), correction is mainly dependent of the intraoperative results. For patients at SS 4 and above, growth modulation contributed to statistically significant but clinically limited improvements (<5°), corroborating clinical observations of reduced growth capacity in these patients (Pahys et al., 2025; Photopoulos et al., 2024). These results emphasize the clinical importance of achieving near-complete intraoperative correction in skeletally mature patients, given that growth modulation alone is unlikely to compensate for suboptimal initial alignment. Conversely, for SS3 A/B patients, caution is required to avoid overcorrection due to their greater growth potential, reinforcing the need for personalized intraoperative targets (Pahys et al., 2025).

## 6.2 Role of spinal flexibility

Spinal flexibility was shown to primarily influence the biomechanical effort required intraoperatively rather than the long-term correction achieved through growth modulation. Stiffer curves necessitated higher tether tension and corrective forces to reach a given alignment target. However, once the desired alignment was achieved, subsequent growth modulation was not significantly affected by flexibility, indicating that flexibility is a critical intraoperative parameter but not a limiting factor for long-term outcomes. It should be noted that considering the exclusion criteria for the study, our cohort is mainly composed by patient with flexible curves. According to surgeons, less flexible curves do not correct as well, so they are less likely to be corrected by VBT and have a higher risk of under-correction.

## 6.3 Impact of weight on long term correction

Patient body weight emerged as another key parameter influencing lumbar VBT outcomes. Heavier patients were more prone to curve progression during growth, even when similar intraoperative corrections were achieved. This finding is consistent with the idea that higher body mass increases spinal loading, possibly reducing the effectiveness of growth modulation. Nevertheless, simulations suggested that when intraoperative correction exceeded 70%, the adverse effect of higher weight was mitigated, emphasizing the importance of achieving sufficient correction intraoperatively. It should be noted that the model assumed constant body weight throughout the simulated period, potentially underestimating the effect of adolescent weight gain on spinal biomechanics. A higher BMI is associated with faster biological maturation, so growth is influenced by the weight of patients. In particular, puberty-related weight gain, depending on whether it occurs before, after or during the growth spurt, may have an effect on growth that has not yet been precisely studied (Durda-Masny et al., 2019).

## 6.4 Inter-patients variability and the need for patient-specific modeling

One of the most important findings from this study is that VBT outcomes can vary a lot from one patient to another. This variability comes mainly from the combined effects of three key factors: how mature the skeleton is at the time of surgery, how flexible the spine is, and how much the patient weighs. This variability challenges the concept of universal correction targets and underscores the relevance of patient-specific biomechanical modelling in surgical planning. The FEM developed in this master thesis provides a solid foundation towards the development of advanced decision-support tool to predict:

- The probability of successful correction based on individual patient characteristics.
- The expected contribution of growth modulation.
- The risk of under- or over-correction depending on intraoperative strategy.

Such predictive modelling promotes a paradigm shift towards a more personalized and biomechanically informed approach to lumbar VBT surgery, reducing empirical decision-making and providing objective, patient-specific surgical targets.

## 6.5 Limitations of the model

Despite encouraging results and validation of the FEM (<3° deviation on average), which is well within the baseline clinical measurement error for scoliosis assessment (Kumar et al., 2024), several limitations must be recognized. Growth modulation was simulated over a fixed period of two years, without extending predictions beyond this timeframe. The model did not account for common complications such as tether breakage - frequent in lumbar curves - or growth retardation. In addition, the patient's weight was considered constant, potentially underestimating biomechanical changes over time. The cohort was mainly composed of flexible curves, which limits the possibilities of generalization to more rigid deformities.

Another important element is the intraoperative cable tension, which was estimated rather than directly measured clinically. It is important to note, however, that the amount of tension applied to the tether does not solely depend on the desired correction but is also strongly influenced by patient positioning during surgery. This positioning can facilitate an initial reduction of the curve, meaning that lower tether forces might be sufficient intraoperatively compared to the forces required to maintain correction in a neutral, upright posture. Ultimately, while the precise intraoperative tension may vary, the critical factor remains the intraoperative alignment target to be achieved. This is precisely what our simulation framework helps to define more reliably, considering patient-specific characteristics and growth potential.

Despite these limitations, the model successfully reproduced the first-order trends of growth-modulated correction within clinically acceptable margins — well aligned with the expected biomechanical behavior and within the variability typically observed in clinical practice. This supports its value as a practical and informative tool to guide preoperative planning of VBT, particularly in providing patient-specific insights to refine surgical strategy and anticipate long-term outcomes.

# CHAPTER 7 CONCLUSION AND PERSPECTIVES

The objective of this study was to biomechanically model and analyze the appropriate intraoperative correction target in lumbar VBT to maximize two-year outcomes while avoiding overcorrection in pediatric idiopathic scoliosis patient, accounting for the presenting deformity, spinal stiffness, body weight and skeletal maturity. Thanks to the FEM developed (Cobetto et al., 2020; Cobetto et al., 2025; Cobetto, Parent, et al., 2018; Gay et al., 2025; Martin et al., 2023) and adapted to the lumbar VBT (Gay et al., 2025; Martin et al., 2023), various parameters combinations were tested in two different studies. The first one tested three levels of intra-operative correction (35%, 50%, 70%) for four different skeletal maturity evaluation (SS: 3A 3B, 4, 5). Our simulations suggest that a target of 70% intraoperative correction may be appropriate for lumbar VBT surgery, except for SS 3A curves, where 50% correction could be sufficient. It also showed that 70% of intra-operative correction could lead to over-correction in SS 3 cases. This was the motivation for the second study. For each case, we tested two different residual growth aiming at finding the intra-operative correction leading to optimal correction at two years (0° ±5°). It has been shown that an optimal intraoperative correction threshold can be identified as a function of SS. Although a retrospective study such as ours can provide guidelines for surgeons, this information needs to be adapted to each individual case. The model could therefore be used for preoperative surgical planning in a prospective study. Additionally, to further enhance clinical applicability, a safety margin could be incorporated into the model to account for cases with higher residual growth potential, thereby minimizing the risk of overcorrection.

This Master thesis aimed to improve the understanding and optimization of lumbar VBT by using a validated patient-specific FEM framework. By capturing the complex biomechanical and biological mechanisms involved in scoliosis correction and growth modulation, this project provides new tools and knowledge to help better plan and personalize VBT surgeries.

The results confirmed the central hypothesis of this work: The intra-operative correction target can be adjusted and optimized to maximize both immediate and long-term (two-year) scoliosis correction, while minimizing the risks of curve progression or over-correction at skeletal maturity. Simulations demonstrated that insufficient intraoperative correction almost systematically resulted in under-correction at two years, regardless of other patient-specific factors. Conversely, adequate correction levels led to favorable outcomes, while excessive intraoperative correction increased the risk of over-correction, particularly in the most immature patients (SS3A).

Moreover, this study identified, for the first time, optimal average intraoperative correction thresholds adapted to the patient's skeletal maturity. These thresholds represent valuable guidance for surgical planning, allowing surgeons to better balance the immediate correction applied during surgery with the anticipated effects of growth modulation. Importantly, these findings were consistent with current clinical knowledge but also offered new, quantitative insight to support surgical decision-making.

Beyond the influence of skeletal maturity, this project also provided new understanding of how other key parameters affect lumbar VBT outcomes. The results confirmed that spinal flexibility mainly impacts technical feasibility and intraoperative effort, without limiting the long-term potential of growth modulation. Additionally, patient body weight was shown to influence both the intraoperative forces required and the risk of curve progression during growth, emphasizing the importance of adapting the surgical strategy in heavier patients.

Perhaps one of the most relevant contributions of this project is the demonstration of the considerable inter-patient variability in VBT outcomes. This variability highlights the limits of applying fixed correction thresholds and reinforces the importance of moving towards a patient-specific approach, where modelling tools can guide the planning process based on the unique characteristics of each patient.

Beyond these results, this project provides solid foundations for the development of predictive and patient-specific tools to support lumbar VBT planning. By improving the understanding of key biomechanical and biological mechanisms involved in VBT outcomes, this work contributes to refining surgical strategies and moving towards a more personalized approach to scoliosis treatment, towards the development of predictive, patient-specific planning tools in lumbar VBT. The potential clinical impact of such tools appears promising. They could support surgeons in better anticipating the evolution of scoliosis post-surgery, tailoring intraoperative correction to patient-specific parameters, and reducing the risk of complications.

Future work should now focus on expanding the modelling framework, including:

- Increasing the number and diversity of clinical cases to strengthen statistical power and improve generalizability.

- Integrating the simulation of potential complications such as tether breakage.
- Accounting for long-term growth and weight evolution dynamics.
- Exploring the integration of additional patient-specific factors such as muscle activation, activity level, and sagittal balance.
- Moving towards the development of a user-friendly planning platform, suitable for clinical integration.

Altogether, this work represents a promising step towards more personalized and optimized surgical planning in lumbar VBT, responding to the needs expressed by surgeons for better tools to understand, anticipate, and control the long-term effects of growth modulation in adolescent idiopathic scoliosis.

# REFERENCES

Abdullah, A., Parent, S., Miyanji, F., Smit, K., Murphy, J., Skaggs, D., Gupta, P., Vitale, M., Ouellet, J., Saran, N., Cho, R. H., Group, P. S. S., & El-Hawary, R. (2021). Risk of early complication following anterior vertebral body tethering for idiopathic scoliosis. *Spine Deform*, *9*(5), 1419-1431. https://doi.org/10.1007/s43390-021-00326-2

Addai, D., Zarkos, J., & Bowey, A. J. (2020). Current concepts in the diagnosis and management of adolescent idiopathic scoliosis. *Child's Nervous System*, *36*(6), 1111-1119. https://doi.org/10.1007/s00381-020-04608-4

Ağırdil, Y. (2020). The growth plate: a physiologic overview. *EFORT Open Rev*, *5*(8), 498-507. https://doi.org/10.1302/2058-5241.5.190088

Aldegheri, R., & Agostini, S. (1993). A chart of anthropometric values. *J Bone Joint Surg Br*, *75*(1), 86-88. https://doi.org/10.1302/0301-620x.75b1.8421044

Amini, S., Veilleux, D., & Villemure, I. (2010). Tissue and cellular morphological changes in growth plate explants under compression. *Journal of Biomechanics*, *43*(13), 2582-2588. https://doi.org/10.1016/j.jbiomech.2010.05.010

Angelliaume, A., Pfirrmann, C., Alhada, T., & Sales de Gauzy, J. (2025). Non-operative treatment of adolescent idiopathic scoliosis. *Orthopaedics & Traumatology: Surgery & Research*, *111*(1, Supplement), 104078. https://doi.org/https://doi.org/10.1016/j.otsr.2024.104078

Arkin, A. M., & Katz, J. F. (1956). The effects of pressure on epiphyseal growth; the mechanism of plasticity of growing bone. *J Bone Joint Surg Am*, *38-a*(5), 1056-1076.

Baker, C. E., Milbrandt, T. A., & Larson, A. N. (2021). Anterior Vertebral Body Tethering for Adolescent Idiopathic Scoliosis: Early Results and Future Directions. *Orthopedic Clinics of North America*, *52*(2), 137-147. https://doi.org/https://doi.org/10.1016/j.ocl.2021.01.003

Baroncini, A., & Courvoisier, A. (2023). The different applications of Vertebral Body Tethering - Narrative review and clinical experience. *J Orthop*, *37*, 86-92. https://doi.org/10.1016/j.jor.2023.02.012

Baroncini, A., Courvoisier, A., Berjano, P., Migliorini, F., Eschweiler, J., Kobbe, P., Hildebrand, F., & Trobisch, P. D. (2022). The effects of vertebral body tethering on sagittal parameters: evaluations from a 2-years follow-up. *European Spine Journal*, *31*(4), 1060-1066. https://doi.org/10.1007/s00586-021-07076-9

Baroncini, A., Migliorini, F., Eschweiler, J., Hildebrand, F., & Trobisch, P. (2022). The timing of tether breakage influences clinical results after VBT. *Eur Spine J*, *31*(9), 2362-2367. https://doi.org/10.1007/s00586-022-07321-9

Baroncini, A., Trobisch, P., Eschweiler, J., & Migliorini, F. (2022). Analysis of the risk factors for early tether breakage following vertebral body tethering in adolescent idiopathic scoliosis. *Eur Spine J*, *31*(9), 2348-2354. https://doi.org/10.1007/s00586-022-07231-w

Boeyer. (2023). *Skeletal Immaturity & VBT: How Utilization of a Sanders Score Can Better Predict Growth Modulation* ICEOS, Boeyer, M. E., Farid, S., Wiesemann, S., & Hoernschemeyer, D. G. (2023). Outcomes of vertebral body tethering in the lumbar spine. *Spine Deform*, *11*, 909-918. https://doi.org/10.1007/s43390-023-00662-5

Boeyer, M. E., Groneck, A., Alanay, A., Neal, K. M., Larson, A. N., Parent, S., Newton, P., Miyanji, F., Haber, L., & Hoernschemeyer, D. G. (2023). Operative differences for posterior spinal fusion after vertebral body tethering: Are we fusing more levels in the end? *Eur Spine J*, *32*(2), 625-633. https://doi.org/10.1007/s00586-022-07450-1

Brinker, M. R., & O'Connor, D. P. (2008). Basic sciences. *Review of Orthopaedics. 5th ed. Philadelphia: Saunders*, 1-36.

Bruno, A. G., Burkhart, K., Allaire, B., Anderson, D. E., & Bouxsein, M. L. (2017). Spinal Loading Patterns From Biomechanical Modeling Explain the High Incidence of Vertebral Fractures in the Thoracolumbar Region. *J Bone Miner Res*, *32*(6), 1282-1290. https://doi.org/10.1002/jbmr.3113

Cheng, J. C., Castelein, R. M., Chu, W. C., Danielsson, A. J., Dobbs, M. B., Grivas, T. B., Gurnett, C. A., Luk, K. D., Moreau, A., Newton, P. O., Stokes, I. A., Weinstein, S. L., & Burwell, R. G. (2015). Adolescent idiopathic scoliosis. *Nat Rev Dis Primers*, *1*, 15030. https://doi.org/10.1038/nrdp.2015.30

Cheriet, F., Laporte, C., Kadoury, S., Labelle, H., & Dansereau, J. (2007). A novel system for thE 3-D reconstruction of the human spine and rib cage from biplanar X-ray images. *IEEE Trans Biomed Eng*, *54*(7), 1356-1358. https://doi.org/10.1109/TBME.2006.889205

Cobetto, N., Aubin, C. E., & Parent, S. (2018a). Contribution of Lateral Decubitus Positioning and Cable Tensioning on Immediate Correction in Anterior Vertebral Body Growth Modulation. *Spine Deform*, *6*(5), 507-513. https://doi.org/10.1016/j.jspd.2018.01.013

Cobetto, N., Aubin, C. E., & Parent, S. (2018b). Surgical Planning and Follow-up of Anterior Vertebral Body Growth Modulation in Pediatric Idiopathic Scoliosis Using a Patient-Specific Finite Element Model Integrating Growth Modulation. *Spine Deform*, *6*(4), 344-350. https://doi.org/10.1016/j.jspd.2017.11.006

Cobetto, N., Aubin, C. E., & Parent, S. (2020). Anterior Vertebral Body Growth Modulation: Assessment of the 2-year Predictive Capability of a Patient-specific Finite-element Planning Tool and of the Growth Modulation Biomechanics. *Spine (Phila Pa 1976)*, *45*(18), E1203-e1209. https://doi.org/10.1097/brs.0000000000003533

Cobetto, N., Fecteau, M.-È., Caouette, C., Gay, M., Larson, A. N., Hoernschemeyer, D., Boeyer, M., El-Hawary, R., Alanay, A., & Aubin, C.-E. (2025). Multicenter Validation of a Surgical Planning Tool for Lumbar Vertebral Body Tethering Simulating Growth Modulation Over Two Years. *Submited to Spine Deformity*.

Cobetto, N., Parent, S., & Aubin, C. E. (2018). 3D correction over 2years with anterior vertebral body growth modulation: A finite element analysis of screw positioning, cable tensioning and postoperative functional activities. *Clin Biomech (Bristol, Avon)*, *51*, 26-33. https://doi.org/10.1016/j.clinbiomech.2017.11.007

Courvoisier, A., Baroncini, A., Jeandel, C., Barra, C., Lefevre, Y., Solla, F., Gouron, R., Métaizeau, J. D., Maximin, M. C., & Cunin, V. (2023a). Vertebral Body Tethering in AIS

Management-A Preliminary Report. *Children (Basel)*, *10*(2). https://doi.org/10.3390/children10020192

Courvoisier, A., Baroncini, A., Jeandel, C., Barra, C., Lefevre, Y., Solla, F., Gouron, R., Métaizeau, J. D., Maximin, M. C., & Cunin, V. (2023b). Vertebral Body Tethering in AIS Management-A Preliminary Report. *Children (Basel)*, *10*(2), 192. https://doi.org/10.3390/children10020192

Delorme, S., Petit, Y., de Guise, J. A., Labelle, H., Aubin, C. E., & Dansereau, J. (2003). Assessment of the 3-d reconstruction and high-resolution geometrical modeling of the human skeletal trunk from 2-D radiographic images. *IEEE Trans Biomed Eng*, *50*(8), 989-998. https://doi.org/10.1109/tbme.2003.814525

Dimeglio, Bonnel, F., & Canavese, F. (2011). Normal Growth of the Spine and Thorax. In *The Growing Spine, Management of Spinal Disorders in Young Children* (pp. 13-42). Springer. https://doi.org/10.1007/978-3-540-85207-0

Dimeglio, A., Bonnel, F., & Canavese, F. (2011). Normal Growth of the Spine and Thorax. In *The Growing Spine* (pp. 13-42). https://doi.org/10.1007/978-3-540-85207-0_2

DiMeglio, A., Canavese, F., & Charles, Y. P. (2011). Growth and adolescent idiopathic scoliosis: when and how much? *J Pediatr Orthop*, *31*(1 Suppl), S28-36. https://doi.org/10.1097/BPO.0b013e318202c25d

Durda-Masny, M., Hanć, T., Czapla, Z., & Szwed, A. (2019). BMI at menarche and timing of growth spurt and puberty in Polish girls - longitudinal study. *Anthropol Anz*, *76*(1), 37-47. https://doi.org/10.1127/anthranz/2019/0920

Farnum, C. E., Nixon, A., Lee, A. O., Kwan, D. T., Belanger, L., & Wilsman, N. J. (2000). Quantitative three-dimensional analysis of chondrocytic kinetic responses to short-term stapling of the rat proximal tibial growth plate. *Cells Tissues Organs*, *167*(4), 247-258. https://doi.org/10.1159/000016787

Figueroa, C., Jozsa, F., & Le, P. H. (2025). Anatomy, Bony Pelvis and Lower Limb: Pelvis Bones. In *StatPearls*. StatPearls Publishing

Copyright © 2025, StatPearls Publishing LLC.

Fries, P., Runge, V. M., Kirchin, M. A., Watkins, D. M., Buecker, A., & Schneider, G. (2008). Magnetic resonance imaging of the spine at 3 Tesla. *Semin Musculoskelet Radiol*, *12*(3), 238-252. https://doi.org/10.1055/s-0028-1083107

Friis, E. A., Arnold, P. M., & Goel, V. K. (2017). 9 - Mechanical testing of cervical, thoracolumbar, and lumbar spine implants. In E. Friis (Ed.), *Mechanical Testing of Orthopaedic Implants* (pp. 161-180). Woodhead Publishing. https://doi.org/https://doi.org/10.1016/B978-0-08-100286-5.00009-3

Gay, M., Cobetto, N., Caouette, C., Larson, A. N., Villemure, I., Hoernschemeyer, D., Boeyer, M., El-Hawary, R., Alanay, A., & Aubin, C.-E. (2025). Patient-Specific Biomechanical Modelling of Intraoperative Scoliosis Correction on the 2-Year Outcomes for Lumbar Vertebral Body Tethering *Submited to Spine Deformity*.

Ghanem, I., & Rizkallah, M. (2020). The impact of residual growth on deformity progression. *Ann Transl Med*, *8*(2), 23. https://doi.org/10.21037/atm.2019.11.67

Guy, A., & Aubin, C. (2023). Finite element simulation of growth modulation during brace treatment of adolescent idiopathic scoliosis. *J Orthop Res*, *41*(9), 2065-2074. https://doi.org/10.1002/jor.25553

Hammad, A. M., Balsano, M., & Ahmad, A. A. (2023). Vertebral body tethering: An alternative to posterior spinal fusion in idiopathic scoliosis? *Front Pediatr*, *11*, 1133049. https://doi.org/10.3389/fped.2023.1133049

Henson, B., Kadiyala, B., & Edens, M. A. (2023). *Anatomy, Back, Muscles*. https://www.ncbi.nlm.nih.gov/books/NBK537074/

Hoernschemeyer, D. G., Boeyer, M. E., Robertson, M. E., Loftis, C. M., Worley, J. R., Tweedy, N. M., Gupta, S. U., Duren, D. L., Holzhauser, C. M., & Ramachandran, V. M. (2020). Anterior Vertebral Body Tethering for Adolescent Scoliosis with Growth Remaining: A Retrospective Review of 2 to 5-Year Postoperative Results. *J Bone Joint Surg Am*, *102*(13), 1169-1176. https://doi.org/10.2106/jbjs.19.00980

Hoernschemeyer, D. G., Boeyer, M. E., Tweedy, N. M., Worley, J. R., & Crim, J. R. (2021). A preliminary assessment of intervertebral disc health and pathoanatomy changes observed two years following anterior vertebral body tethering. *Eur Spine J*, *30*(12), 3442-3449. https://doi.org/10.1007/s00586-021-06972-4

Kumar, S., Awadhiya, B., Ratnakumar, R., Thalengala, A., Areeckal, A. S., & Nanjappa, Y. (2024). A Review of 3D Modalities Used for the Diagnosis of Scoliosis. *Tomography*, *10*(8), 1192-1204. https://doi.org/10.3390/tomography10080090

Lin, H., Aubin, C.-E., Parent, S., & Villemure, I. (2009). Mechanobiological bone growth: comparative analysis of two biomechanical modeling approaches. *Medical and Biological Engineering and Computing*, *47*(4), 357-366. https://doi.org/10.1007/s11517-008-0425-9

Lonner, B., Weiner, D. A., Miyanji, F., Hoernschemeyer, D. G., Eaker, L., & Samdani, A. F. (2022). Vertebral Body Tethering: Rationale, Results, and Revision. *Instr Course Lect*, *71*, 413-425.

Louer, C. R., Jr., Upasani, V. V., Hurry, J. K., Nian, H., Farnsworth, C. L., Newton, P. O., Parent, S., & El-Hawary, R. (2024). Growth modulation response in vertebral body tethering depends primarily on magnitude of concave vertebral body growth. *Spine Deform*, *12*(6), 1689-1698. https://doi.org/10.1007/s43390-024-00909-9

Louer, C. R., Upasani, V. V., Hurry, J. K., Nian, H., Farnsworth, C. L., Newton, P. O., Parent, S., El-Hawary, R., & Pediatric Spine Study, G. (2024). Growth modulation response in vertebral body tethering depends primarily on magnitude of concave vertebral body growth. *Spine Deformity*, *12*(6), 1689-1698. https://doi.org/10.1007/s43390-024-00909-9

Martin, S., Cobetto, N., Larson, A. N., & Aubin, C. E. (2023). Biomechanical modeling and assessment of lumbar vertebral body tethering configurations. *Spine Deform*, *11*, 1041-1048. https://doi.org/10.1007/s43390-023-00697-8

Mathew, S. E., Hargiss, J. B., Milbrandt, T. A., Stans, A. A., Shaughnessy, W. J., & Larson, A. N. (2022). Vertebral body tethering compared to posterior spinal fusion for skeletally immature adolescent idiopathic scoliosis patients: preliminary results from a matched case-control study. *Spine Deform*, *10*(5), 1123-1131. https://doi.org/10.1007/s43390-022-00519-3

McDonald, T. C., Shah, S. A., Hargiss, J. B., Varghese, J., Boeyer, M. E., Pompliano, M., Neal, K., Lonner, B. S., Larson, A. N., Yaszay, B., Newton, P. O., & Hoernschemeyer, D. G. (2022). When successful, anterior vertebral body tethering (VBT) induces differential segmental growth of vertebrae: an in vivo study of 51 patients and 764 vertebrae. *Spine Deform*, *10*(4), 791-797. https://doi.org/10.1007/s43390-022-00471-2

Mehlman, C., Araghi, A., & Roy, D. (1997). Hyphenated history: the Hueter-Volkmann law. *American journal of orthopedics (Belle Mead, N.J.)*, *26*, 798-800.

Menger, R. P., & Sin, A. H. (2025). Adolescent Idiopathic Scoliosis. In *StatPearls*. StatPearls Publishing

Copyright © 2025, StatPearls Publishing LLC.

Mishreky, A., Parent, S., Miyanji, F., Smit, K., Murphy, J., Bowker, R., Al Khatib, N., & El-Hawary, R. (2022). Body mass index affects outcomes after vertebral body tethering surgery. *Spine Deform*, *10*(3), 563-571. https://doi.org/10.1007/s43390-021-00455-8

Newton, P. O., Bartley, C. E., Bastrom, T. P., Kluck, D. G., Saito, W., & Yaszay, B. (2020). Anterior Spinal Growth Modulation in Skeletally Immature Patients with Idiopathic Scoliosis: A Comparison with Posterior Spinal Fusion at 2 to 5 Years Postoperatively. *The Journal of bone and joint surgery. American volume*, *102*(9), 769-777. https://doi.org/10.2106/JBJS.19.01176

O'Brien, Kuklo, Blanke, & Lenke. (2005). *Radiographic Measurement Manual* (M. Michael F. O'Brien, M. Timothy R. Kuklo, R. Kathy M. Blanke, & M. Lawrence G. Lenke, Eds.). Medtronic Sofamor Danek.

Oliver, J., & Middleditch, A. (1991). *Functional Anatomy of the Spine*.

Otomo, N., Funao, H., Yamanouchi, K., Isogai, N., & Ishii, K. (2022). Computed Tomography-Based Navigation System in Current Spine Surgery: A Narrative Review. *Medicina (Kaunas)*, *58*(2). https://doi.org/10.3390/medicina58020241

Pahys, J. M., Hwang, S. W., McGarry, M., Quinonez, A., Grewal, H., & Samdani, A. F. (2025). Incidence and Predictors of Growth Modulation and Overcorrection after Anterior Vertebral Body Tethering. *Spine (Phila Pa 1976)*. https://doi.org/10.1097/brs.0000000000005306

Pehlivanoglu, T., Oltulu, I., Erdag, Y., Akturk, U. D., Korkmaz, E., Yildirim, E., Sarioglu, E., Ofluoglu, E., & Aydogan, M. (2021). Comparison of clinical and functional outcomes of vertebral body tethering to posterior spinal fusion in patients with adolescent idiopathic scoliosis and evaluation of quality of life: preliminary results. *Spine Deform*, *9*(4), 1175-1182. https://doi.org/10.1007/s43390-021-00323-5

Petit, Y., Aubin, C. É., & Labelle, H. (2004). Patient-specific mechanical properties of a flexible multi-body model of the scoliotic spine. *Medical and Biological Engineering and Computing*, *42*(1), 55-60. https://doi.org/10.1007/BF02351011

Photopoulos, G., Hurry, J., Bansal, A., Miyanji, F., Parent, S., Murphy, J., El-Hawary, R., & Pediatric Spine Study, G. (2024). Differential vertebral body growth is maintained after vertebral body tethering surgery for idiopathic scoliosis: 4-year follow-up on 888 periapical vertebrae and 592 intervertebral discs. *Spine Deformity*, *12*(5), 1369-1379. https://doi.org/10.1007/s43390-024-00874-3

Raballand, C., Cobetto, N., Larson, A. N., & Aubin, C. E. (2023). Prediction of post-operative adding-on or compensatory lumbar curve correction after anterior vertebral body tethering. *Spine Deform*, *11*(1), 27-33. https://doi.org/10.1007/s43390-022-00558-w

Raitio, A., Syvänen, J., & Helenius, I. (2022). Vertebral Body Tethering: Indications, Surgical Technique, and a Systematic Review of Published Results. *J Clin Med*, *11*(9), 2576. https://doi.org/10.3390/jcm11092576

Raj, P. P. (2008). Intervertebral disc: anatomy-physiology-pathophysiology-treatment. *Pain Pract*, *8*(1), 18-44. https://doi.org/10.1111/j.1533-2500.2007.00171.x

Risser, J. C. (1958). The Iliac apophysis; an invaluable sign in the management of scoliosis. *Clin Orthop*, *11*, 111-119.

Rushton, P. R. P., Nasto, L., Parent, S., Turgeon, I., Aldebeyan, S., & Miyanji, F. (2021). Anterior Vertebral Body Tethering for Treatment of Idiopathic Scoliosis in the Skeletally Immature: Results of 112 Cases. *Spine (Phila Pa 1976)*, *46*(21), 1461-1467. https://doi.org/10.1097/brs.0000000000004061

Ryan, P. M., Puttler, E. G., Stotler, W. M., & Ferguson, R. L. (2007). Role of the triradiate cartilage in predicting curve progression in adolescent idiopathic scoliosis. *J Pediatr Orthop*, *27*(6), 671-676. https://doi.org/10.1097/BPO.0b013e3181373ba8

Sanders, J. O. (2015). Normal growth of the spine and skeletal maturation. *Seminars in Spine Surgery*, *27*(1), 16-20. https://doi.org/https://doi.org/10.1053/j.semss.2015.01.005

Sanders, J. O., Howell, J., & Qiu, X. (2011). Comparison of the Paley method using chronological age with use of skeletal maturity for predicting mature limb length in children. *J Bone Joint Surg Am*, *93*(11), 1051-1056. https://doi.org/10.2106/jbjs.J.00384

Sanders, J. O., Khoury, J. G., Kishan, S., Browne, R. H., Mooney, J. F., 3rd, Arnold, K. D., McConnell, S. J., Bauman, J. A., & Finegold, D. N. (2008). Predicting scoliosis progression from skeletal maturity: a simplified classification during adolescence. *J Bone Joint Surg Am*, *90*(3), 540-553. https://doi.org/10.2106/jbjs.G.00004

Sanders, J. O., Qiu, X., Lu, X., Duren, D. L., Liu, R. W., Dang, D., Menendez, M. E., Hans, S. D., Weber, D. R., & Cooperman, D. R. (2017). The Uniform Pattern of Growth and Skeletal Maturation during the Human Adolescent Growth Spurt. *Sci Rep*, *7*(1), 16705. https://doi.org/10.1038/s41598-017-16996-w

Sarwark, J., & Aubin, C.-É. (2007). Growth Considerations of the Immature Spine. *JBJS*, *89*(suppl_1), 8-13. https://doi.org/10.2106/JBJS.F.00314

Saurabh, S. (2019). *DIRECT NUMERICAL SIMULATION OF HUMAN PHONATION*

Sauri-Barraza, J. C. (2023). [Early-onset scoliosis: pathophysiology, diagnosis and treatment]. *Acta Ortop Mex*, *37*(2), 99-105. (Escoliosis de inicio temprano: fisiopatología, diagnóstico y tratamiento.)

Shankar, D., Eaker, L., von Treuheim, T. D. P., Tishelman, J., Silk, Z., & Lonner, B. S. (2022). Anterior vertebral body tethering for idiopathic scoliosis: how well does the tether hold up? *Spine Deform*, *10*(4), 799-809. https://doi.org/10.1007/s43390-022-00490-z

Stokes, I. A. (2002). Mechanical effects on skeletal growth. *J Musculoskelet Neuronal Interact*, *2*(3), 277-280.

Stokes, I. A., Aronsson, D. D., Dimock, A. N., Cortright, V., & Beck, S. (2006). Endochondral growth in growth plates of three species at two anatomical locations modulated by mechanical compression and tension. *J Orthop Res*, *24*(6), 1327-1334. https://doi.org/10.1002/jor.20189

Stokes, I. A., Mente, P. L., Iatridis, J. C., Farnum, C. E., & Aronsson, D. D. (2002). Enlargement of growth plate chondrocytes modulated by sustained mechanical loading. *J Bone Joint Surg Am*, *84*(10), 1842-1848. https://doi.org/10.2106/00004623-200210000-00016

Stokes, I. A., Spence, H., Aronsson, D. D., & Kilmer, N. (1996). Mechanical modulation of vertebral body growth. Implications for scoliosis progression. *Spine (Phila Pa 1976)*, *21*(10), 1162-1167. https://doi.org/10.1097/00007632-199605150-00007

Todderud, J., Milbrandt, T., Baroncini, A., Petcharaporn, M., Marks, M., Hoernschemeyer, D., Newton, P., Parent, S., Alanay, A., Miyanji, F., Lonner, B., Neal, K., Yaszay, B., Blakemore, L., Shah, S., Haber, L., Samdani, A., & Larson, A. N. (2025). Outcomes and complications of vertebral body tethering by patient gender. *Spine Deformity*. https://doi.org/10.1007/s43390-024-01035-2

Treuheim, T. D. P. v., Eaker, L., Markowitz, J., Shankar, D., Meyers, J., & Lonner, B. (2023). Anterior Vertebral Body Tethering for Scoliosis Patients With and Without Skeletal Growth Remaining: A Retrospective Review With Minimum 2-Year Follow-Up. *International journal of spine surgery*, *17*(1), 6-16. https://doi.org/10.14444/8357

Trobisch, P., Baroncini, A., Berrer, A., & Da Paz, S. (2022). Difference between radiographically suspected and intraoperatively confirmed tether breakages after vertebral body tethering for idiopathic scoliosis. *Eur Spine J*, *31*(4), 1045-1050. https://doi.org/10.1007/s00586-021-07107-5

Trobisch, P. D., & Baroncini, A. (2021). Preliminary outcomes after vertebral body tethering (VBT) for lumbar curves and subanalysis of a 1- versus 2-tether construct. *Eur Spine J*, *30*(12), 3570-3576. https://doi.org/10.1007/s00586-021-07009-6

Trobisch, P. D., Castelein, R., & Da Paz, S. (2023). Radiographic outcome after vertebral body tethering of the lumbar spine. *European Spine Journal*, *32*(6), 1895-1900. https://doi.org/10.1007/s00586-023-07740-2

vBizzoca, D., Piazzolla, A., Moretti, L., Vicenti, G., Moretti, B., & Solarino, G. (2022). Anterior vertebral body tethering for idiopathic scoliosis in growing children: A systematic review. *World J Orthop*, *13*(5), 481-493. https://doi.org/10.5312/wjo.v13.i5.481

Voller, T., Cameron, P., Watson, J., & Phadnis, J. (2020). The growth plate: anatomy and disorders. *Orthopaedics and Trauma*, *34*(3), 135-140. https://doi.org/https://doi.org/10.1016/j.mporth.2020.03.006

Wan, S. H. T., Guldeniz, O., Yeung, M. H. Y., Cheung, J. P. Y., Kwan, K. Y. H., & Cheung, K. M. C. (2023). Inter-screw index as a novel diagnostic indicator of tether breakage. *Spine Deform*. https://doi.org/10.1007/s43390-023-00679-w

Weinstein, S. L., Dolan, L. A., Wright, J. G., & Dobbs, M. B. (2013). Effects of bracing in adolescents with idiopathic scoliosis. *N Engl J Med*, *369*(16), 1512-1521. https://doi.org/10.1056/NEJMoa1307337

Weiss, H. R., Karavidas, N., Moramarco, M., & Moramarco, K. (2016). Long-Term Effects of Untreated Adolescent Idiopathic Scoliosis: A Review of the Literature. *Asian Spine J*, *10*(6), 1163-1169. https://doi.org/10.4184/asj.2016.10.6.1163

Yang, M. J., Samdani, A. F., Pahys, J. M., Quinonez, A., McGarry, M., Grewal, H., & Hwang, S. W. (2023). What Happens After a Vertebral Body Tether Break? Incidence, Location, and Progression with 5-Year Follow-up. *Spine (Phila Pa 1976)*. https://doi.org/10.1097/brs.0000000000004665

Yucekul, A., Akpunarli, B., Durbas, A., Zulemyan, T., Havlucu, I., Ergene, G., Senay, S., Yalinay Dikmen, P., Turgut Balci, S., Karaarslan, E., Yavuz, Y., Yilgor, C., & Alanay, A. (2021). Does vertebral body tethering cause disc and facet joint degeneration? A preliminary MRI study with minimum two years follow-up. *Spine J*, *21*(11), 1793-1801. https://doi.org/10.1016/j.spinee.2021.05.020

Yucekul, A., Yilgor, C., Demirci, N., Gurel, I. E., Orhun, O., Karaman, M. I., Durbas, A., Lim, H. S., Zulemyan, T., Yavuz, Y., & Alanay, A. (2025). A comparative analysis of axial and appendicular skeletal maturity staging systems through assessment of longitudinal growth and curve modulation after VBT surgery. *Eur Spine J*, *34*(1), 251-262. https://doi.org/10.1007/s00586-024-08488-z

Zhang, H., Fan, Y., Ni, S., & Pi, G. (2022). The preliminary outcomes of vertebral body tethering in treating adolescent idiopathic scoliosis: a systematic review. *Spine Deform*, *10*(6), 1233-1243. https://doi.org/10.1007/s43390-022-00546-0

Zimmermann, E. A., Bouguerra, S., Londono, I., Moldovan, F., Aubin, C.-E., & Villemure, I. (2017). In situ deformation of growth plate chondrocytes in stress-controlled static vs dynamic compression. *Journal of Biomechanics*, *56*, 76-82. https://doi.org/10.1016/j.jbiomech.2017.03.008

# APPENDIX A ARTICLE 3: MULTICENTER VALIDATION OF A SURGICAL PLANNING TOOL FOR LUMBAR VERTEBRAL BODY TETHERING SIMULATING GROWTH MODULATION OVER TWO YEARS

## A1.1 Presentation of the article

The article presented in this section develops the adaptation and validation of a finite element model used to simulate VBT surgery followed by growth and growth modulation over a two-year period, making it possible to predict residual deformation at two years with an accuracy of 3° ± 2°.

This article entitled “Multicenter Validation of a Surgical Planning Tool for Lumbar Vertebral Body Tethering Simulating Growth Modulation Over Two Years” was accepted by the journal Spine Deformity on May 22$^{nd}$, 2025 with a 10% author's contribution.

## A1.2 Article 3: MULTICENTER VALIDATION OF A SURGICAL PLANNING TOOL FOR LUMBAR VERTEBRAL BODY TETHERING SIMULATING GROWTH MODULATION OVER TWO YEARS

Nikita Cobetto, PhD, Eng.[1,2], Marie-Ève Fecteau [1,2], Christiane Caouette, PhD, Eng.[1,2], Marine Gay [1,2], A. Noelle Larson, MD[3], Dan Hoernschemeyer, MD[4], Melanie Boeyer, PhD[4], Ron El-Hawary, MD[5], Ahmet Alanay, MD[5], Carl-Eric Aubin, PhD, ScD P.Eng.[1,2]

**Affiliations**

1- Department of Mechanical Engineering, Polytechnique Montréal, Montreal, Quebec, Canada
2- Research Center, Sainte-Justine University Hospital Center, Montreal, Quebec, Canada
3- Department of Orthopedic Surgery, Mayo Clinic, Rochester, Minnesota, USA
4- Department of Orthopaedic Surgery, University of Missouri, Columbia, Missouri, USA
5- Division of Orthopedic Surgery, IWK Health Centre, Halifax, Nova Scotia, Canada
6- Department of Orthopedics and Traumatology, Acibadem Mehmet Ali Aydinlar University School of Medicine, Istanbul, Turkey

**Abstract**

**Purpose:** Vertebral body tethering (VBT) for lumbar curves is gaining popularity due to greater growth potential than thoracic spine and benefits of preserved flexibility. Predicting long-term correction remains challenging, with high revision rates and complications (14%-32%) including under-/over-correction, tether breakage, adding-on. This study aimed to validate a planning tool for lumbar VBT using a patient-specific finite element model (FEM) integrating mechanobiological growth modulation as a function of preoperative skeletal maturity.

**Methods:** Thirty-five retrospective idiopathic scoliosis patients who underwent lumbar VBT, with or without concomitant thoracic VBT, were included. A personalized FEM calibrated to preoperative spine deformity, flexibility and weight was created using 3D radiographic reconstructions. The FEM was linked to an algorithm integrating spine growth and mechanobiological growth modulation, calibrated using preoperative Sanders score. VBT surgery was simulated to replicate immediate postoperative correction and predict two-year correction. Simulated Cobb angles, sagittal curves, and apical axial rotation were compared to actual two-year radiographic measurements.

**Results:** Preoperative Cobb angles averaged 37 ± 12° (thoracic) and 48 ± 9° (thoraco-lumbar/lumbar). Immediate postoperative correction was 38 ± 15% and 59 ± 16%, with two-year corrections of 44±24% and 73±21%, respectively. Simulated postoperative correction was accurate within 3° (Cobb angles), while simulated two-year outcomes were accurate within 3° (Cobb), 2° (kyphosis), 4° (lordosis), and 3° (axial rotation), showing no significant differences from reference results ($p<0.05$; statistical power 90%).

**Conclusion:** The patient-specific FEM and growth modulation algorithm accurately predicted two-year correction. This tool can support preoperative planning, reduce surgeon variability, and potentially improve VBT outcomes by providing a predictive tool to help surgical planning.

**Keywords:** Idiopathic Scoliosis – Growth modulation – Vertebral Body Tethering – Finite element modeling – Biomechanics

## Introduction

For the treatment of idiopathic pediatric scoliosis with progressive Cobb angle above 40°, surgical intervention may be considered to prevent further curve progression [1,2]. Vertebral body tethering (VBT) is a promising fusionless technique for children with remaining growth potential. The surgery involves tensioning a cable connected to vertebral implants on the convex side of the scoliotic curve [3]. According to the Hueter-Volkmann principle, the aim is to induce growth modulation, with the tensioned cable applying compressive forces to epiphyseal growth plates of vertebrae on the convex side thus limiting growth, while promoting growth on the concave side. The instrumentation has the potential to allow the deformity to be corrected progressively, using the patient's remaining growth [4].

VBT is gaining popularity to treat lumbar curves in addition to thoracic curves, because it better maintains spinal flexibility compared to other surgeries such as spinal fusion [5,6]. The patients' long-term quality of life has shown to correlate with preserved spinal motion [7]. However, since the lumbar segment supports higher loads and has increased mobility, long-term correction following lumbar VBT remains difficult to predict and the revision rate is high (14% and 32%) [8,9]. Frequent complications can occur, such as under- or overcorrection, broken tether, and junctional deformities (adding-on). Current reoperation rates exceed those of spinal fusion surgeries, potentially endangering the use of the VBT procedure [10].

To further understand the biomechanics of VBT, a finite element model (FEM) was developed to simulate the postoperative correction and evaluate forces exerted by the device on vertebral epiphyseal growth plates. Previous studies aimed to predict postoperative correction immediately after thoracic VBT and achieved accurate simulations to within 4° of actual correction following two years of growth and vertebral modulation [11,12]. However, this model was only validated for thoracic VBT. Subsequently, a preliminary study adapted the planning tool for lumbar VBT, but was limited to a small number of cases from a single center and did not account for patients' skeletal maturity at treatment initiation [13].

The aim of this study was to further improve and validate the predictive capacity of a surgical planning tool applied to lumbar VBT, enabling the biomechanical effect of growth modulation to be modeled and predicted over 2 years as a function of preoperative skeletal maturity, in a multicenter study.

**Methods**

**Patient data.** This multicenter study was conducted retrospectively on patients who underwent VBT at three participating centers. Inclusion criteria included cases with idiopathic scoliosis, treated with lumbar VBT with or without a concomitant thoracic VBT, with a minimum of two-year postoperative follow-up. Cases with a suspected broken tether, double rows, or non-idiopathic scoliosis (e.g., muscular or congenital scoliosis) were excluded.

**Patient specific finite element modeling**. For each case, a 3D reconstruction of the spine, pelvis and rib cage was built from preoperative coronal and sagittal radiographs, using an in-house validated software. The 3D reconstruction was used to generate a patient-specific osseo-ligamentous FEM using the Ansys 20.2 finite element software package (Ansys Inc., Canonsburg, Pennsylvania, USA) (Fig. 1A). Thoracic and lumbar vertebrae, pelvis, rib cage, intervertebral disks, ligaments and costo-transverse joints were modeled using 3D beams, tension-only springs and contact elements. Modeling of vertebrae included vertebral bodies, distinct upper and lower epiphyseal growth plates, pedicles, transverse and spinous processes. Local deformations (wedging) of the vertebrae and intervertebral discs were considered during the construction of the FEM through detailed vertebral modeling based on positioning of vertebral body corners from the 3D reconstruction. The mechanical properties attributed to the elements were taken from the literature and determined through experiments on human cadavers [14-18]. The FEM was calibrated to the patient's preoperative weight and flexibility, using available fulcrum bending, lateral bending or traction films. A flexibility index was assigned based on the percentage reduction of the curve during the flexibility tests, and intervertebral disks mechanical properties were calibrated to the previously determined flexibility index [19].

**Simulation of intraoperative positioning and gravity forces.** To simulate VBT surgery, intraoperative lateral decubitus positioning of the patient was first modeled. To numerically represent this position change and corresponding curvature correction, forces representing the patient's weight were applied to the center of mass of each vertebra, while lateral forces were applied on the convex side of the major curve. Force magnitudes were based on published values [20-22]. Boundary conditions included blocking the pelvis and ribs on the concave side of the instrumented curve in all three planes to represent contact with the operating table, while T1 only movement in the caudal-cranial direction was allowed.

**Simulation of immediate VBT correction.** The VBT device installation was simulated on the lateral decubitus geometry, following the actual surgical approach. Vertebral screws were modeled on vertebrae's lateral side at selected instrumented levels. Screws were represented as hollow cylinders with titanium mechanical properties, modeled using 3D beam elements, rigidly fixed to the vertebrae. The cable, modeled with 3D beam elements and polyethylene properties, was sequentially tightened. For the tightening sequence, one cable end was fixed to the cranial screw, while the other end passed through the next caudal screw. Tensioning was achieved by applying a downward compressive intervertebral force and securing the cable to the caudal screw, progressing level by level. A temporary lateral force averaging 25% of cable tension was applied during tightening to simulate the surgeon's force. Tension peaked at the apex and decreased towards the ends of the instrumented levels. For bilateral VBT, the same steps were applied, with the addition of a patient repositioning step to install the thoracic and lumbar VBT on either side (Fig. 1B).

The model was returned to an upright position to obtain immediate postoperative correction and force equilibrium, with adjustments made to match intraoperative corrections and first postoperative radiographs. Vertical and lateral forces from previous step were removed, and gravitational forces were applied to vertebral centers of mass. To globally represent muscle and soft tissue effects, an optimization process defined the compensatory transverse forces based on preoperative curve magnitude, patient's weight and flexibility. Boundary conditions remained consistent with those used in the earlier steps.

**Simulation of 2 years of spine growth and mechanobiological growth modulation.** Simulated immediate postoperative results were used to model the remaining spine growth and the mechanobiological growth modulation of the instrumented spine over two years using a validated algorithm [23-25] (Fig. 1C). This algorithm relies on in-vivo correlations and mechanobiological principles based on Hueter-Volkman principle, expressed by an equation relating actual stresses ($\sigma$) and normal physiological stresses ($\sigma_m$) at vertebral epiphyseal growth plates [23, 24] (1). The final longitudinal growth rate (G) was calculated as a function of these stresses:

$$G = G_m * (1 - \beta * (\sigma - \sigma_m)) \quad (1)$$

The sensitivity parameter ($\beta$), averaged at 1.6 $MPa^{-1}$ [26], determined growth response. When $\beta*(\sigma - \sigma_m)$ exceeded 1, G was set to 0, representing growth arrest. The baseline growth rate ($G_m$) was adjusted to patient's preoperative skeletal maturity status, with $G_m$ varying according to Sanders score (SS). Growth rates were modeled for SS1 to SS7, differentiating stages SS3A and SS3B, and represented as constants based on growth duration at each stage and were obtained from in-house data (Table 1).

Interface for the simulation tool. A Matlab-based interface (MATLAB version 9.14.0, R2023a, The MathWorks Inc, Natick, Massachusetts, USA) was developed to streamline and sequence simulation steps, using the tool without requiring programming skills. Users can input parameters such as X-rays, 3D reconstructions, flexibility, weight, SS, instrumented vertebral levels, intervertebral correction to be achieved, and the growth period. The remaining simulation steps are automated, guiding users seamlessly through the interface.

**Simulation tool validation.** The FEM was validated following the ASME V&V40:2018 framework [27]. The context of use (COU) pertains to a tool designed to simulate biomechanical effects of growth modulation following VBT, aiming to predict correction at two years. Its ultimate purpose is to support surgical planning by enabling scenario comparisons, allowing the surgeon to confirm their choice prior to instrumentation. The risk linked to the simulation tool (combining model influence and decision-making impact) was categorized as high-low. The model's influence was deemed high, as its results strongly shape surgical planning decisions. However, the impact was classified as low since the final decision depends on the interplay between biomechanical data and surgeon expertise. Based on the COU, verification, validation and uncertainty quantification (VVUQ) actions were undertaken. Verification included comparative studies assessing sensitivity to patient-related parameters (spinal flexibility, weight, growth rate) and surgical parameters (instrumented levels, cable tension) [13,28-30]. To enhance the reliability of computed compressive stresses, these were compared to published data from in silico and in vivo studies [31-35] and were found to be consistent with these data. Validation consisted of comparisons with actual radiographic data, to show the concordance between simulated and real postoperative corrections. Main thoracic (MT) and thoracolumbar/lumbar (TLL) constant Cobb angles (considering preoperative upper- and lower-end vertebrae for all measurements), as well as T4-T12 kyphosis, L1-L5 lordosis and lumbar apical axial rotation, were measured on 2-yr postoperative radiographs, and on simulated 3D geometries. Radiographic measurements were performed by two examiners to minimize bias. Transverse plane rotation of apical vertebrae [11-13] was derived from the 3D reconstruction or automatically generated as simulation outputs.

Statistical analysis was conducted using Minitab 18 Statistical Software (Minitab Inc., State College, Pennsylvania, USA). Data normality was verified with a Shapiro-Wilk test. Equivalence between simulated and actual angles was tested using a paired equivalence statistical test (alpha level=0.05). A 5° variability threshold, based on reported 3D indices measurement variability

(Cobb angles, kyphosis, lordosis and apical axial rotation) [36], was used to determine equivalence. The test assessed whether simulated indices were sufficiently close to actual corrections. In the case of a statistical equivalence test, a value of $p<0.05$ confirms equivalence. Statistical power analysis, based on study data (sample size, equivalence limits of ±4° from prior studies [11,12], mean difference of 3°, and standard deviation of 2°), confirmed the sample size provided adequate power.

**Results**

The study included 35 cases, with 23 undergoing single lumbar VBT and 12 receiving bilateral instrumentation. Mean presenting Cobb angle was of 37±12° (12°-63°) for the MT curve and 48±9° (29°-66°) for TLL. Mean presenting T4-T12 kyphosis angle was 30°±9° (13°-46°), while the L1-L5 lordosis angle was of 49°±16° (19°-66°). The mean apical vertebra rotation for the instrumented lumbar segment before VBT instrumentation was of 7°±13° (5°-26°). Average preoperative skeletal maturity Sanders score was of 4±1 (2-7), while the Risser stage was 1±1 (0-4). Mean preoperative patient weight was 45±9kg (29-69kg). According to the Shapiro-Wilk statistical test, all preoperative indices followed a normal distribution ($p>0.05$).

The immediate average actual correction was of 23±6° for MT Cobb angle, and 20±9° for TLL which were respectively simulated to within 3±2° and 2±1° (absolute difference) when using the FEM (23±7° and 20±8° for simulated MT and TLL Cobb angles respectively). After two years of growth, actual corrections were of 20±9° for MT and 13±11° for TLL, whereas simulated Cobb angles after two years of spine growth and mechanobiological growth modulation were of 20±10° and 13±10°. For the simulated two years postoperative correction, the average of the differences was of 3±2° for both MT and TLL Cobb angles (statistically equivalent, $p<0.05$, with a 90% statistical power; Table 2).

The average of actual T4-T12 kyphosis and L1-L5 lordosis angles showed slight changes immediately after surgery and after two years, but these differences were not statistically significant ($p<0.05$). Simulated kyphosis and lordosis were predicted within 4° at two years postoperatively. For the actual L1-L5 lordosis, two patients were excluded due to significant posture variations between follow-ups, as confirmed by radiographic evidence. Axial rotation assessment was not possible in a subgroup of 10 patients due to poor image quality on certain radiographs at preoperative or two-year visits, preventing identification of key anatomical landmarks. After two years, actual lumbar apical rotation showed slight correction, averaging 1±7°. Simulated predictions for axial rotation changes were accurate within 3±2° over the same period (Table 2). Equivalence tests confirmed that simulated and actual postoperative measurements at two years were statistically equivalent ($p<0.05$), with a 90% statistical power (Table 2).

Mean stress values at the lumbar apical vertebral epiphyseal growth plates of the instrumented segment were 0.5 MPa (convex side) and -1.3 MPa (concave side) before surgery. Post-surgery, stresses were inverted to reach -0.9 MPa on the concavity and -0.3 MPa on the convexity of the lumbar curve (positive stress values indicate tension loads, while negative values indicate compression loads) (Fig2).

**Discussion**

This study highlights the predictive capabilities of our advanced numerical simulation tool for modeling the effects of growth modulation after lumbar VBT surgery. Unlike traditional surgical planning methods, which often rely on heuristics and empirical approximations, this tool leverages a physics-based approach to provide reliable, patient-specific predictions of VBT's complex and time-dependent effects. By offering actionable insights, it aims to reduce variability and uncertainty in surgical outcomes, empowering surgeons to make more informed preoperative decisions and ultimately improving long-term patient care.

The simulations accurately predicted immediate and two-year postoperative Cobb angle corrections with clinically relevant accuracy (absolute difference<3°), aligning with prior studies [11-13]. The simulation results also show reasonable agreement in the sagittal plane for kyphosis and lordosis angles, with slightly greater variability in the lumbar segment remaining statistically non-significant. This variability likely stems from experimental factors, such as non-standardized radiographic acquisition methods across centers or visits, and differences in patient posture or arm positioning affecting sagittal angle measurements [37]. However, as VBT's primary effect is in the coronal plane, this variability minimally influences the assessment of the device’s growth modulation effect. Also, the assessment of pressures exerted on vertebral endplates confirmed that VBT correction predominantly occurs in the coronal plane, with the instrumentation effectively rebalancing epiphyseal growth plate stresses, underscoring VBT's potential for growth modulation.

Calibrating the tool to patient-specific preoperative skeletal maturity status expanded its applicability to a broader pediatric population undergoing VBT, enhancing accessibility for more surgeons. The multicenter trial added variability to the validation population, considering factors like skeletal maturity, weight, spine flexibility and surgical techniques. Building on prior models for thoracic and lumbar VBT [12,13], this study enhances the tool's clinical utility and scope.

This model was developed following the ASME V&V40 standard, a valuable framework for comprehensively evaluating the relevance and adequacy of VVUQ activities to establish model credibility. While results confirm the model's adequacy based on 3D measurement indices, complementary sensitivity studies and additional patient data from other centers would enhance statistical power and account for variability in surgical techniques, increasing generalizability.

Certain simplifications were made based on the simulation tool's COU, with limitations to be acknowledged. Muscle modeling and activation were not explicitly represented but were indirectly accounted for by considering the overall efforts required to stabilize the spine. Prior studies suggest that improved balance post-correction reduces muscle activity needed to maintain posture [11]. Further analyses are needed to clarify relationships between instrumentation parameters, balance changes, and forces on growth plates, and risks like adding-on, progression and cable breakage. Second, rib cage stiffness was modeled globally, without explicit rib cage growth, as the focus was on lumbar spine correction rather than thoracic volumetric or rotational changes. While rib hump correction with lumbar VBT remains poorly understood and its influence on outcomes appears minimal, this simplification aligns with the study's scope. Lastly, spinal flexibility was estimated using various types of flexibility films, prone to variability and low reproducibility. These factors may affect flexibility calibration, force estimates, and growth modulation. Nonetheless, when applied as a comparative tool for surgical scenario analysis, these limitations are minimized since all scenarios are uniformly impacted.

**Conclusion**

This study validates the numerical simulation tool for predicting correction results immediately after lumbar VBT and following two years of growth modulation. It also improves biomechanical understanding of the stresses exerted on the growth plates during device use; insights unattainable with the radiographs currently used in clinical practice. Over time, this tool has the potential to improve surgical planning and reduce uncertainty associated with VBT by factoring in complementary biomechanical parameters.

Future studies could leverage this tool to analyze the effect of tether tension or breakage, as well as to develop strategies to prevent over- or under-correction by accounting for each patient's residual growth potential. Although this study retrospectively used FEM to validate two-year correction outcomes, prospective applications could assess its utility in planning lumbar VBT procedures and refining surgical parameter selection. Ultimately, the tool could serve as an aid to rationalize and optimize surgical planning, guide intraoperative corrections, and tailor configurations to each patient’s specific treatment needs.

**Tables and Figures Legends** (listed in order of appearance in the text)

**Fig. 1** A) Presenting deformity, 3D reconstruction obtained from biplanar radiographs, and the corresponding FEM calibrated to patient's flexibility, weight and skeletal maturity (Sanders score); B) Predicted and actual immediate postoperative correction; C) Predicted and actual 2-year growth and growth modulation (ligaments and vertebral posterior elements not shown for clarity)

Table 1 – Growth rate used for growth and growth modulation simulation based on Sanders score and corresponding to skeletal maturity at treatment beginning.

Table 2 – Actual vs. simulated 2-year surgical 3D outcomes

(* Indicates a p-value<0.05, confirming equivalence)

**Fig. 2** A) Presenting deformity; B) Visual representation of stresses distribution on the lumbar apical growth plates (back view) for the presenting deformity; C) Simulated immediate postoperative correction; D) Visual representation of stresses distribution on the lumbar apical growth plates (back view) following immediate postoperative (first erect)

**References**


1. Lonstein JE, Carlson JM (1984) The prediction of curve progression in untreated idiopathic scoliosis during growth. J Bone Joint Surg Am 66(7):1061-71. PMID: 6480635.
2. Charles YP, Daures JP, de Rosa V, Diméglio A (2006) Progression risk of idiopathic juvenile scoliosis during pubertal growth. Spine (Phila Pa 1976). 1;31(17):1933-42. doi: 10.1097/01.brs.0000229230.68870.97. PMID: 16924210.
3. Shankar D, Eaker L, von Treuheim TDP, Tishelman J, Silk Z, Lonner BS (2022) Anterior vertebral body tethering for idiopathic scoliosis: how well does the tether hold up? Spine Deformity 10(4):799-809. doi: 10.1007/s43390-022-00490-z. Epub 2022 Mar 8. PMID: 35258844.
4. Louer, C.R., Upasani, V.V., Hurry, J.K. et al. (2024) Growth modulation response in vertebral body tethering depends primarily on magnitude of concave vertebral body growth. Spine Deform 12, 1689–1698 https://doi.org/10.1007/s43390-024-00909-9
5. Buyuk AF, Milbrandt TA, Mathew SE, Larson AN (2021) Measurable Thoracic Motion Remains at 1 Year Following Anterior Vertebral Body Tethering, with Sagittal Motion Greater Than Coronal Motion. J Bone Joint Surg Am. 103(24):2299-2305. doi: 10.2106/JBJS.20.01533. PMID: 34270505.
6. Pahys JM, Samdani AF, Hwang SW, Warshauer S, Gaughan JP, Chafetz RS (2022) Trunk Range of Motion and Patient Outcomes After Anterior Vertebral Body Tethering Versus Posterior Spinal Fusion: Comparison Using Computerized 3D Motion Capture Technology. J Bone Joint Surg Am. 104(17):1563-1572. doi: 10.2106/JBJS.21.00992.
7. Pehlivanoglu T, Oltulu I, Erdag Y, Akturk UD, Korkmaz E, Yildirim E, Sarioglu E, Ofluoglu E, Aydogan M (2021) Comparison of clinical and functional outcomes of vertebral body tethering to posterior spinal fusion in patients with adolescent idiopathic scoliosis and evaluation of quality of life: preliminary results. Spine Deformity 9(4):1175-1182. doi: 10.1007/s43390-021-00323-5.
8. Hoernschemeyer DG, Boeyer ME, Robertson ME, Loftis CM, Worley JR, Tweedy NM, Gupta SU, Duren DL, Holzhauser CM, Ramachandran VM (2020) Anterior Vertebral Body Tethering for Adolescent Scoliosis with Growth Remaining: A Retrospective Review of 2 to 5-Year Postoperative Results. J Bone Joint Surg Am. 102(13):1169-1176. doi: 10.2106/JBJS.19.00980. PMID: 32618924

9. Baker, C.E., Kiebzak, G.M., Neal, K.M (2021) Anterior vertebral body tethering shows mixed results at 2-year follow-up. Spine Deform. 9:481–489. doi.org/10.1007/s43390-020-00226-x
10. Roser MJ, Askin GN, Labrom RD, Zahir SF, Izatt M, Little JP (2023) Vertebral body tethering for idiopathic scoliosis: a systematic review and meta-analysis. Spine Deform. 11(6):1297-1307. doi: 10.1007/s43390-023-00723-9
11. Cobetto N, Aubin CE, Parent S (2018) Surgical Planning and Follow-up of Anterior Vertebral Body Growth Modulation in Pediatric Idiopathic Scoliosis Using a Patient-Specific Finite Element Model Integrating Growth Modulation. Spine Deform. 6(4):344-350. doi: 10.1016/j.jspd.2017.11.006. PMID: 29886903.
12. Cobetto N, Aubin CE, Parent S (2020). Anterior Vertebral Body Growth Modulation: Assessment of the 2-year Predictive Capability of a Patient-specific Finite-element Planning Tool and of the Growth Modulation Biomechanics. Spine (Phila Pa 1976). 45(18): E1203-E1209. doi: 10.1097/BRS.0000000000003533. PMID: 32341305.
13. Martin S, Cobetto N, Larson AN, Aubin CE (2023) Biomechanical modeling and assessment of lumbar vertebral body tethering configurations. Spine Deform. 11(5):1041-1048. doi: 10.1007/s43390-023-00697-8. Epub 2023 May 13. PMID: 37179281.
14. Panjabi M, Brand R, White A (1976) Three-dimensional flexibility and stiffness properties of the human thoracic spine. *J Biomechanics* 9:185-192
15. Chazal J, Tanguy A, Bourges M, Gaurel G, Escande G, Guillot M, Vanneuville G (1985) Biomechanical properties of spinal ligaments and a histological study of the supraspinal ligament in traction. J Biomech. 18(3):167-76. doi: 10.1016/0021-9290(85)90202-7
16. Martin F (1990) Analyse expérimentale du comportement du rachis lombaire, Génie biologique et médical option biomécanique, E.N.S.A.M., Paris
17. Boudreault F (1994) Comportement mécanique des unités fonctionnelles : T3- T4, T7- T8 et T12-Ll saines et lésées du rachis humain, Mechanical Engineering Departement, Polytechnique Montreal, Montreal, Québec, Canada
18. Pezowicz C, Głowacki M (2012) The mechanical properties of human ribs in young adult. Acta Bioeng Biomech. 14(2):53-60. doi: 10.5277/abb120207

19. Petit Y, Aubin CE, Labelle H (2004) Patient-specific mechanical properties of a flexible multi-body model of the scoliotic spine, Med Biol Eng Comput. 42(1):55-60. doi: 10.1007/BF02351011. PMID: 14977223
20. Clauser C E, McConville J T, Young J W (1969). Weight, volume, and center of mass of segments of the human body. AMRL technical report TR-69-70, Available at: http://www.dtic.mil/dtic/tr/fulltext/u2/710622.pdf. Accessed November 2024.
21. Schultz A, Andersson G, Ortengren R, Haderspeck K, Nachemson A (1982) Loads on the lumbar spine. Validation of a biomechanical analysis by measurements of intradiscal pressures and myoelectric signals. J Bone Joint Surg Am. 64(5):713-20. PMID: 7085696.
22. Pearsall DJ, Reid JG, Livingston LA (1996) Segmental inertial parameters of the human trunk as determined from computed tomography. Ann Biomed Eng. 24(2):198-210. doi: 10.1007/BF02667349. PMID: 8678352.
23. Stokes IA, Aronsson DD, Dimock AN, Cortright V, Beck S (2006) Endochondral growth in growth plates of three species at two anatomical locations modulated by mechanical compression and tension. J Orthop Res. 24(6):1327-34. doi: 10.1002/jor.20189
24. Stokes IA (2007) Analysis and simulation of progressive adolescent scoliosis by biomechanical growth modulation. Eur Spine J16(10):1621-8. doi: 10.1007/s00586-007-0442-7.
25. Villemure I, Aubin CE, Dansereau J, Labelle H (2002) Simulation of progressive deformities in adolescent idiopathic scoliosis using a biomechanical model integrating vertebral growth modulation. J Biomech Eng. 124(6):784-90. doi: 10.1115/1.1516198
26. Sarwark J, Aubin CE (2007) Growth considerations of the immature spine. J Bone Joint Surg Am. 89 Suppl 1:8-13. doi: 10.2106/JBJS.F.00314
27. Viceconti M, Pappalardo F, Rodriguez B, Horner M, Bischoff J, Musuamba Tshinanu F (2021) In silico trials: Verification, validation and uncertainty quantification of predictive models used in the regulatory evaluation of biomedical products. Methods. 185:120-127. doi: 10.1016/j.ymeth.2020.01.011
28. Cobetto, N (2017) Planification chirurgicale pour la correction 3D de la scoliose pédiatrique progressive à l'aide d'un dispositif sans fusion flexible, Biomedical Engineering Departement, Polytechnique Montreal, Montreal, Québec, Canada; https://publications.polymtl.ca/2627/

29. Cobetto N, Aubin CE, Parent S (2018) Contribution of Lateral Decubitus Positioning and Cable Tensioning on Immediate Correction in Anterior Vertebral Body Growth Modulation. Spine Deform. 6(5):507-513. doi: 10.1016/j.jspd.2018.01.013
30. Cobetto N, Parent S, Aubin CE (2017) 3D correction over 2years with anterior vertebral body growth modulation: A finite element analysis of screw positioning, cable tensioning and postoperative functional activities. Clin Biomech (Bristol, Avon). 51:26-33. doi: 10.1016/j.clinbiomech.2017.11.007.
31. Nachemson AL (1981) Disc pressure measurements. Spine (Phila Pa 1976) 6(1):93-7. doi: 10.1097/00007632-198101000-00020
32. Sato K, Kikuchi S, Yonezawa T (1999) In vivo intradiscal pressure measurement in healthy individuals and in patients with ongoing back problems. Spine (Phila Pa 1976). 24(23):2468-74. doi: 10.1097/00007632-199912010-00008
33. Meir AR, Fairbank JC, Jones DA, McNally DS, Urban JP (2007) High pressures and asymmetrical stresses in the scoliotic disc in the absence of muscle loading. Scoliosis. 2:4. doi: 10.1186/1748-7161-2-4. PMID: 17319969
34. Driscoll M, Aubin CE, Moreau A, Villemure I, Parent S (2009) The role of spinal concave-convex biases in the progression of idiopathic scoliosis. Eur Spine J. 18(2):180-7. doi: 10.1007/s00586-008-0862-z
35. Driscoll M, Aubin CE, Moreau A, Parent S (2011). Biomechanical comparison of fusionless growth modulation corrective techniques in pediatric scoliosis. Med Biol Eng Comput. 49(12):1437-45. doi: 10.1007/s11517-011-0801-8
36. Morrissy RT, Goldsmith GS, Hall EC, Kehl D, Cowie GH (1990) Measurement of the Cobb angle on radiographs of patients who have scoliosis. Evaluation of intrinsic error. J Bone Joint Surg Am. 72(3):320-7. PMID: 2312527.ref
37. Cheung PWH, Wong HL, Lau DSL, Cheung JPY (2023) Directed Versus Nondirected Standing Postures in Adolescent Idiopathic Scoliosis: Its Impact on Curve Magnitude, Alignment, and Clinical Decision-Making. Spine (Phila Pa 1976). 48(19):1354-1364. doi: 10.1097/BRS.0000000000004731

**Tables and Figures** (listed in order of appearance in the text and the legend section)

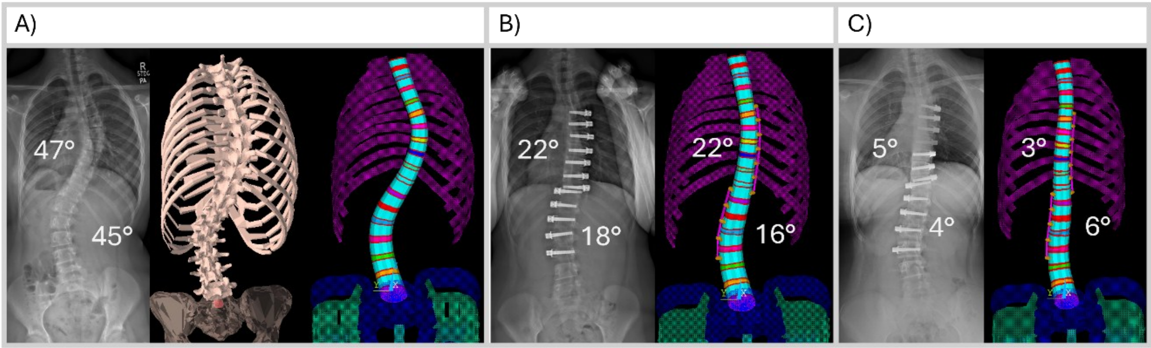


| Skeletal maturity (SS) at treatment beginning | Thoracic (T1-T12) growth rate (mm/vert/year) | Lumbar (L1-L5) growth rate (mm/vert/year) |
|---|---|---|
| Sanders 1 | 0.64 | 0.78 |
| Sanders 2 | 0.81 | 0.99 |
| Sanders 3A | 0.94 | 1.15 |
| Sanders 3B | 0.47 | 0.57 |
| Sanders 4 | 0.36 | 0.44 |
| Sanders 5 | 0.26 | 0.31 |
| Sanders 6 | 0.18 | 0.22 |
| Sanders 7 | 0.13 | 0.16 |

| Indices | Actual 2-year correction | Predicted 2-year correction | Difference (ABS) |
|---|---|---|---|
| MT Cobb | 20° ± 9° | 20° ± 10° | **3°± 2° *** |
| TL/L Cobb | 13° ± 11° | 13° ± 10° | **3°± 2° *** |
| T4-T12 Kyphosis | 31° ± 11° | 30° ± 9° | **2°± 1° *** |
| L1-L5 Lordosis | 50° ± 13° | 54° ± 14° | **4°± 4° *** |
| Apical axial rotation variation | 1° ± 7° | 2° ± 7° | **3°± 2° *** |

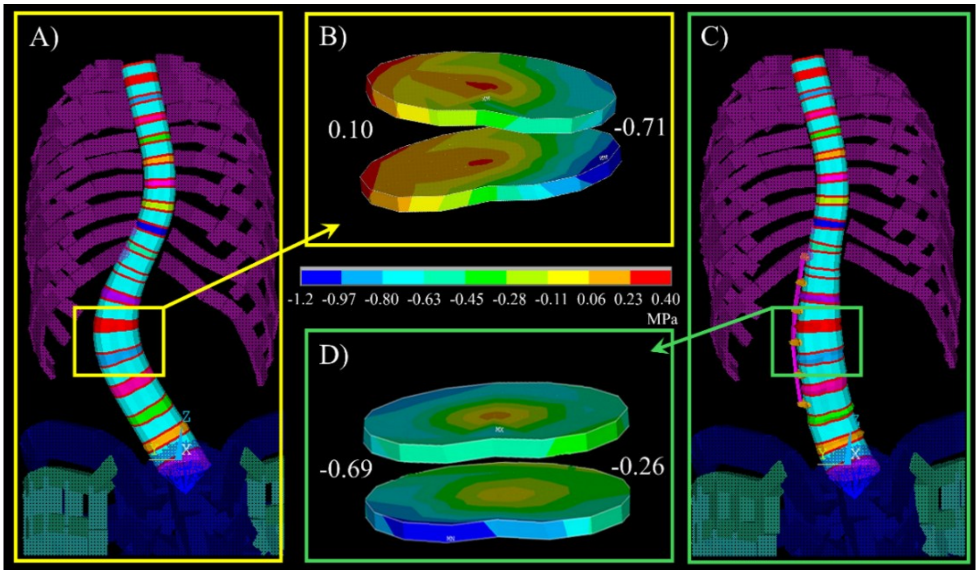
A)
B)
0.10
-0.71
C)
-1.2 -0.97 -0.80 -0.63 -0.45 -0.28 -0.11 0.06 0.23 0.40
MPa
D)
-0.69
-0.26

**CONSORT Flowchart**

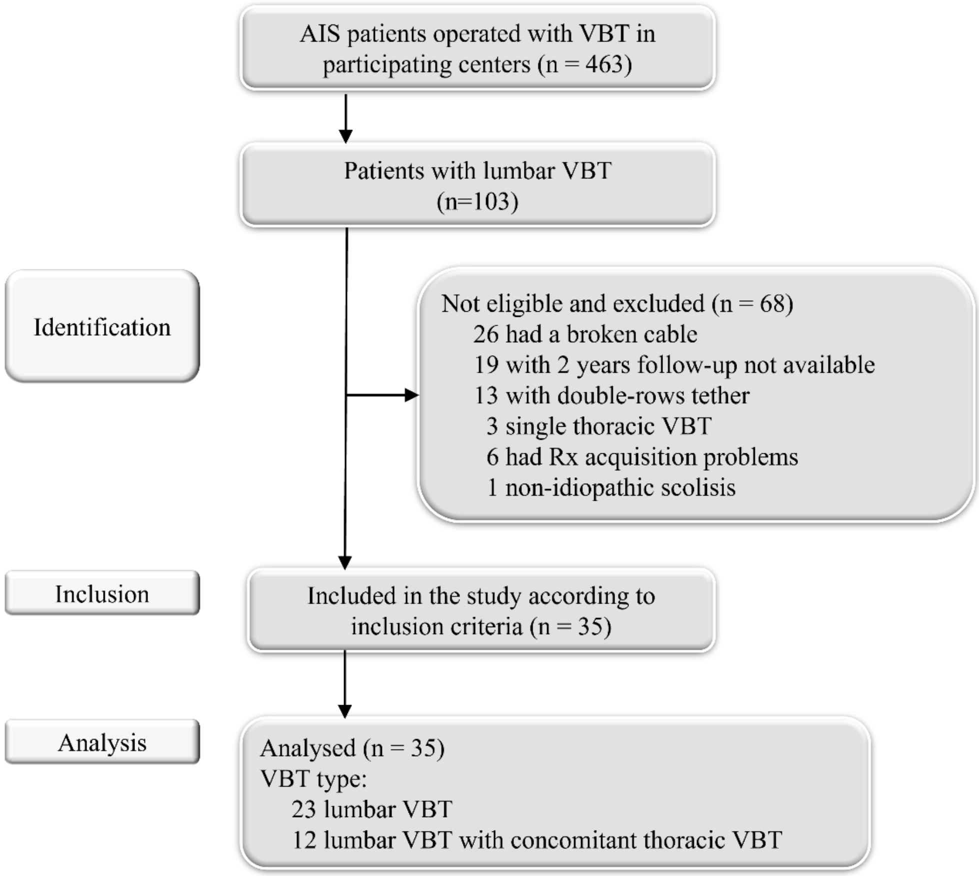


CONSORT flowchart of patients recruited from the participating centers, excluded and included in analysis following inclusion criteria